Determination of the Pre-Qualification Rules for the Acceptance Testing Of MVDC Cable System

A. SANTOSH

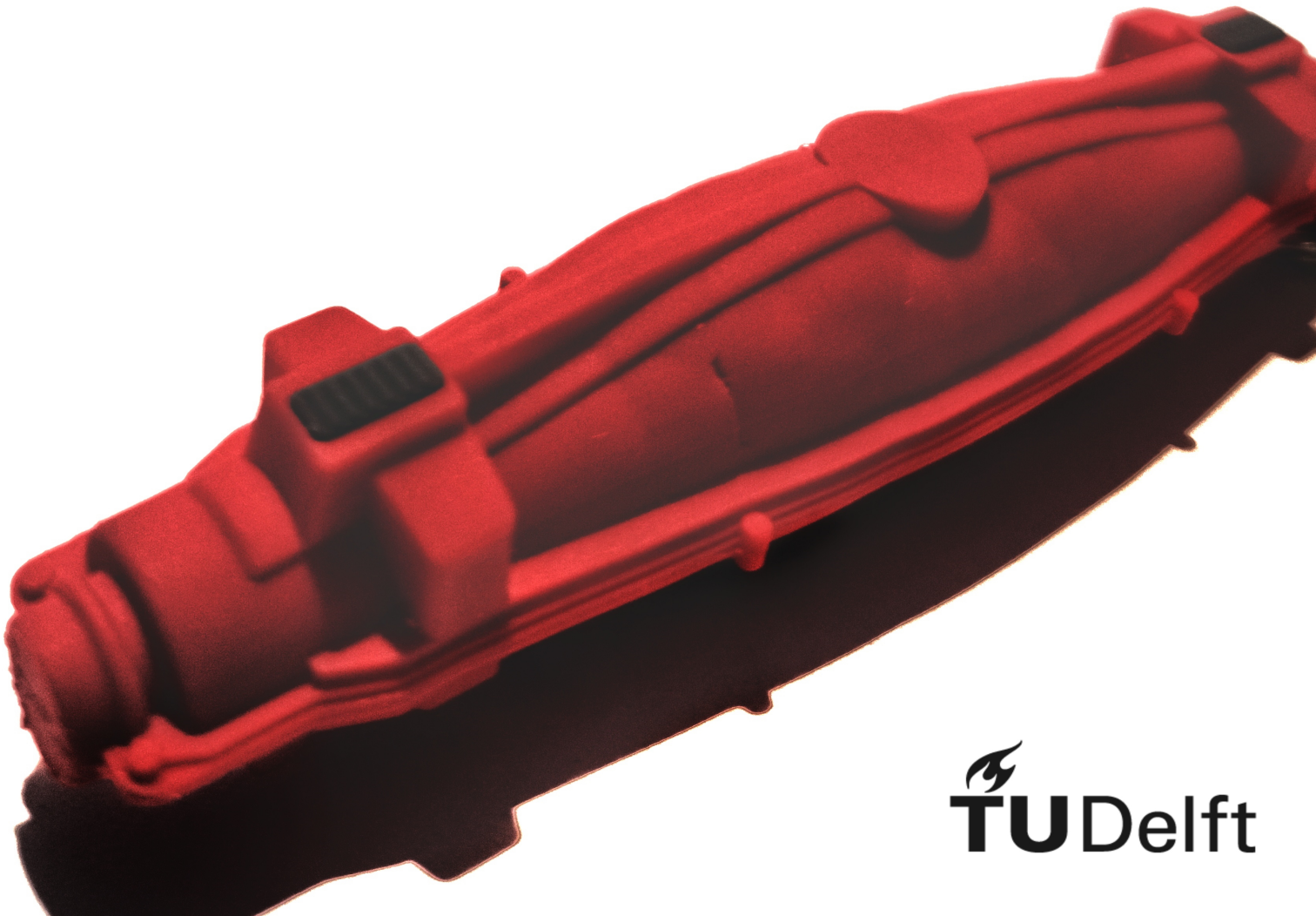

TU Delft

Determination of the Pre-Qualification Rules for the Acceptance Testing of MVDC Cable System.

by

A. Santosh

to obtain the degree of Master of Science
at the Delft University of Technology,
to be defended publicly on Wednesday August 26, 2020 at 10:00 AM.

Student number:	4809416	
Project duration:	November 25, 2019 – August 25, 2020	
Thesis committee:	Prof. Dr. R. Ross,	TU Delft
	Dr. ir. M. Ghaffarian Niasar,	TU Delft, supervisor
	Dr. ir. M. Cvetkovic,	TU Delft
	Dr. ir. L. Chmura,	Lovink Enertech B.V., supervisor
	Ir. D. Bergsma,	Lovink Enertech B.V.

This thesis is confidential and cannot be made public until December 31, 2022.

TU Delft

Acknowledgment

I want to thank Lovink Enertech B.V. for giving me this excellent opportunity to work on this research project for my thesis. I am grateful to Lukasz Chmura for guiding me throughout the last one year period. Under his guidance in the past year, I have developed as a researcher and as a person. I want to thank Marco Van Helmond for always being available to help me during my testing and examination phase. The knowledge I gained of various type tests and standards under the guidance of both Lukasz and Marco has been an invaluable experience. I am thankful to Dennis Bergsma for allowing me to work as part of the Engineering and Development team at Lovink.

I want to thank my supervisor from TU Delft, Professor Mohamad Ghaffarian Niasar for guiding me and supporting me throughout the last nine months. I can't be grateful enough to Prof. Mohamad for motivating me and agreeing to discuss my research at the shortest of notices. I want to thank Prof. Rob Ross for agreeing to chair my thesis committee. I am grateful to Prof. Milos Cvetkovic for agreeing to be the external expert as part of my thesis committee.

I would like to finally thank my family and friends for constantly supporting me, guiding me and believing in me throughout. I express my sincere gratitude to Govind Padmakumar who is the brain behind the cover page design. I look forward to the future adventures!

Abstract

In the transmission and distribution network of the future, there is expected to be a mix of both Alternating Current (AC) and Direct Current (DC). In the high voltage division owing to technical and economic aspects, there is a wider use of High Voltage Direct Current (HVDC) instead of High Voltage Alternating Current (HVAC). However, when observing the medium voltage network, it is noticed that it is completely AC in nature. One major reason for this preference of AC in the medium voltage network is the better know-how of an AC network and the presence of well established and reliable MVAC components and the ability to transform (step up and down) voltage in AC. A switch to Medium Voltage Direct Current (MVDC) is expected as the cost of power electronic components is decreasing with time, and there is an improvement in their performance. Therefore, switching to MVDC would provide advantages in the form of improved transfer capacity and better power control.

MVDC grids are debated to be a vital member of the future distribution network. In the present scenario, there is an absence of such an MVDC grid. Thereby, there are also no MVDC accessories available which can be used in such a grid. Therefore, there is also the absence of a testing procedure for the same. CIGRE TB 496 provides the testing strategies for DC cable systems up to 500 kV, but it does not take into consideration the difference between an MVDC system and an HVDC system. The systems may have a striking difference in construction, such as concerning materials. Additionally, there is also a difference concerning max field stresses and thickness of the insulation.

The possibility of using the AC accessories for DC application needs to be analysed, and it needs to be verified how such an AC accessory would behave under the influence of prolonged DC stresses. The use of existing MVAC accessories for DC would be beneficial given the high production standards and the voluminous supply chain of MVAC systems. Additionally, this also opens possibilities of reusing existing AC cable system for DC stress. It needs to be noticed that in DC, the field distribution would depend on the conductivity (σ) of the material which is different from AC where the field distribution depends on the permittivity (ϵ) of the material. The permittivity of insulation is virtually independent of the temperature. However, conductivity has a strong relation to temperature and electric field, which makes DC field distribution more complex when compared to AC field distribution for any geometry.

The test criteria of MVAC and prequalification test for HVDC are well known and need to be utilised in proposing and motivating the test sequence and test voltages for the accessories to be used in the future MVDC network. These accessories to be used in this future MVDC cable system needs to be analysed using Finite Element Method (FEM). The field simulations would give identification of locations in the joint which are undergoing maximum stresses during DC application. These maximum values of stresses are used to calculate the voltage life of the system based on electro-thermal life laws. The test results based on the representative testing procedure would help in understanding the performance and lifetime of the cable systems under DC stress. Therefore, to understand all items previously mentioned, a representative testing procedure needs to be proposed and motivated to test the use of existing MVAC accessories in the future MVDC network.

Contents

List of Figures

List of Tables

1 Introduction

1.1. Contemporary Cable System

The power system architecture consists of power generating stations, power transmission and distribution systems and consumers. The power generation takes place generally far from the point of power consumption. This power needs to be transferred to the point of consumption, either using overhead lines or underground cables. The cable system is a key party of this transmission and distribution architecture. In earlier decades, the use of overhead lines was considered to be the most reliable method for the transmission of power [7], [25]. However, it was found in SAIDI (System Average Interruption Index) for a local distribution company in Australia that the majority of outages as high as 70% are on the overhead line and the rest on the underground network [7]. As per [25], factors such as the deregulation of energy markets and also increasing attention to environmental aspects has changed the way how future electrical infrastructures would be planned and constructed.

Underground cables have seen increased participation in the power transmission and distribution architecture when compared to their overhead counterparts owing to the environmental benefits and also because they do not add to visual pollution [35]. The switch to underground cables from overhead lines took place over time with the cable technology becoming more economical and reliable and also given the reason that the latter was prone to adversities such as storms and vehicular accidents [7]. As per [49], the DC systems at medium and lower voltage level is yet to achieve the same level of maturity as that of the system at higher voltage level. The DC system at higher voltage level is reaping benefits when used for long distance transmission and connection to offshore wind parks [49]. The research aims to understand better the feasibility of DC cable system at the medium voltage level specifically the use of MVAC cable system for DC stressing.

1.1.1. Underground Cables

Underground cables are a critical part of the power system architecture, and they are preferred over their overhead counterparts more and more for the reasons mentioned above. In the United States of America, 15-20% of the installed distribution capacity is fulfilled by the underground cable system and this number can reach the high of 50% in Europe [58]. In the Netherlands, the total length of the overhead line is capped, and a principle of compensation has been implemented [54]. According to this principle, every new kilometre of the overhead line which is built should be compensated by changing a kilometre of overhead line to underground cable in some other location [54]. In many parts of Europe, the use of underground cables has increased over time in order to integrate more and more renewable energy sources into the grid [54].

When discussing underground cables and their utilisation over overhead lines, we need to understand that:

- Underground cables are more complex to construct as the insulation layer part of the system is also subjected to mechanical, environmental stresses [45], [47].

- As the cables are laid underground, the cable should be constructed such that it can dissipate the heat generated during operation [47].

- The length of the underground cables are limited due to their higher capacitance as it requires greater charging current for power transfer [45]. The reason for this higher capacitance of underground cables when compared to overhead lines is the lower insulation thickness of the former [45]. Another reason being that in comparison to air, the cable insulation (XLPE) has a higher permittivity.

Underground cable system with all the advantages it brings into the power transmission and distribution architecture, it also has some disadvantages, both of which can be seen as per the following table:

Advantages	**Disadvantages**
The frequency of outages is lower for the underground cable systems.	Underground system require higher capital costs.
Operation/Maintenance costs are lower when considering underground electrical system.	Due to the fact they are buried underground and are out of sight they tend to have longer repair time in case of outages
Underground cable system doesn't add up to the visual pollution	Reactive power compensation is a setback to long AC cable systems

Table 1.1: Advantages and Disadvantages of Underground Cable Systems [58].

The major classification of underground cable system based on their voltage level (Rated phase to phase voltage V_N) of operation can be seen as follows [45]:

- Low Voltage Cables: V_N<1 kV
- Medium Voltage Cables: 1 kV < V_N < 45 kV
- High Voltage Cables: 45 kV < V_N < 150 kV
- Extra High Voltage Cables: V_N > 150 kV

Underground cables typically compromise of conductors with screens and metal sheath along with the dielectric insulation. This type of construction gives rise to a radial electric field distribution, the electric stress can be given as follows [45]:

$$E(x) = \frac{V_0}{[x.ln\frac{R}{r}]} \tag{1.1}$$

In the above equation 1.1:

- V_0 : Operating Voltage
- R: Outer radius of the cable
- r: Inner radius of the cable
- x: Continuous radial coordinate

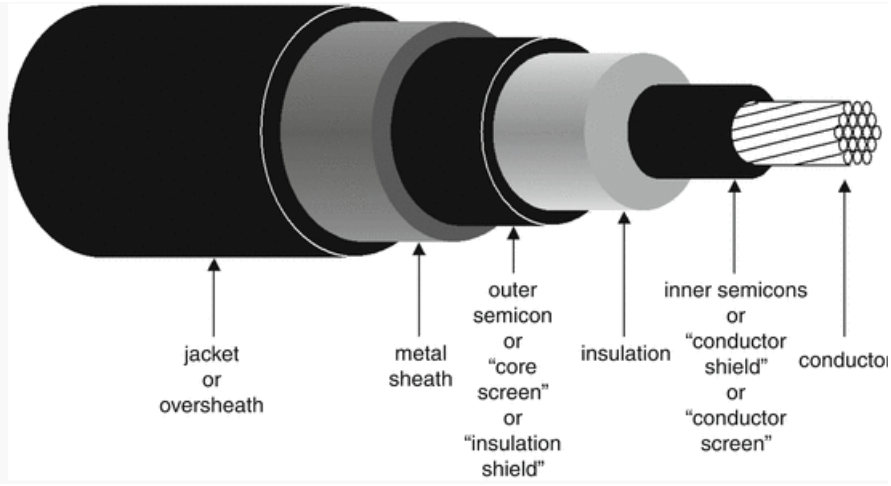

Figure 1.1: Different layers in a cable design [58].

The major elements which are part of the cable construction as seen in figure 1.1 can be briefly explained as follows [45]:

1. **Conductor**

   The conductor is responsible for the current transmission and should have losses as low as possible. Aluminium and copper are widely used material in conductor construction. Copper owing to its higher conductivity and lower cross-sectional area for the same current carrying capacity is superior but owing to cost when compared to aluminium, it takes the back seat. Aluminium owing to its lower density is lighter than copper for the same current carrying capacity. Thereby it is widely used as a conductor material in the current transmission and distribution architecture.

2. **Insulation**

   Insulation is a layer of dielectric between the conductor and the sheath, and it should possess higher breakdown strength and should tend to avoid causes (voids, intrusions) which may lead to field enhancements. Impregnated paper and Cross-Linked Polyethylene (XLPE) are widely used for cable insulation. The dielectric insulation is the most critical part of the cable system and often defines the long term behaviour of the system.

   - **Impregnated Paper:** Narrow strips of paper are placed helically on the cable conductor, and constant butt gaps are provided. Butt gaps facilitate the impregnation of the cable with the dielectric media and also helps towards bending of the cable.
   - **Extruded Polymer:** Dielectrics of the variant PE (Polyethylene) and especially XLPE (Cross-Linked Polyethylene) owing to its thermoelastic properties help in operating the cable system under higher temperatures. In these type of systems, care must be taken during production to avoid voids as in such insulation as there is an absence of any form of flowing dielectric media which would fill the voids. The extruded system can be mass-produced, and this solves the major time-consuming production steps taken for the preparation of paper and impregnating media in the case of impregnated paper cables.

3. **Semi-conductive Screen**

   Semi-conductive screen present on either side of the insulation layer in order to ensure a cylindrical field. These layers serve two main purposes:

   - It prevents any local field enhancements which can take place due to the presence of any inhomogeneities.
   - It helps in prevention of void formation between the conductor and insulation layer owing to mechanical and thermal stress and ensures a strong bond. The presence of such voids would cause partial discharges in the cable. In order to ensure the prevention of void formation, the

chosen semi-conductive screen material should have its coefficient of thermal expansion in close similarity to the dielectric in use as part of the cable construction.

Carbon paper is an example of a semi-conductive screen, and carbon black is incorporated into the carbon paper to attain the required levels of conductivity.

4. **Metal Sheath**

   The metal sheath provides protection against penetration of moisture into cables and leakage of oil when taking into account oil-paper cables. The sheath also helps in the conduction of fault current in case of a fault. The types of metallic sheaths which are normally seen are:

   - Copper wire screen with Aluminum laminated sheath

     These are light weight and are longitudinally watertight in nature but offer limited mechanical protection.

   - Lead Sheath

     These don't require corrugation and are longitudinally watertight but require pressure protection when being used for oil filled cable.

   - Corrugated Aluminium Sheath

     These type of metal sheath offer good mechanical protection and are light weight in nature. The downside of using this metal sheath is the difficulty in attaining longitudinal water tightness.

   - Steel pipes

     Steel pipes when used as metal sheath offer the best mechanical protection but tend to take higher effort for installation.

5. **Polymeric Outer Sheath**

   The outer sheath provides cable mechanical protection and also helps prevent moisture ingress. High-Density Polyethylene (HDPE) or Medium-Density Polyethylene (MDPE) is commonly used in this area due to its favourable characteristics.

The underground cable system in addition to their differentiation in voltage class are also segregated based on the type of dielectric technology in application as seen previously. The choice of underground cable system based on the technology can be divided into four major types as follows [58]:

1. **Polymeric:** This can be either XLPE (Cross-Linked Polyethylene), EPR (Ethylene Propylene Rubber), or WTRXLPE (Water Tree Retardant Cross-linked Polyethylene).
2. **Self Controlled Fluid Filled (FF or LPOF or PILC):** These cables were introduced in the 1890s. These type of cable system compromises of paper or PPL (Poly Propylene Laminated) which is impregnated with a liquid dielectric and a metal sheath is also present as part of the construction.
3. **Mass Impregnated non-draining (MIND or solid):** These types do cable system are widely used in medium voltage and high voltage submarine application. The cable system compromises of cable in which paper is impregnated with a poly-butene compound of high viscosity, a metal sheath is also present as part of the construction.
4. **High pressure fluid-filled (Pipe Type or HPOF):** A non-biodegradable fluid is used to impregnate the paper and, the whole system is kept under high pressure.

In the earlier times as per [15], oil filled and mass impregnated cables were majorly used for DC application. The environmental impact caused by these cable technology such as leakage and also the development of extruded technology such as XLPE led to the use of extruded cables for DC application [15].

1.1.2. Cable Accessories

Cables can be produced for long continuous lengths, but the post-production handling and transportation results in limiting cable length to an acceptable value [20], [12], [45]. Cable joint is an accessory which is used for the connection of two sections of cables, it may also incorporate field grading mechanisms. These sections can be either composed of similar insulation or be composed of different insulation [45]. Termination is a type of cable accessory used at cable section ends in order to terminate the system electrically or to grade the electric field [12]. Cable accessories are also the most problematic part of the cable system as they are prone to the most breakdowns [45]. It is stated in [53], that almost 55% of times the cable joints were responsible for the premature remove of DC cable system from operation. In an inspection performed on a total of 170 cable system failures by DNV GL, it was found that the majority of times the accessory was responsible for the failure and not the cable [59]. In an investigation as part of the southern power grid in China, 85.5% of the times the failure happened in an accessory [61].

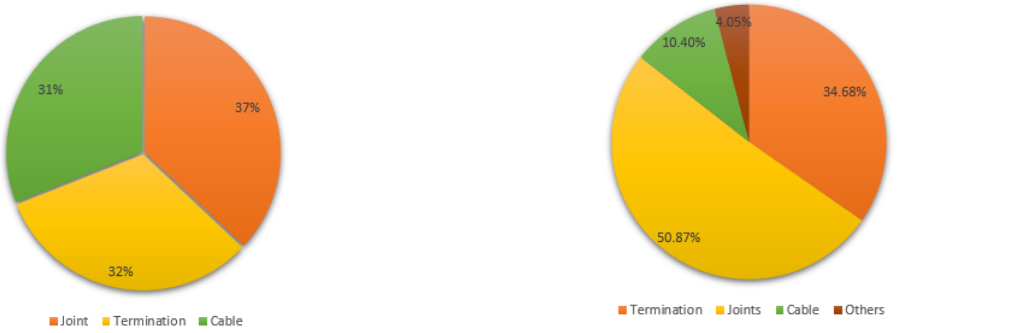

(a) Failure Location in the 170 cases investigated by DNV GL [59].

(b) Failure Location in the 110-220 kV cable systems as per the data collected by China Southern Power Grid.

Figure 1.2: Distribution of Failure in two different investigations.

As the fault in an accessory can affect the reliability of the whole cable system, accessories should preferably have performance in resemblance to the cables [12]. One major reason for high failure rate in the accessories as per [36], [51], [61] is because these accessories are assembled in field and are prone to contamination owing to human error. The major factors which needs to be considered when designing an accessory are [37]:

- The accessory should be able to control the field at the screen interruption. As the screen interruption may cause field enhancement which needs to be mitigated.
- The accessory should be able to mitigate high electrical stress which may occur along with the interfaces inside the accessory.
- The accessory should be able to mitigate any field disturbances which may tend to come up around the connector.

The different type of cable joints as per [36], [45] can be seen as follows:

1. **Straight joints:** Straight joints as the name suggests are type of joints are used to connect cable sections with similar insulation.
2. **Transition joints:** Transition joints as the name suggests are type of joints are used to connect cable sections with different insulation. These type of joints can be used to connect a paper insulated cable to a section of cable of the extruded insulation type.

The cable system in order to connect an accessory is stripped layer by layer, in the absence of field control mechanism a high field is witnessed at the end of the semiconducting layer [61].

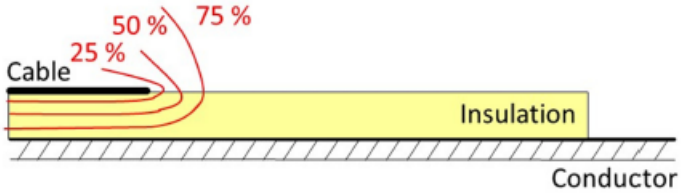

Figure 1.3: Electric Field Distribution in the Absence of Field Grading [61].

The accessories make use of multiple mechanism to keep the electric field under the permitted level, these can be briefly explained as follows:

1. **Capacitive Field Control:** Capacitive field control is used in controlling the electric field in systems such as the high voltage cable system for a long time [45], [61]. A stress cone which is normally utilised for capacitive field grading, it makes use of conductive layer to form equipotential surfaces which thereby reduces field concentration [37], [61].

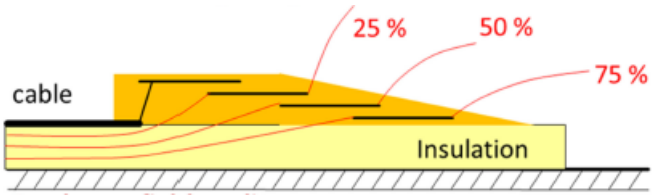

Figure 1.4: Electric Field Distribution with Capacitive Field Grading [61].

2. **Geometric Field Control:** Geometric Field Control which is also utilised in our test object makes use of deflector arrangement to control the electric field [45]. This type of field grading is one of the commonly used methods when considering polymeric cables and accessories [61]. The deflector arrangement shapes the field and also increases the V_a (Inception voltage for preliminary discharges) [45]. In [19] it is mentioned that the major disadvantage concerning such a method of field grading is the fact they require additional material and space.

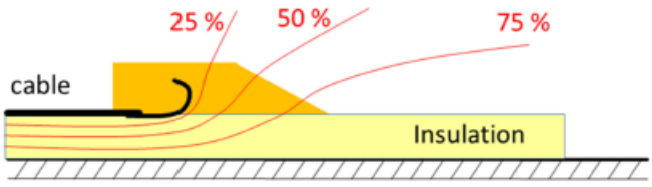

Figure 1.5: Electric Field Distribution with Geometric Field Grading [61].

3. **Non-linear Resistive Field Control:** Non-linear Resistive Field Grading utilises a layer of non resistive material to control the electric field. These material have conductivity varying with electric field and thereby helps in preventing field concentrations [61], [19]. This is achieved by utilising fillers like SiC (Silicon Carbide), FeO (Ferrous Oxide) in the field grading material.

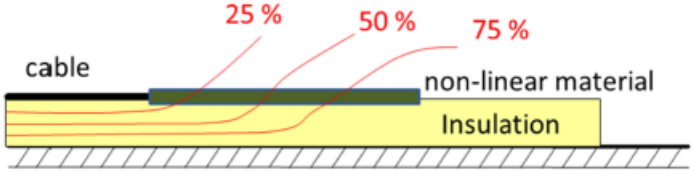

Figure 1.6: Electric Field Distribution with Non-Linear Resistive Field Grading [61].

4. **Refractive Field Control:** Refractive field control makes use of materials with high permittivity to move the equipotential lines away from the semi-conductive screen edge [61]. The compactness of this field grading method is an added advantage but this particular field grading cannot be used for DC voltages [61].

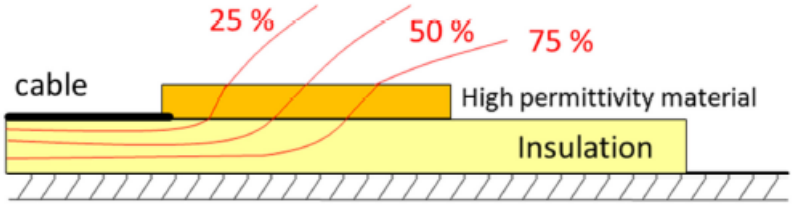

Figure 1.7: Electric Field Distribution with Refractive Field Grading [61].

1.2. Future of Distribution Grid

To ensure the reliable supply of power, enhanced power capacity and the better integration with renewable sources of power generation it is a natural process of updating existing power lines, one of these ways is to achieve this is to convert AC lines to operate under DC [31]. AC transfer has been the most popular method of power transmission for an extended period of time, but the maximum distance of power transmission is restricted owing to the reactive power compensation [15]. In the higher voltage level switching from AC to DC mode of power transmission resulted in increased power control and enhanced power transfer capacity, in the same manner, increase in transfer capacity can be achieved by converting Medium Voltage AC lines to DC [15], [62], [42].

When discussing the medium voltage network, the other major advantages of switching from Medium Voltage AC to a Medium Voltage DC network are as follows:

- The existing network components can be re-purposed rather than doing a complete overhaul [10].
- This use of the existing network component would prevent the need for additional investment for reinforcing the network [10].
- Power electronics which are to be used in the future MVDC grid would not contribute to fault current [10].
- Converters used in such an MVDC grid would also provide reactive power and voltage control [10], [62].
- The conversion to DC would provide ease of connection to renewables [62].

A key aspect of this study which would also be discussed below is to find out the possibilities of the switch from a medium voltage AC network to a DC one. The research would focus on the use of existing MVAC components to make this transition.

1.3. Need for this Study

The medium voltage network which contributes to the distribution side of a power system is operated using AC. The conversion of these medium-voltage lines to work under DC instead of AC would lead to improved system reliability and savings in term of investment which would have gone in refurbishing the existing AC lines and also there would be improved transfer capacity [31], [10]. When switching to DC there are certain phenomena which need to be kept in consideration that are not present in AC such as field inversion, space charge accumulation and thermal runaway, and these would be discussed in detail in the later chapters.

The MVDC networks discussed here would require the presence of MVDC accessories, and such an MVDC accessory would be required to pass a pre-qualification test procedure [14]. The need for conducting such a pre-qualification test procedure is to ensure the long term performance of the cable system [3]. The pre-qualification test of a DC cable system up to 500 kV is done with the help of CIGRE TB 496: ”Recommendations for Testing DC Extruded Cable Systems for Power Transmission at Rated

Voltage up to 500 kV". The CIGRE TB 496 suggests a universal test procedure for pre-qualification and type test of cable system up to 500 kV but does not take into consideration the difference between a medium voltage and a high voltage cable system with respect to insulation thickness, conductor cross-section and maximum field stresses [14].

The use of MVAC cable system for DC application needs to be tested. MVAC cable system due to its existing presence and wide usage leads to quality assurance and voluminous supply possible [14]. The test would also focus on how MVAC cable systems would work under prolonged DC stress as the field distribution in DC is different when compared to AC. The thesis research would focus on motivating test rules for the pre-qualification testing of such an MVAC cable system for the future DC distribution network.

1.4. Thesis Outline

The aim of this study is to understand the possibility of using an MVAC cable system in DC application. This can be exlpained as:

1. How do the existing MVAC accessories behave under DC stress, will DC due to its complex field distribution be critical to the accessory?
2. Will the MVAC cable system when put under a modified Pre-Qualification test program ensure a long term performance of the system for operation under DC stress?

The objective of this research is to understand the behavior on an MVAC cable system under DC stress, the aim of the pre-qualification is to understand if the system would deliver satisfactory long term performance. The examination phase which follows the pre-qualification test procedure helps in understanding what types of stresses the system witnessed during the whole test program.

In Chapter 2, the literature review written as part of the thesis research is present. The chapter focuses on the difference in AC and DC field distribution and how, for longer distances, the choice of DC would be the appropriate choice. The literature review also focuses on the rise of XLPE cables with the advancement in converter technologies. The advantages of DC at the distribution level and advancements in the pre-qualification test procedure are discussed as part of this chapter. Towards the end of the literature review, the significant causes of failures and their visual identifications for AC cable accessories are found.

In Chapter 3 the difference in AC and DC field distribution is highlighted. The chapter also talks about various phenomena in DC such as field inversion and space charge accumulation which are not witnessed in AC. The chapter also highlights medium voltage network under both AC and DC and also information about conversion of existing AC network to DC and the advantages involved.

In Chapter 4 we use COMSOL Multiphysics to understand how the field would distribute inside the MVAC accessory under DC stress. Temperature dependent field distribution and a few specific cut lines are also discussed as part of this chapter. Life time of the most stressed using electro-thermal life laws is also included as part of this chapter.

In Chapter 5 the requirement of a pre-qualification test procedure prior to the acceptance of the system into the field is understood. The pre-qualification test procedure which exists for high voltage DC system and the testing standards for MVAC system are also highlighted in this chapter. The knowledge of these existing test programs is utilised in preparing and motivating the modified test program.

Chapter 6 discusses the test object which is made to undergo the modified test program for its pre-qualification test. The pre-requisites to the tests and preparation of reference cable is also present in the chapter. The section on examination would help in understanding the impact of the pre-qualification tests on the test object.

Chapter 7 discusses the results from the FEM simulation and the observation made post the completion of the pre-qualification test procedure. The chapter concludes by answering the research questions which were formed as part of this research.

Chapter 8 describes the future recommendation which can be considered as part of future research in this domain.

2

Literature Review

It is well known that the electric field distribution in any high voltage equipment plays a major role in the lifetime of the equipment [16]. As per [55], the field distribution in AC depends on the permittivity of the material. It needs be understood here that the field distribution in DC depends on the conductivity of the material, which has a further dependency on the temperature and electric field strength [18], [22]. When considering AC field distribution in a cable, the maximum stress occurs on the conductor and minimum on the electric screen [32]. However, in DC this would change when cable transitions from no load to full load, this can be seen as per the following figure:

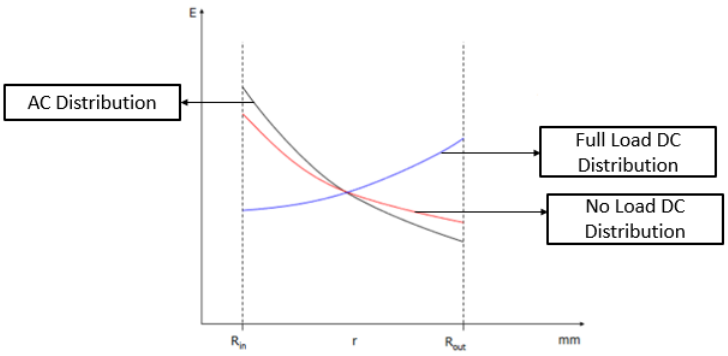

Figure 2.1: Difference in field distribution between AC and DC cable [11].

H.Kasuga et al. in their paper, discuss how long-distance transmission of power using AC would lead to serious power losses and also may cause instability in the network [26]. M. Tefferi et al. in their paper report that the usage high voltage DC transmission leads to a reduction in power losses, leads to stability enhancement, and moreover, it does not require reactive power to function [55], [15]. When long-distance power transmission is taken into consideration, DC would be the only feasible option [13], [26], [21]. A. Buchner et al. in their paper point that owing to the technical, operational and also economic reasons the further expansion of AC lines is not possible and thereby there would increase the use of high voltage DC [14]. When considering DC, we need to account for phenomena such as space charge and field inversion, and these phenomena are not relevant when considering AC [15].

In [56] K. Terashima et al. mention how the XLPE (Cross-Linked Polyethylene) cables are used widely in AC transmission owing to their superior dielectric and fire prevention properties. The authors also mention that for DC transmission OF (Oil Filled) and MI (Mass Impregnated) insulation are used over

XLPE insulation as for XLPE the breakdown strength of the insulation would decrease when at higher temperatures and would have a dependency on the thickness of the insulation [56]. K.P. Meena et al. in their paper state the increased use of XLPE cable for both medium/high voltage application is due to its better characteristics both thermally and electrically when compared with paper cables [35]. Y. Murata et al. in their paper on the development of high voltage DC cable system state that XLPE insulation with its environmental benefits is therefore chosen over oil-filled and mass impregnated type cables for DC application [41]. C. Stancu et al. in their paper mentions that when comparing DC cables with AC cables, the former has the upper hand owing to lower environmental impact, lower losses and enhanced transmission capacity [53], [14]. The paper also states that the interface charge would be seen in the presence of dielectrics when there is difference in the values permittivity (ϵ) or conductivity (σ), these charges would enhance the electric field in DC to a value twice than the scenarios without space charge [53]. W. Choo et al. in their paper mention the reason for XLPE cables taking over the oil-impregnated cables is owing to their positive characteristics such as higher dielectric strength, lower production cost and also they tend to have a higher resistance to moisture [18]. The major issue in using these XLPE cables for the high voltage DC transmission is their degradation due to the formation of space charge in the insulation under higher stresses [18], [12]. Y. Murata et al. in their paper compared AC-XLPE to DC-XLPE (prepared by addition of nano-sized particles) for space charge accumulation by utilising a field enhancement factor (FEF), the factor helps in understanding the effect of space charge on field enhancement in both the materials [41]. The authors find that the FEF of AC-XLPE increased with time and increase was greater with higher stresses but for DC-XLPE, the FEF was stable for a range of days [41]. K. Wu et al. in their paper on the effect of space charge on the aging of XLPE material for HVDC application state that space charge behaviour cannot be ignored as it may also change the IPL (Inverse Power Law) exponent [60]. M. Tefferi et al. states in their paper that owing to the temperature dependence of conductivity for DC field distribution, it is suggested to use materials with conductivity having lower temperature coefficient (α) [55], [61]. It is thereby pointed out that Ethylene Propylene Rubber with lower temperature coefficient (α) in comparison to XLPE may therefore be better for DC application.

In [3] the working group gives an explanation about the VSC (Voltage Source Converter) and LCC (Line Commuted Converter) systems, as per [3], LCC systems attain bidirectional flow of power using polarity reversal while VSC is a type of converter system which for the bidirectional flow of power does not require a change in polarity. T. Nguyen et al. state that the availability of VSC based converter systems combined with advancements in the field of power electronics opens up the possibility of integrating wind turbine with DC rather than AC [42]. M. Tefferi et al. in their paper, discuss how there is an increase in the usage of XLPE cables over the mass impregnated cables [55]. The reason for this is owing to the emergence of VSC systems which do not require polarity reversal for bidirectional power flow which is required by an LCC system [55], [13], [17], [24]. H. Kasuga et al. in their paper also mention that the use of XLPE cables is also beneficial when taking into account the fact that the cables tend to remain clean and free from maintenance in the case of an accident [26]. Y. Liu et al. in their paper on using an AC line for DC operation for an existing XLPE cable system make use of VSC based converter system in order to avoid polarity reversal which would be fatal for XLPE [31].

Work Group B1.32 in their book [3] state how pre-qualification testing is done in order to ensure the desired long term performance of the system. K. Terashima et al. in their paper [56] discuss the research and development ±250 kV DC XLPE cables, the long term performance test consist of a 200 m long cable which incorporates factory joints. The testing in [56] makes use of current transformers to generate the necessary heating cycles to carry out the tests.

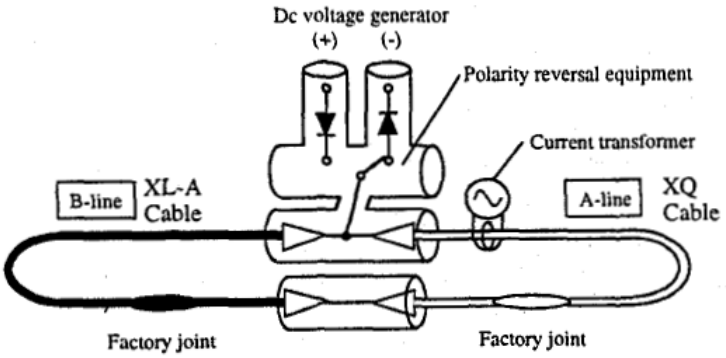

Figure 2.2: Layout of long term aging test [56].

The authors in [56] make use of a 24-hour cycle for heating consisting of 8/16 hours of heating/cooling. This cycle is similar to what is seen in [3], [13]. The test duration in [56] is a total of 260 days which was selected by the authors after considering the CIGRE recommendation for the testing of fluid-filled cables and the results obtained from prior testing of DC XLPE cables. The test duration in [56] is different from what is seen in [3] by a total of 100 days. The test program used by K. Terashima et al. in their paper can be shown in the following figure:

Step	Test Voltage	Days	Remarks
1	+ 500kV	30	$2V_0$
2	- 500kV	30	$2V_0$
3	±375kV	10	Polarity reversal $1.5V_0$
4	-500 kV	90	$2V_0$
5	±375kV	10	Polarity reversal $1.5V_0$
6	+ 500kV	90	$2V_0$

Table 2.1: Test program as in [56]

The load cycle test program as seen in figure 2.1 is different from the test program suggested by the [3] in section 5.2. A. Braun et al. in [13] came out with a prequalification test procedure which surpasses the one provided by [3]. The authors in their paper check the possibility of a 525 kV extruded cable for the transfer of power from the north sea to industrial areas in the south-west of Germany. A. Braun et al. in their paper [13] make use of conditions like different cable laying techniques such a directly buried, buried in tunnel/pipe in order to simulate real-life conditions which may occur in the field. The author also mentions how a DTS (Distributed Temperature Sensing) system can be used to monitor the temperature of the loop. The test setup as made in [13] can be shown as follows

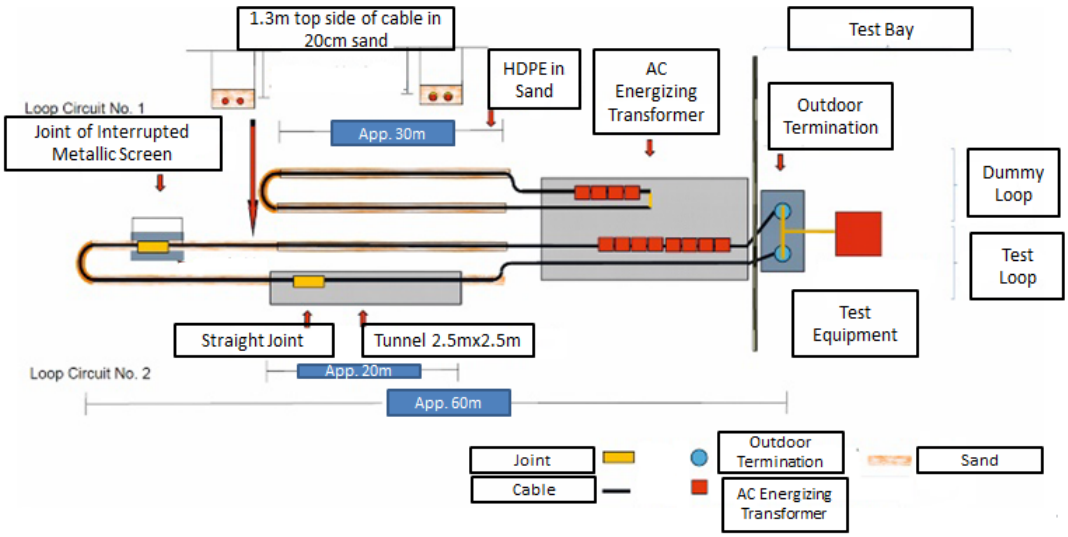

Figure 2.3: Test setup as in [13]

The test program followed by A. Braun et al. in their paper is similar to what is suggested by the Work Group in [3]. In the paper [21], H. He et al. suggest that during prequalification testing the temperature gradient should be efficiently maintained and a superimposed voltage test also needs to be conducted. The authors in [21] suggest this as an improvement to the prequalification test as suggested in [3]. The authors, in order to maintain ΔT across the cable wind a heating cable in helical fashion over the cable insulation. The heating cables of 6m x 50mm are wound over thin layers aluminium foil to ensure equal temperature distribution. H. He et al. also makes use two programs one to control the temperature at the conductor and the other at the cable insulation, the programs mutually interact to maintain a constant ΔT [21].

The paper [21] highlights a test setup where the temperature gradient is controlled to a temperature of Δ15K. The temperature distribution across the insulation with the presence of heating cable is shown as follows:

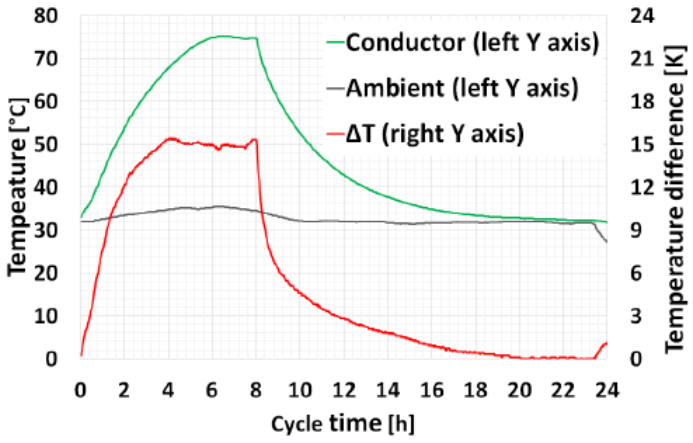

Figure 2.4: Temperature gradient with the presence of heating cable [21]

A. Buchner et al. in their paper [14] make use of a modified test program to test MVAC cables for DC application. The test setup consists of 2 cable loops which are 10m in length incorporated with 12/20 kV slip on termination and heat shrink joint with refractive field control. The choice of voltage for the PQ

test is 55 kV which was selected based on a few preliminary tests.

T. Nguyen et al. in their work state how when considering both MVAC and MVDC for the deployment of wind generation, MVDC offers multiple advantages in the form of safety when experiencing a fault [42]. Y. Liu et al. in their paper state that in order to enhance power transfer capacity of an AC line, one method would be to convert the lines as DC lines [31], [10]. The authors also address that with such a conversion as in [31], there would be better power quality and system reliability also ensure project savings. An increase in transmission capacity by 185% is stated in [10] when converting a 33 kV AC distribution system to MVDC. Similarly, as the breakdown voltage under DC is superior to AC, therefore for an insulation thickness of 10.5 mm, the DC voltage suggested would be 20kV or higher when the chosen ratio is two [31].

G. Bathurst et al. in their paper state that the majority of loads being served by today's AC network are primarily DC and thereby open up a possibility of upgrading the AC lines using DC [10]. J. Yu et al. discuss the significant challenges for the future of their existing distribution architecture in [62] as follows:

- Difficulty to obtain the right of way for additional distribution network for the UK.
- The current distribution network would be under high pressure with the increasing concentration of DER (Distributed Energy Resources) in the grid.

D. Antoniou states that the ability to run the AC systems at peak AC voltage when utilising it for DC application would lead to enhanced transfer capacity [8]. The author also mentions that utilising the existing AC system for DC application would lead to economic savings considering the cost of digging and putting newer cables [8]. J. Yu et al. mention that along with the increase in transfer capacity when switching to DC, the system would also facilitate the connection of renewable generation and provide more control over the circuit [62]. The author also mentions the choice of permissible DC voltage is of paramount importance when switching to DC, and the author makes use of peak AC value as the safe DC value [62].

Therefore when re-purposing a 33kV AC line for DC, we get a safe DC voltage of 27kV.

$$V_{DC} = \frac{33 \times \sqrt{2}}{\sqrt{3}} = 27kV \tag{2.1}$$

The authors in [17] state that the choice of DC voltage can be as high as two times the AC RMS voltage, this is because the insulation headroom present in AC cables can be used for higher voltages in DC. Y. Murata et al. during their testing of AC XLPE cable for DC application highlighted that space charge were found to be a major factor of concern at voltage stresses in the range of 20-50 kV/mm [41]. G. Bathurst et al. in their paper mentions how MVDC due to increased current and voltage and also due to the absence of voltage drop would provide increased power transfer capacity [10]. A. Shekhar et al. in their paper mention how when considering AC systems a voltage corresponding to $\sqrt{3} \times V_n$ can be witnessed in AC in case of faults, therefore when switching to DC a $\sqrt{2}$ increase in voltage is possible [49]. A. Burstein et al. in their paper, speak about an enhancement of 47% in transmission capacity as the insulation headroom, which is used for AC can be reduced when using for DC application [17]. The authors discuss how safe DC voltage to be applied on MVAC cable systems needs to be researched more. Y. Liu et al. in their paper discuss that when transitioning existing AC cable systems for DC applications, it should be verified how materials designed for AC behave under DC stress and also that if they accumulate space charge [31], [10]. The author also mentions that when transitioning existing AC systems to DC the performance of the overall system would need to be evaluated. J. Yu et al. discuss the same problem in their paper and state that when using AC cable systems for DC application, the oldest section of the complete cable system would act as the bottleneck owing to its thermal duty [62].

I.A. Metwally in their paper [36] state that accessories have higher failure rates, the reason for this behaviour:

- They see higher stresses electrically, thermally and also mechanically.
- They are prone to impurities as they are assembled and mounted in field.

- They require higher quality of workmanship.

In an MVAC cable system around 60-70% failure are result of an internal defect as part of the insulation, the reason for occurrence of such defects are the operational, environmental stresses and also due to poor handling of accessories [36].

When discussing about pre-qualification testing, K.P. Meena et al. in their paper research about the failure of medium voltage AC cable accessorises during qualification tests, and the paper mentions how joints and terminations with regards to stresses and ageing have the highest chance of failing [35]. The authors in their paper highlight a few general causes of cable failure and the visual identification on how they are identified, this can be seen in the following table:

Failure Causes	**Visual Identification**
Improper stress grading.	The failure point is witnessed close to the insulation screen.
Low clearance between conductor and shield terminus.	Insulation fails along the surface between the conductor lug and the screen terminus.
Missing semi-conductive layer (partly/completely) over stress control.	Insulation Failure
Cut seen at the insulation where the semi conducting layer ends.	Puncture in the insulation in the region surrounding the termination screen.
Improper Jointing.	Insulation around the joint show signs of overheating.
Sheath not grounded.	Joint insulation degradation and failure.
Joint not sealed properly.	Water ingress induced deterioration.
Cut marks or presence of semi conducting material traces on the surface of insulation.	Insulation degradation and failure.
Accessory being overloaded.	Change in color, charring of insulation over the joint and near the lug.
Termination not given necessary protective covering.	Tracking and erosion witnessed at the termination and insulation surface.

Table 2.2: Failure causes of cable accessories and their visual identification [35]

H. Gramespacher et al. in their paper [20], discuss how in an AC cable accessory, the causes of failure can range from error in production, installation error or the presence of a inhomogeneity such as void/bubble in the insulation. A failure rate of 1 joint for every 2000 joint is seen for AC joints working in voltage range 220 kV- 500 kV [20]. O. Siirto et al. in their paper discuss the reliability of medium voltage network of a specific distribution operator in Finland and mentions that electrical degradation (partial discharges, electrical and water trees) is the major cause of concern in polymeric insulation [51].

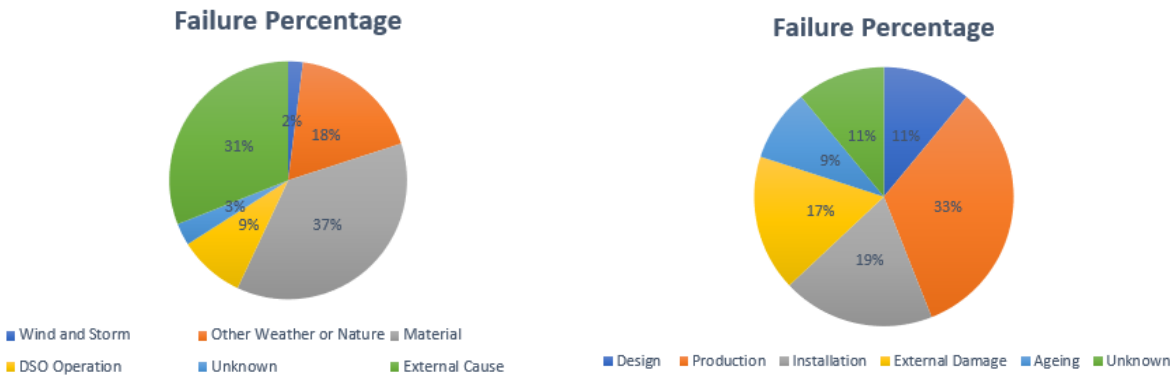

(a) Faults in the medium voltage AC network, 2010 [51]

(b) Causes of cable system failure as per a total of 170 investigations [59]

Figure 2.5: Failure Causes in AC cable system.

The medium voltage AC network in Helsinki saw almost two times the increase in faults in the year 2010 when compared to the previous year, and this can be seen in figure 2.5a. In figure 2.5b, we notice the cause of failures for a total of 170 failure of cable systems as investigated by DNV GL. BV Maanen et al. in their paper state that how production accounted for a majority of failures, these may arise due to voids, inclusion or in cases of mechanical damage to the cable during handling or transport [59]. The paper thereby brings up an important point that during some scenarios, defects may not appear when performing the acceptance testing but later may cause the breakdown of the whole system during operation. It can be seen that from both [51] and [59] that the material and its production is the major contributor to the cause of failures of the cable system.

3

Medium Voltage Network and Associated Accessories

As mentioned in previous chapters, Medium Voltage AC is the method for power transfer in the medium voltage distribution network. Medium voltage DC is debated to be the upcoming key player for power transfer in the medium voltage network. The major difference between both of them occurs from the use of either Alternating Current (AC) or Direct Current (DC) for power transfer. It is necessary to understand how AC and DC are different when it comes to their usage for power transfer.

3.1. AC vs DC

Alternating Current (AC) vs Direct Current (DC) for power transfer has been a debate which has been spanning for a long time. Alternating Current consists of a periodic reversal in the electric charge flow and is excessively used for the transfer of power over a long distance. AC can be transferred from lower voltages to higher voltages and vice versa easily using a transformer.

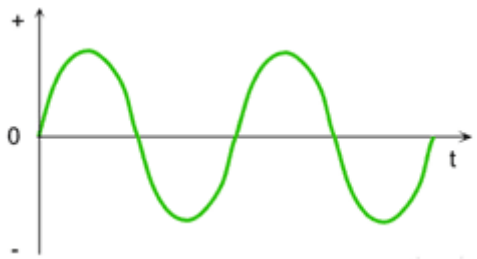

Figure 3.1: AC Waveform.

On the other hand, in DC (Direct Current), there would be a steady flow of electric charge. Household batteries to the batteries used in automobiles are the simple example of DC application. The DC waveform shown in figure 3.2 can be either positive or negative.

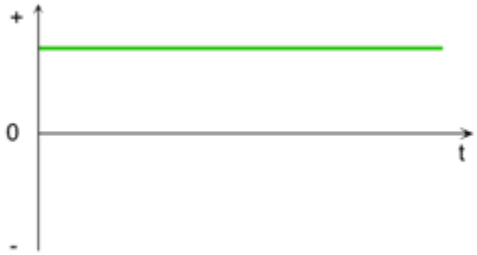

Figure 3.2: DC Waveform.

The choice of AC or DC for power transfer led to a series of events referred to as the war of currents. The war of currents took place when the need for a power transmission system was understood in the early 1890s, and It is also famously referred to as ”battle of currents” [6]. After the discovery of the incandescent bulb in 1880 by Edison, there originated a need of transmission network for the transfer of power for commercial use [6]. The first commercial power transmission system was in Edison's Pearl street where a 24 kilometre long DC line consisting of copper conductors was installed at 110 V for lighting the area of Lower Manhattan [10]. Around the same time, George Westinghouse developed an alternating current system which made use of transformers to step up and down the voltage [6]. Over time AC became the preferred way of long-distance power transmission owing to the lower losses and lower current requirements when compared to its DC counterpart [10]. The paper by [10] also mentions that with the emergence of transformers, the AC systems were the most suitable power system to ensure a reliable power supply. In the present times, with the groundbreaking progress of DC technologies such as cables and semiconductor devices, there is an increasing debate about using DC as the new favourite for power transmission [10]. When considering long-distance power transmission taking into account renewable sources, DC has the upper hand due to the following reasons [58]:

- The issues arising due to the connection of sections with different AC frequency value is absent.
- Absence of losses in DC owing to skin effect.

3.2. Field Distribution under AC

Field distribution in AC depends on the material property such as the permittivity (ϵ) of the insulation [36]. In the modern cable system, which is composed of polymeric insulation, it is also understood that the permittivity (ϵ) of the material does not have a strong dependence on temperature [55]. The dependence of permittivity on AC distribution can be explained considering two layers of dielectrics with varying values of permittivity as follows:

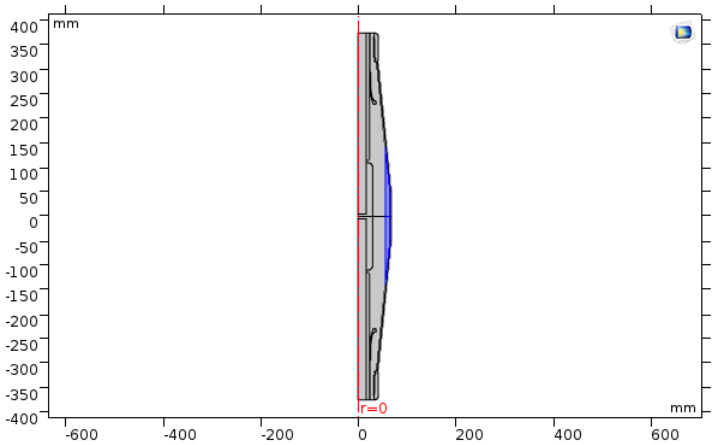

Figure 3.3: 12kV Joint with a layer of solid Lovisil.

In the above figure 3.3, the simulation of an AC joint is seen, the highlighted blue part represents a solid

layer of liquid Lovisil. The influence of permittivity on the AC electric field distribution can be seen by changing the value of permittivity of the solid Lovisil layer in the following scenario:

1. **Similar Values of Permittivity**

   In this case, we set the value of permittivity of solid Lovisil (ϵ= 2.9) to a similar value of that seen in liquid Lovisil (ϵ= 2.73).

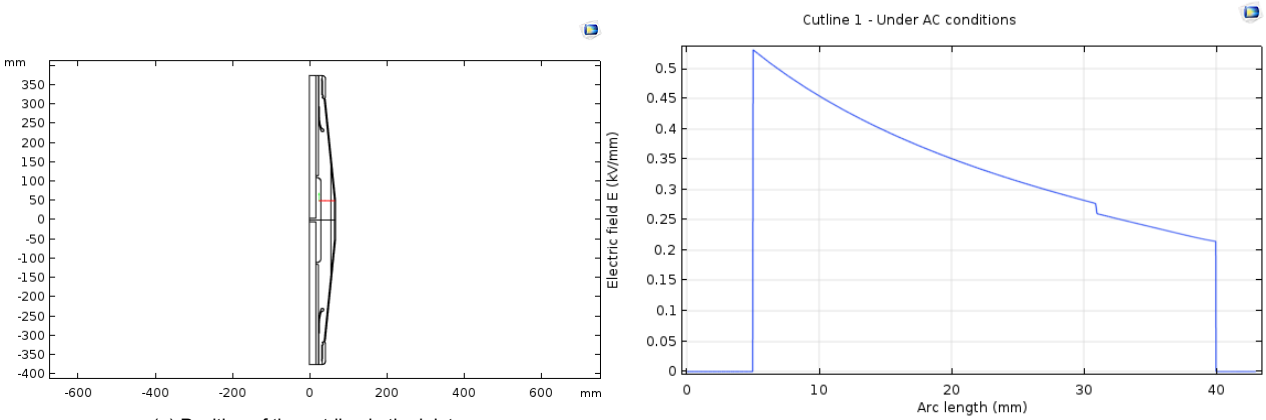

(a) Position of the cut-line in the joint

(b) AC Field Distribution.

Figure 3.4: AC Field Distribution in the presence of layers with similar permittivities.

In the above figure 3.4 we have two subfigures, figure 3.4a highlights the cut line over which the electric field distribution is witnessed. The cut line passes at the cable connector and passes through both liquid and solid Lovisil. As per figure 3.4b, we notice that the field distribution in the presence of layers of similar values of permittivity is not distorted much. Due to the slightly lower value of permittivity in liquid Lovisil (ϵ= 2.73), we see that the field is higher in that region and drops by a small value as it enters comparatively higher permittivity (ϵ= 2.9) region of solid Lovisil. This variation in field distribution between layers is because AC field distribution depends on the permittivity of the material and the field would tend to concentrate in the area of lower permittivity [27], [36].

2. **Varying Values of Permittivity**

   In this case, we assume the value of permittivity of solid Lovisil as one (ϵ= 1), which is very different to the value seen in liquid Lovisil (ϵ= 2.73).

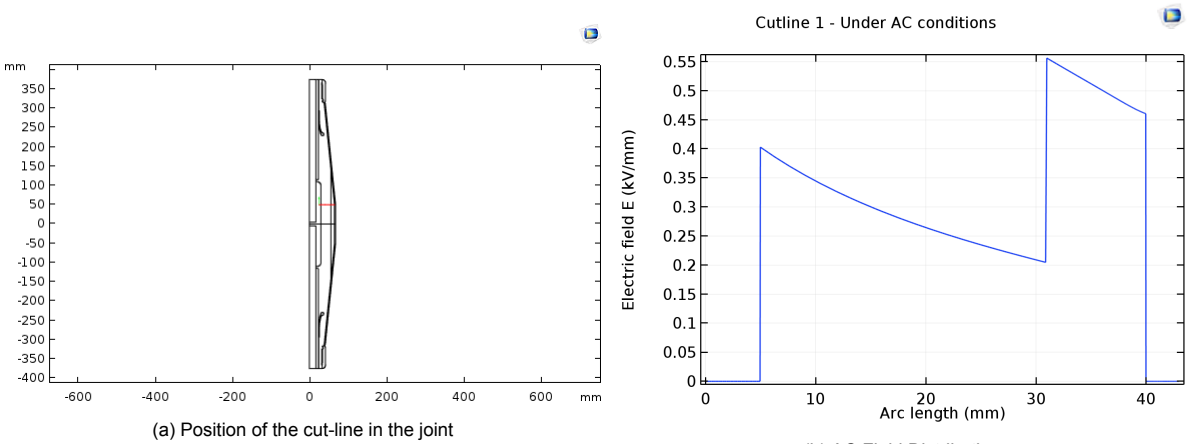

(a) Position of the cut-line in the joint

(b) AC Field Distribution.

Figure 3.5: AC Field Distribution in the presence of layers with different permittivities.

In the above figure 3.5, we notice that the field distribution in the presence of layers of varying permittivity concentrates in the layer with the lower value of permittivity. Due to the lower assumed value of permittivity in solid Lovisil (ϵ= 1), the electric field under AC tends to concentrate here rather than in the liquid Lovisil.

3.3. Field Distribution under DC

Field distribution under DC is different from AC, as explained earlier, the field distribution in AC depends on the permittivity (ϵ) of the material [55]. In the case of DC, the field distribution depends on the resistivity (ρ) of the material [58], [20], [18]. In contrast to AC, the resistivity of insulation material has a huge dependence on both temperature and electric field for DC field distribution [18]. The dependence of resistivity on temperature for a few insulation materials can be shown as follows:

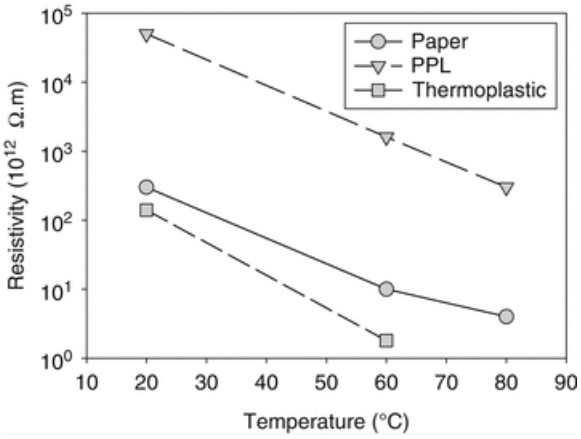

Figure 3.6: Variation of Resistivity at Different Temperatures [58].

In figure 3.6, we notice how the value of resistivity of different insulation material changes over a range of temperature. This change in resistivity over a range of temperature would make DC field distribution complex. In [27], it is discussed that how the permittivity of different material may vary within a decade on the same hand the conductivity of different material may vary in the range of several decades. The relationship of conductivity to temperature during the presence of a temperature gradient in DC during operation results in the shift of higher field strength from conductor to the sheath [13]. There are a certain number of phenomena which are exclusive to DC cables and are not seen in AC cables such as field inversion, space charge accumulation [15]. These phenomena would be further explained down the line.

Field Inversion:

Field inversion in DC cables happens due to the dependency of DC field distribution on conductivity and dependence of conductivity on temperature and electric field [13]. During operation, heat losses result in temperature gradient which is present in DC cable from the conductor to the sheath [15], [55]. We understand from figure 3.6 that for insulation materials, the conductivity increases with the increase in temperature, and there due to this temperature gradient, we would have higher conductivity at the conductor and lower conductivity at the sheath. Owing to this it would be seen that in DC cables the highest field strength shifts from the conductor to the sheath [15], [21]. The occurrence of such field inversion phenomena in the cable also adds to the space charge formation [55]. In a DC accessory such as a cable joint also this phenomena of field inversion during the application of DC voltage can be witnessed.

The field distribution shown below is on a joint manufactured at Lovink Enertech B.V., the cut-line of the field distribution lies between the cable connector and the joint insulation. Field inversion is observed by witnessing the field distribution in the cut-line show in the figure 3.7a for both AC and DC conditions. The cut line is made in a normal manner at the cable connector and joins insulation interface. The field distribution witnessed in the liquid dielectric would show variation when plotted for both AC and DC

condition.

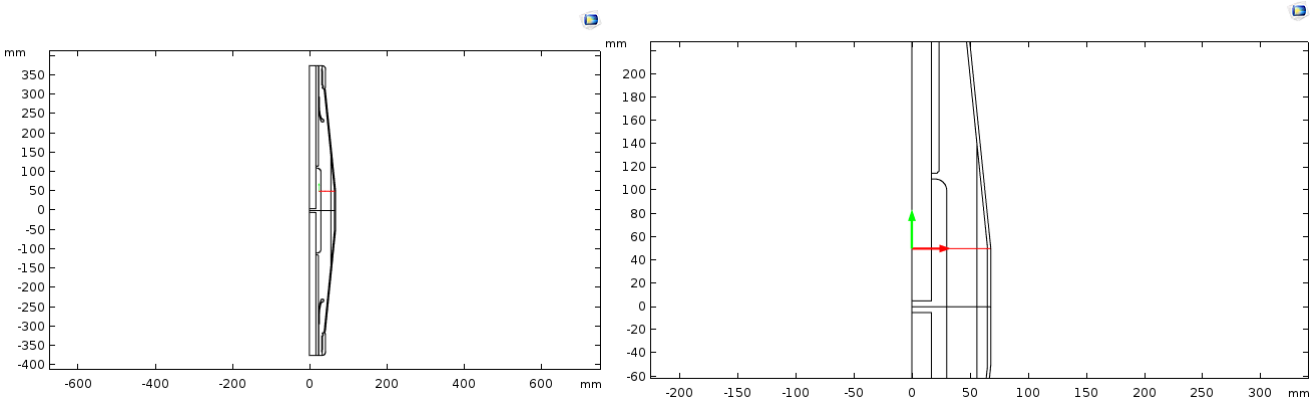

(a) Position of the cut-line in the joint

(b) Zoomed in cross-section

Figure 3.7: Normal cut-line made on Cable Connector + Joint Insulation

In the case of AC field distribution shown in figure 3.8a, it is seen that the max field strength occurs at the conductor throughout, and there is no field inversion taking place [32]. In the case of DC field distribution, we see that with that at lower temperatures the maximum field strength occurs near the conductor and with the increase in temperature this peak electric field strength shifts from the conductor towards the sheath.

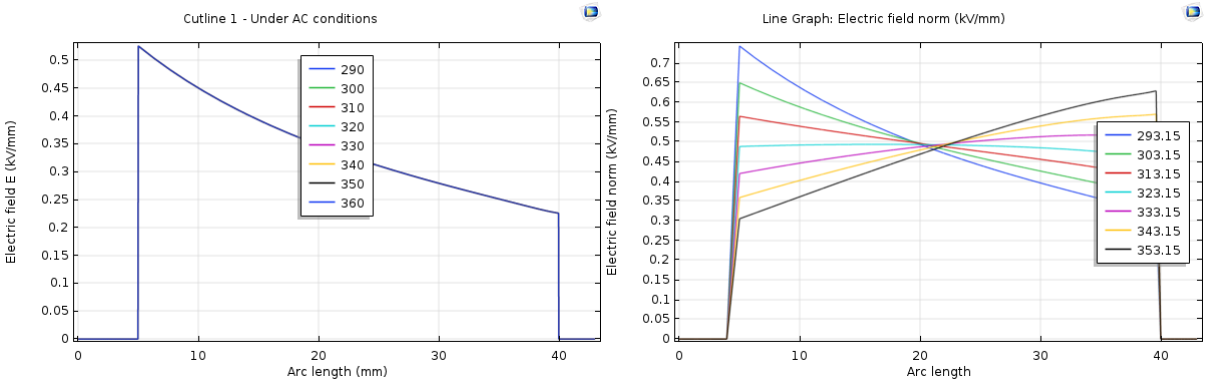

(a) AC Field Distribution.

(b) DC Field Distribution.

Figure 3.8: AC and DC field Distribution for a range of temperature 293-363 K.

The materials used for DC application should favourably possess higher breakdown strength for both DC and impulse voltages [55]. The material shouldn't accumulate much space charge and also it should have a conductivity characteristic which shows a lower temperature dependence [55].

Space Charge Accumulation

Polymeric insulation material like cross-linked polyethylene can store charges, and these free charge carriers can affect the way the electric field distributes inside the insulation material [14]. These charges are not that critical in AC since due to the periodic voltage shift, they are not pushed inside the insulation mass. On the other hand, when considering DC, these charges and can influence the electric field distribution and may cause field enhancements [24], [53], [16].

These charges can also get accumulated in the material, if charge entering the insulation is different from the amount of charge leaving the insulation, and this would lead to a space charge accumulation [16]. When considering the development of cables with polymeric insulation for DC application, space charge tends to be a significant issue as it tends to electric field distortion [12]. In cases where the maximum

field strength is low when considering both full load and no-load operation, then the phenomena of space charge accumulation in the solid insulation (XLPE) is not critical [31]. The reasons leading to the generation of space charges in a polymer material can be given as [29]:

- **Conduction:** Generation of space charge owing to the movement of charges inside the dielectric.
- **Injection:** Generation of space charge owing to its injection/extraction into the dielectric from the electrodes.
- **Trapping:** Generation of space charge owing to trapping of charges in various location in the bulk of the dielectric.

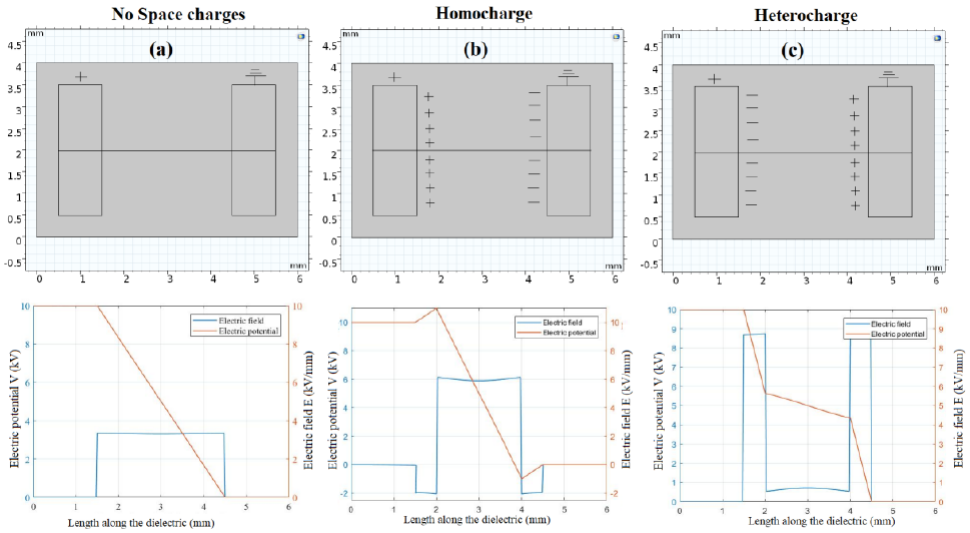

Figure 3.9: Electric Field and Potential Distribution, (a) In the absence of space charge (b) In the presence of homocharges (c) In the presence of hetrocharges [16].

The major regions where space charge accumulation can occur are listed below [38]:

- Electrode - Dielectric interface
- Dielectric - Dielectric interface
- In the presence of a temperature gradient
- In the presence of gross inhomogeneities
- In the presence of morphological inhomogeneities

The above figure 3.9 shows an electrode-dielectric interface, and this is one of the regions where space charge can accumulate if the current density is divergent. In an electrode-dielectric interface, there are two major mechanisms which are the charge injection/extraction mechanism and the charge transport mechanism [38]. The injection/extraction mechanism is responsible for the flow of charges across the interface while the charge transport mechanism handles the flow of charge through the bulk of the dielectric [38]. If the injected/extracted charge is not equal to the charge transported we get space charge accumulation [38]:

$$J_{inj}(E,T) - J_{tra}(E,T) = \Delta J_{interface} \tag{3.1}$$

In the above equation 3.1:

- J_{inj}: Charge injection density
- J_{tra}: Charge transport density
- $\Delta J_{interface}$: Charge accumulation density

The different cases which can be seen due to the difference in injection/extraction and transport charge density can be explained as follows [38]:

1. $J_{inj}(E,T) = J_{tra}(E,T)$

   In such a scenario where both the injection and transport charge density is the same, there won't be any charge accumulation. As shown in figure 3.9(a), this scenario won't lead to any distortion of the electric field and potential.

2. $J_{inj}(E,T) > J_{tra}(E,T)$

   In such a scenario where the transport charge density is lower than the injection charge density, we get a homocharge accumulation. Homocharges tend to accumulate on the electrode with similar polarity as that of the charge [24]. This is owing to the reason that the dielectric bulk doesn't transport charge at the same rate as which the electrode injects. The formation of homocharges as shown in figure 3.9(b) leads to the enhancement of electric field in bulk and the increase of transport current. In contrast, the electric field at the interface drops and so does the injection current. The steady-state is obtained when both the currents are on the same level.

3. $J_{inj}(E,T) < J_{tra}(E,T)$

   In such a scenario where the injection charge density is lower than the transport charge density, we get a heterocharge accumulation. Heterocharge accumulates on electrode of opposite polarity as that of the charge [24]. The accumulation is because the interface does not inject charge at the same rate as which the dielectric transports. Heterocharges as shown in figure 3.9(c) leads to the reduction of the electric field in bulk and the reduction of the transport current the interface, and similar enhancement is seen in the injection current. The steady-state is obtained when both the currents are on the same level.

Thermal Runaway:

As explained previously under Field Inversion, insulation material show very low resistivity at a higher temperature. High direct leakage current is witnessed in the cable insulation, which results in further heating of the insulation, this may result in the thermal breakdown of the cable insulation [14], [15]. This phenomena is called thermal runaway [14], [15]. Modern XLPE cables owing to newer technologies and materials in the insulation see a lower risk of thermal runaway, these cables can be operated up to a maximum conductor temperature of 90°C [14], [15].

3.4. MVAC and MVDC

The Medium Voltage Cable system is pivotal towards ensuring the reliability of the distribution network [35]. When considering distribution level, the choice between AC and DC become more complex as the MVAC system, which is currently being made us of is cost-efficient and widely established [10], [42]. When utilising an AC system for power transfer, the transmission efficiency takes a hit owing to the losses such as skin effect [15]. In addition to losses the requirement for reactive power as per [15] would put a cap on the maximum length of cable. The option to increase the voltage in the AC system would lead to an increase in the absolute losses, and also the generated heat would add to the accelerated ageing of the system [8]. These AC systems also face an ageing architecture and restrictions to expansion which makes a switch to DC viable. Multiple pieces of research such as what is given in [42] states that the usage of MVDC system in place MVAC would help in achieving increased power transfer capacity. In a combination of that, the future requirement problems to be faced by the passive network can be mitigated utilising the MVDC technology [62]. When re-purposing AC cable systems for DC, there are also savings in terms of infrastructure cost and the cost for digging and laying newer cables [8], [50]. As per [49], the major reasons for the increase in power transfer capacity when using an MVAC system for DC operation is as follows:

1. An increase in current rating is present in DC compared to AC conditions owing to the improved thermal limit. The rise in thermal limit is due to the following reasons:

   - In AC condition losses happen due to the presence of skin effect and proximity effect, and these contribute to heating which puts a cap on the thermal limit of the cable.

- AC tends to witness both dipole and dielectric losses, and these dipole losses would be insignificant when considering DC.
- Leakage current due to capacitive effect is high in the cable insulation in AC condition, and such a capacitive effect is absent in DC condition.

2. The presence of power factor in AC and its value has an impact on the power transfer capacity. As the power factor in AC is a value smaller than unity would lead to reduced power transfer capacity in the AC condition when compared to its DC counterpart.
3. The possibility to achieve higher voltage at the receiving end in DC compared to AC leads to increased transfer capacity. The choice of higher voltage rating is one of the major factors leading to an increase in transfer capacity when switching from AC to DC [17].
    - The transmission line is made of resistance ($R_{cab,AC}$) and inductance (L_{cab}), the voltage drop across them both lead to a reduction in voltage at the receiving end in AC. In DC, it is seen that the inductance (L_{cab}) is absent and due to the absence of skin effect the losses due to resistance ($R_{cab,DC}$) is also lower.
    - In DC the sending in voltage can be raised by a minimum factor of $\sqrt{2}$ as the same insulation headroom required for AC is not necessary for DC.

The advantage of switching to an MVDC network also lies in the fact that it would support the connection of more and more renewable to the network and the use of power converters would facilitate both voltage and power control [62]. MVDC system as per [55] is considered the scaled-down version of the HVDC system. As per [17] the impact of all factors cannot be scaled down directly for medium voltage applications from the knowledge of this phenomena in high voltage application. The field inversion as mentioned before in section 3.3 is a severe concern in HVDC system, but when considering an MVDC system owing to the lower field stresses, these will not be critical to the system [17]. When considering the deployment of distributed wind generation in [42] using either MVDC or MVAC system, the former showed better performance over the latter. The major limiting factors in an AC system such as the losses due to skin effect and proximity effect are not dominant in DC and thereby gives more reason on switching to a DC system [17], [49]. MVDC can be used to integrate the distributed resources, and such a system is essential when we plan to interconnect both transmission and distribution systems [55]. These systems can power activities such as DC ships, future power systems and also for the electrification of marine infrastructure [55].

The major limiting factors which can arise when integrating an MVDC system are as follows:

1. The equipment's which are to be used in an MVDC system have shorter life span [10].
2. The lower production standards of medium voltage cables in comparison to their high voltage counterparts [17].

As part of this research, we will be determining the possibility of utilising an MVAC cable system for DC application. The accessories manufactured for AC application are designed such that they facilitate AC field distribution. The inherent difference between AC and DC field distribution needs to be considered, and the behaviour of the accessory needs to be investigated when subjected to DC stressing.

3.5. Running AC systems under DC

Upgrading existing AC lines to DC or re-purposing existing AC lines for DC application is done in order to ensure reliable power supply [31]. Multiple challenges face the existing network as the loads are increasing, and so does the decentralized generation in the grid [17]. The usage of DC distribution in place of the existing AC distribution would lead to increases power transfer capacity, and also it would facilitate the ancillary services [17]. The following challenges as per [62] were faced by SP Energy Networks when considering the future development of their distribution network:

- Increasing pressure on the network in terms of voltage management and maintaining the thermal limit with an increase in connections with distributed energy resources.
- Difficulty in obtaining the right of way for the construction of supporting network in the UK.

The choice of permissible DC voltage is of paramount importance when switching to DC, and the authors in [62] makes use of peak AC value as the safe DC value. Therefore when re-purposing a 33 kV AC line for DC, we get a safe DC voltage of 27 kV [62]. As per [8], [17] also when re-purposing MVAC cables for DC application, the peak AC voltage is taken as the safe DC voltage. In our case, for a 12 kV AC system, the safe voltage is therefore found as follows:

$$V_{DC} = 12 \times \sqrt{2} = 17kV \tag{3.2}$$

Ageing as per [49], [33] has strong relations to factors such as breakdown and lifetime of the cable. When switching to DC from AC, it needs to be considered that the design and construction of the system were to facilitate AC application. In cases of high thermal loading post switching to DC, the system undergoes accelerated thermal ageing [17]. Similarly, higher electrical stress post-conversion to DC would lead to failure due to accelerated electrical ageing [17]. Thereby it needs to be made sure that the choice of DC voltage and current after re-purposing does not lead to accelerated ageing of the system. When re-purposing existing AC system for DC application, the overall condition assessment is important as some ageing would have already taken place and this thereby influences the selection of the current and DC voltage [62]. It needs to be seen if components of cable such as the insulation would develop space charge under DC stressing [31]. In a case where the cable system is made of multiple sections of cables with varying insulation types then the oldest section of the cable would be the bottleneck owing to its thermal constraint [62].

The choice of DC-link topology has an impact on capacity enhancement when switching from AC to DC for power transfer [49]. The major DC-link topology used when converting AC lines for DC operation as per [49], [8] can be seen as follows:

1. **Unipolar System**

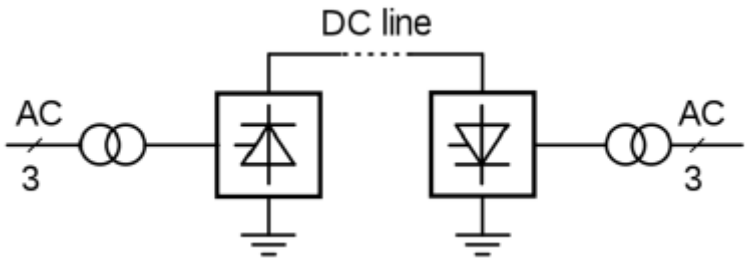

Figure 3.10: Unipolar System [8].

As seen in figure 3.10, a unipolar system makes use of a single metallic conductor for current transfer, the return current is via earth return [8]. The absence of a metallic return path leads to advantage such as cost savings but may lead to corrosion which is a major disadvantage [49].

2. **Bipolar System**

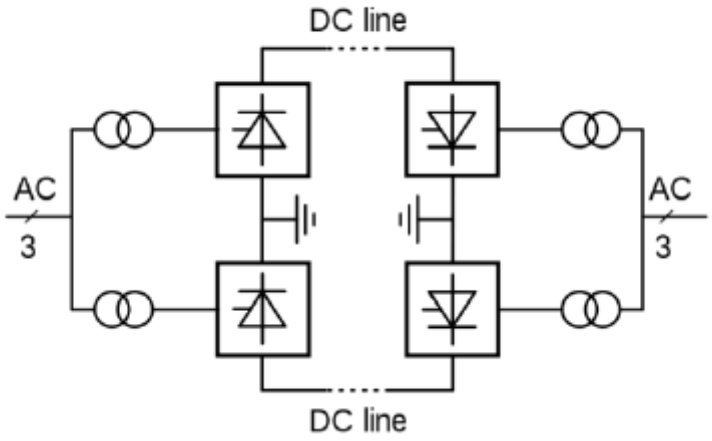

Figure 3.11: Bipolar System [8].

A Bipolar configuration, as seen in figure 3.11, makes use of two metallic conductors, these conductors carry current in opposite polarities [8]. Such a system has an advantage that in case of failure of one of the conductor, the system can keep functioning at half its capacity, but the extra line leads to added costs [8]. In [31], for the conversion of a 33 kV AC cable system for DC application, the use of a bipolar system is highlighted.

3.6. Failure Processes in DC

Failure of any system prevents it from providing the necessary functions expected. Cable systems, as previously mentioned, play a pivotal role in the power transmission and distribution architecture. The failure in cable systems would affect the reliability of the whole architecture as it takes days/weeks and in the case of subsea connection months to repair [58]. The importance of finding the root cause of failure can be understood as follows [59]:

- The knowledge of failure helps in identifying the root cause and thereby mitigating the issue for future cable systems.
- It helps in identifying the party who was responsible for the failure.
- The knowledge of the root cause helps in analysing scenarios of the failure in different circumstances and the safety hazards which would be part of it.

The significant causes of failure of medium voltage AC cable accessories and their visual indication during qualification testing are discussed in the Literature Review. As per [58], phenomena such as water treeing/ingress, thermo-electric ageing and extrinsic defects are the significant causes of insulation breakdown in cable systems under AC. The cable system part of our test object consists of both solid and liquid dielectric. The reasons for a breakdown in these individual dielectrics would be explained below as per [29].

3.6.1. Breakdown in Solid Dielectrics

In similarity to breakdown under AC, the major mechanisms for a breakdown under DC are intrinsic breakdown, thermal breakdown, breakdown due to discharges and also treeing.

Intrinsic Breakdown

Intrinsic breakdown strength of a material is the breakdown strength achieved when the effect of any external interference is nullified. These breakdown strengths are generally high and can be obtained in a lab environment only.

Thermal Breakdown

Thermal breakdown tends to take place in a dielectric if the heat removal from the dielectric by thermal conduction is slower than the heat generated. The heat generated here is owing to the leakage current and applied voltage. In [29], it is stated how under DC stress, thermal breakdown does not take place normally.

Treeing

Treeing is a phenomena owing to which field concentration takes place at the edge of a defect (sharp gap, sharp inclusion, protrusion) [29]. The phenomena of treeing take place at comparatively higher field strengths as per [29] when compared to AC.

Partial Discharge

Partial discharge phenomena in DC as per [40] does not have the same recurrence and magnitude when compared to what is witnessed in the AC condition. As per [29], the direct or indirect breakdown in DC owing to partial discharges is still a matter of question, but from the knowledge of tests, it is understood that this phenomena weakens the dielectric.

3.6.2. Breakdown in Liquid Dielectrics

Breakdown in liquids is not much different when comparing both AC and DC [29]. It is also stated in [29] that owing to the sensitivity towards dust in DC, the breakdown voltages obtained may be slightly lower than what is witnessed in AC.

Intrinsic Breakdown on Liquid

Intrinsic breakdown strength of a material is the breakdown strength achieved when the effect of any external interference is nullified [27]. These breakdown strengths are generally high and can be obtained in a lab environment only.

Polarization Phenomena

Insulation liquids such as oil even after undergoing multiple filtering processes may still have some minute particles left which would then coagulate to form larger particles [27]. These particles tend to move towards the area of higher field strength, and this process is not dependent on the potential at the electrode [27].

Particle Induced Breakdown

As mentioned Polarization Phenomena, the coagulated particles tend to move towards the area of higher field strength. The particle with higher permittivity would lead to a concentration in the field due to itself thereby attracting more particles and which in result would lead to a bridge formation across the two electrodes [27]. The formation of such a particle bridge affects the breakdown strength of the liquid greatly, the formation of such a particle bridge can be shown using the following figure:

Figure 3.12: Particles bridging the electrodes [27]

4

Finite Element Analysis

Finite Element Method (FEM) is used to understand the electric field distribution when taking into account complex constructions. Many software's are available today to simulate and understand the distribution of field in various geometries and out of these we make use of a software called COMSOL Multiphysics. COMSOL Multiphysics makes use of triangular elements to divide the area between the electrodes. The formation of these triangular elements is a process called meshing. The size of these elements is controlled to understand better the field distribution. A finer mesh is used in places where the field concentrates, and a coarser mesh is used in the other parts.

4.1. Material Analysis

In order to simulate the cross section of the joint show in figure 4.3 under DC stressing, conductivity of both joint and cable insulation needs to be made temperature and electric field dependent. The AC cable insulation is made of XLPE which is a type of polymeric insulation. In order to simulate under DC, as per [16], the conductivity of polymeric insulation can be defined by the following equation:

$$\sigma = \sigma_0 e^{\alpha(T-T_0)} e^{\gamma(E-E_0)} \tag{4.1}$$

In the above equation 4.1,

σ_0 = Conductivity at temperature T_0 and electric field strength E_0.

α = Temperature dependent coefficient of conductivity.

γ = Electric Field dependent coefficient of conductivity.

Liquid Lovisil is the silicon based dielectric joint insulation used by Lovink Enertech B.V. in their medium voltage AC joints. The liquid insulation tends to cure and solidify in the presence of moisture, and this behaviour is beneficial because once the outer layer solidifies, it prevents further ingress of moisture towards the core of the cable. In order to understand the behaviour of the system when stressed under DC, we make use of the FEM based software COMSOL Multiphysics. In order to simulate the liquid Lovisil in COMSOL Multiphysics, the conductivity of the liquid insulation needs to be both temperature and electric field dependent. This dependency on temperature and electric field in DC is because the field depends on the conductivity of the insulation where the conductivity has a dependence on both temperature and electric field. In [16] the conductivity measurement of the liquid silicon insulation is shown at a temperature of 20°C and 40°C. The conductivity measurement performed in [16] takes into account a set period of 24 hours in order to let the sample reach a steady state of conductivity. This is done in consideration to the ion drift process, which takes place in liquid dielectric because of which the initial conductivity values would be different from the conductivity values at a later stage [16].

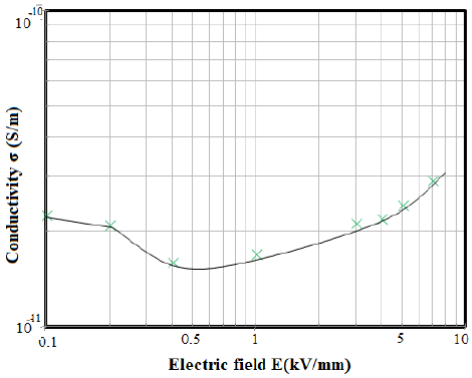

(a) Conductivity vs Electric field at 20°C

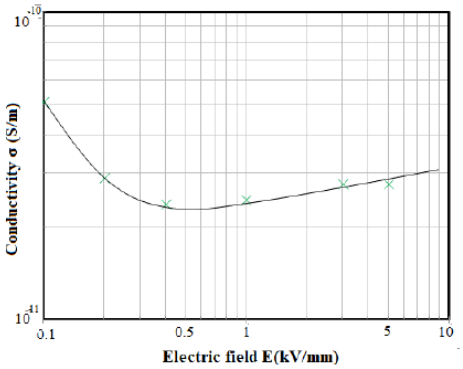

(b) Conductivity vs Electric field at 40°C

Figure 4.1: Conductivity vs Electric Field as per [16].

In the above sub-figure 4.1a the Conductivity (S/m) vs Electric Field (kV/mm) is given for a temperature of 20°C and 4.1b is for a temperature of 40°C. It can be also noticed that with the rise in temperature there is a definite rise in conductivity in the liquid dielectric. As previously mentioned, in order to understand how an MVAC accessory would behave under DC stress it needs to be initially simulated in COMSOL multiphysics. In this simulation the conductivity of dielectric need to be made both temperature and electric field dependent to understand how the electric field would distribute when considering DC. The change of conductivity with respect to both temperature and electric field is input to COMSOL as an equation. In order to construct this equation for liquid Lovisil we make use of the curve fitting tool in MATLAB. The curve shown in figure 4.1a is plotted in MATLAB and then utilizing the curve fit tool an exponential equation is made for the same.

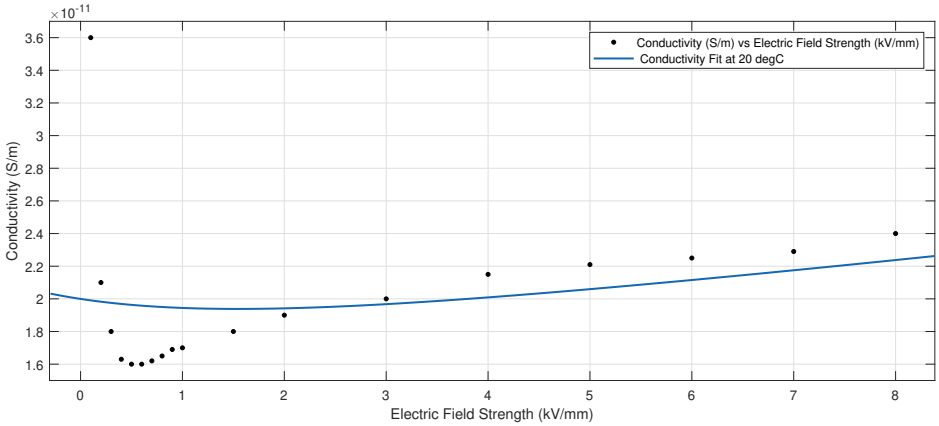

Figure 4.2: Curve Fitting of the conductivity curve

The exponential curve fit show in figure 4.2 provides an equation for the Electric Field vs Conductivity of the liquid dielectric at 20°C. The curve is extrapolated at lower field stress to assume a uniform trend as the curve at 40°C. The choice of exponential curve fit is with the aim to keep the number of coefficients to a minimum as the equation is to be further used as part of simulation in COMSOL Multiphysics. In order to make this equation work for other temperatures above 20°C, a factor of multiplication is computed in accordance with the change in conductivity with respect to temperature as seen in figures 4.1a, 4.1b. This factor of multiplication shifts the curve by 0.0725 for every increase of 1°C. The factor of multiplication when shifting the curve from 20°C to 40°C is 1.45, therefore for every increase of 1°C it is 0.0725. As the conductivity current measurement is only available for two temperature ranges which is 20°C and 40°C, it is assumed here that the same behavior would continue at higher temperatures.

The equation governing liquid Lovisil's behaviour with respect to conductivity can be seen as follows:

$$((a_1 * exp(b_1 * (ec.normE)) + c_1 * exp(d_1 * (ec.normE)) * (T - T_0) * 0.0725) \quad (4.2)$$

Here a_1, b_1, c_1 and d_1 as in the equation 4.2 are coefficients of the curve and their value as per curve fit performed in MATLAB can be given as follows:

- a_1 = $2.25e^{-12}$
- b_1 = -0.648
- c_1 = $1.775e^{-11}$
- d_1 = 0.02892

4.2. Field Simulations

The DC simulations were performed on the model created in COMSOL Multihpysics for the MVAC joint. The MVAC joint simulated here is a 12 kV joint of the M85 type manufactured at Lovink Enertech B.V. The respective material characteristics were entered into all the different domains in order to get the DC simulation result. The joint to be simulated can be seen as follows:

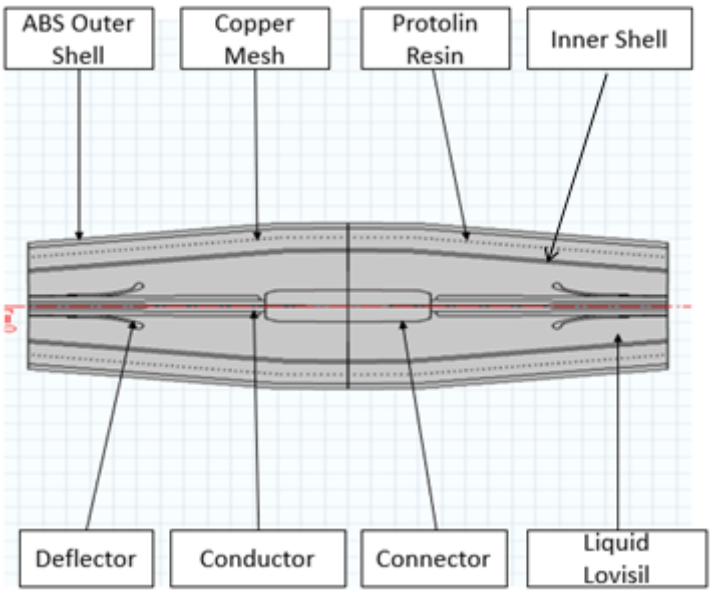

Figure 4.3: Cable joint model.

The choice of DC voltage to be applied to it is of importance. Peak AC voltage is considered safe DC voltage [17], therefore for our 12 kV AC joint, the safe DC voltage would be:

$$\text{Safe DC Voltage} = AC_{RMS} * \sqrt{2} = 12 * \sqrt{2} = 17\text{kV} \quad (4.3)$$

The electrical boundary condition (ground and high voltage) for the joint model can be seen as follows:

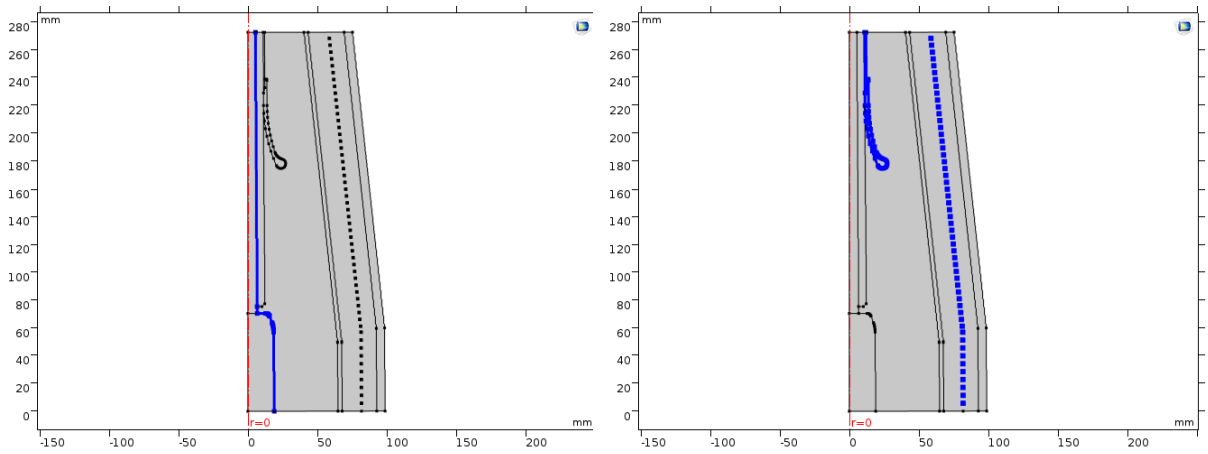

(a) High Voltage (b) Ground

Figure 4.4: Electric Boundary Conditions of the joint model used for simulation.

In addition to performing the simulation at 17 kV, the simulations would also be performed for a voltage of 26.5 kV which is the test voltage utilised in our modified test program. The selection of this test voltage would be further explained in section 5.4. The following images show the field simulations at three different cutlines, the cutlines are made on the following locations in the joint:

- Starting of the joint, near the field grading.
- Middle of the joint
- End of the joint, at the connector.

The field distribution in each of these cut-lines are shown below:

Near the Field Grading:

The cut-line is made such that it passes both the cable insulation which is made of XLPE and joint insulation which is made of liquid Lovisil and also through the field grading which is placed to mitigate field concentration owing to screen interruptions. The cut line passes through the triple point of all the three material with different material characteristics and is needed to see if any field concentrations are witnessed. The position of the cut line and the field distribution in the cutline is given as follows:

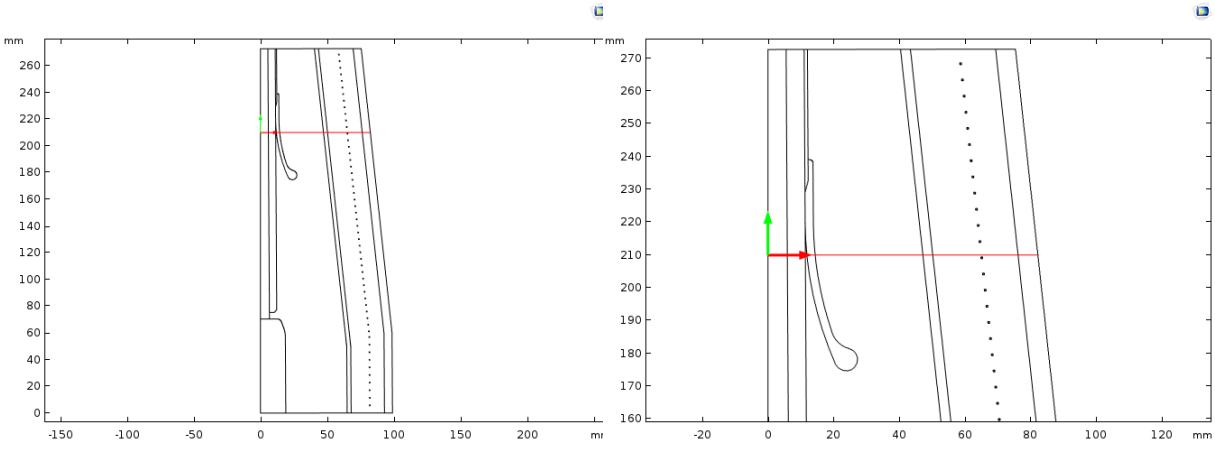

(a) Position of the cut-line in the joint (b) Zoomed in cross-section

Figure 4.5: Cut-line made near to the Field Grading

The electric field distribution at the cut line shown in figure 4.5 is given below:

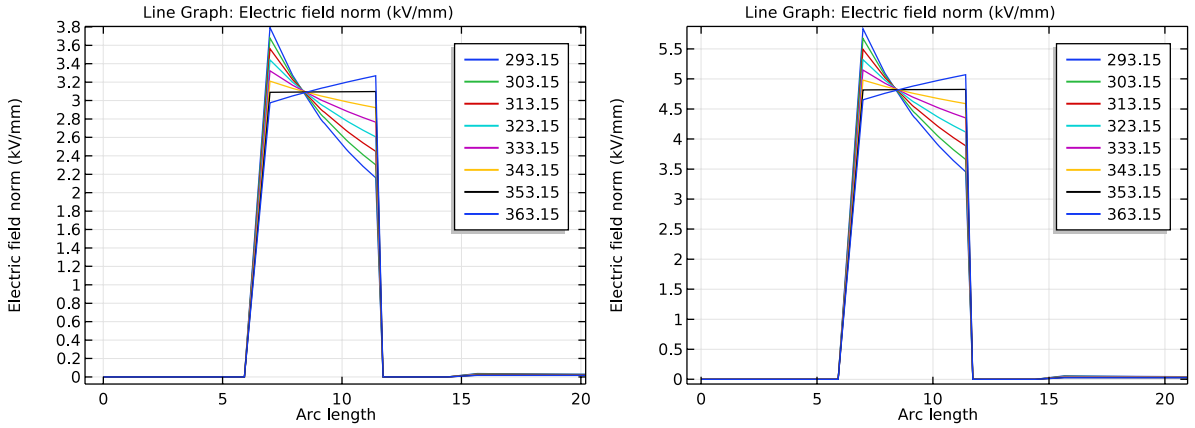

(a) Electric field distribution at 17 kV.

(b) Electric field distribution at 26.5 kV.

Figure 4.6: Electric Field distribution at 17 and 26.5 kV for different conductor temperatures.

In the above figure 4.6 the electric field distribution along the cut line given in figure 4.5 is witnessed. It can be seen from figure 4.6 that a definite field inversion takes place in the cable insulation (XLPE) with the rise in temperature. It can be seen that initially the maximum field strength is witnessed near the conductor and this maximum field strength shifts away from the conductor side to the sheath side in the XLPE layer at higher temperatures. The maximum field strength in the simulations at 17 kV and 26 kV are about 3.8 kV/mm and 5.6 kV/mm respectively. The electric field strength at the sheath side post field inversion does not exceed the maximum field strength seen at lower temperature gradient at the conductor side.

Middle of the Joint

The cut-line is made such that it passes both the cable insulation made of XLPE, joint insulation which is made of liquid Lovisil, inner shell made of polyester, polyurethane resin and the copper mesh. The interface between two different dielectrics is a critical area from electrical point of view as the material parameters at the interfaces changes considerably. This cut line is aimed at seeing what is the maximum field strength which would be witnessed at such an interface. The position of the cut line is given as follows:

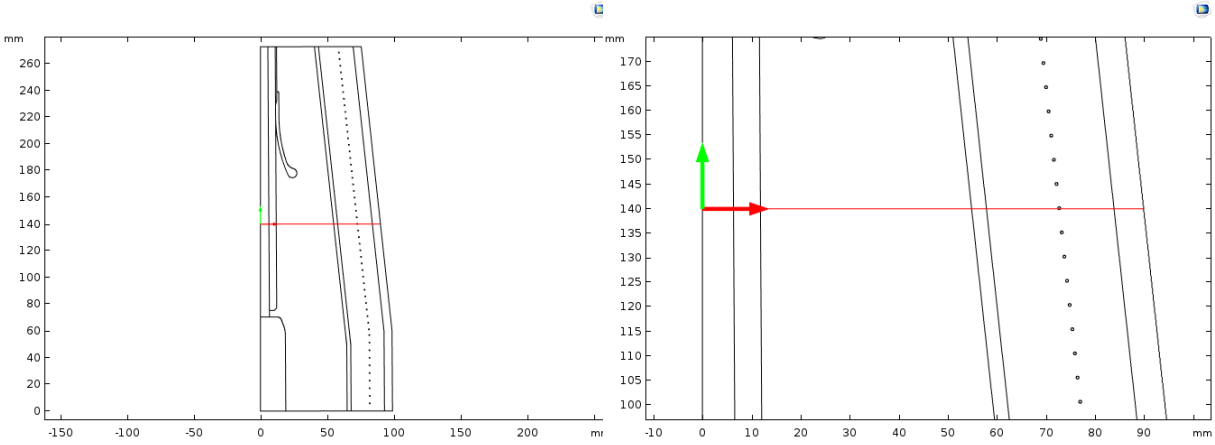

(a) Position of the cut-line in the joint

(b) Zoomed in cross-section

Figure 4.7: Cut-line made on Cable Insulation + Joint Insulation

The electric field distribution at the cut line shown in figure 4.7 is given below:

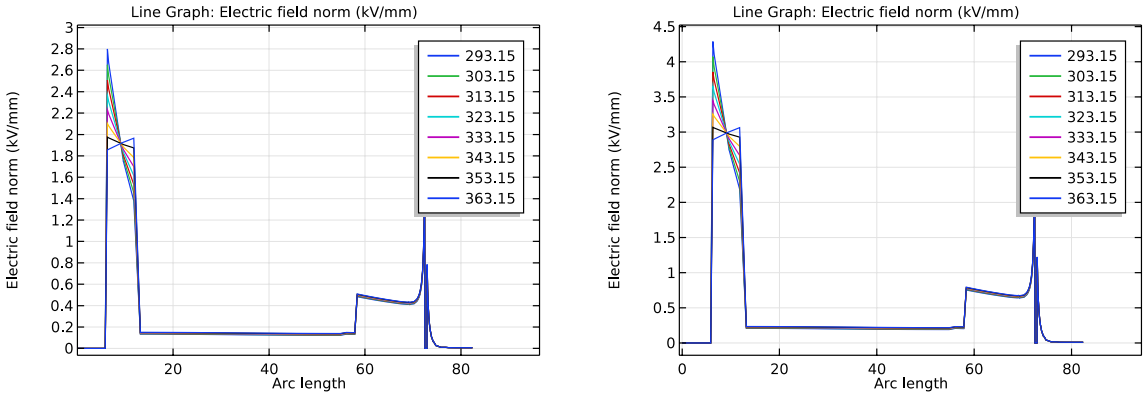

(a) Electric field distribution at 17 kV.

(b) Electric field distribution at 26.5 kV.

Figure 4.8: Electric Field distribution at 17 and 26.5 kV as per the cut line in the middle of the joint model for different conductor temperatures.

In the above figure 4.8 we notice that with the increase in temperature there is a definite field inversion taking place. The location of the field inversion when observed in the zoomed in cross-section as per figure 4.7b is in the the cable insulation (XLPE layer) inside the joint. The field here concentrates in the cable insulation and not in the joint insulation owing to the lower conductivity of the cable insulation layer. We also notice that in figures 4.8a, 4.8b that the maximum field strength is witnessed in the XLPE layer and it accounts to about 2.8 kV/mm and 4.3 kV/mm for 17 and 26.5 kV conditions respectively. The electric field drops to a low value of about 0.2 kV/mm in the liquid Lovisil layer and then rises as it enters the Protolin resin layer as this resin layer has a lower conductivity compared to the liquid Lovisil. Inside the resin layer the field strength gradually decreases across its length before taking a sharp increase and peaking in the periphery of the copper mesh. The peak field strength is a result of the field enhancement due to sharp edges in the copper mesh post which the field drops to a nil value inside the mesh. The electric field rises to a small value behind the mesh before dropping to zero.

End of the joint, at the Connector

The cut-line is made at the connector and passes through the liquid Lovisil, inner shell, copper mesh and polyurethane resin. This specific cut line helps in analysing the maximum field strength which may be witnessed inside the liquid Lovisil insulation at this area. The position of the cut line is given as follows:

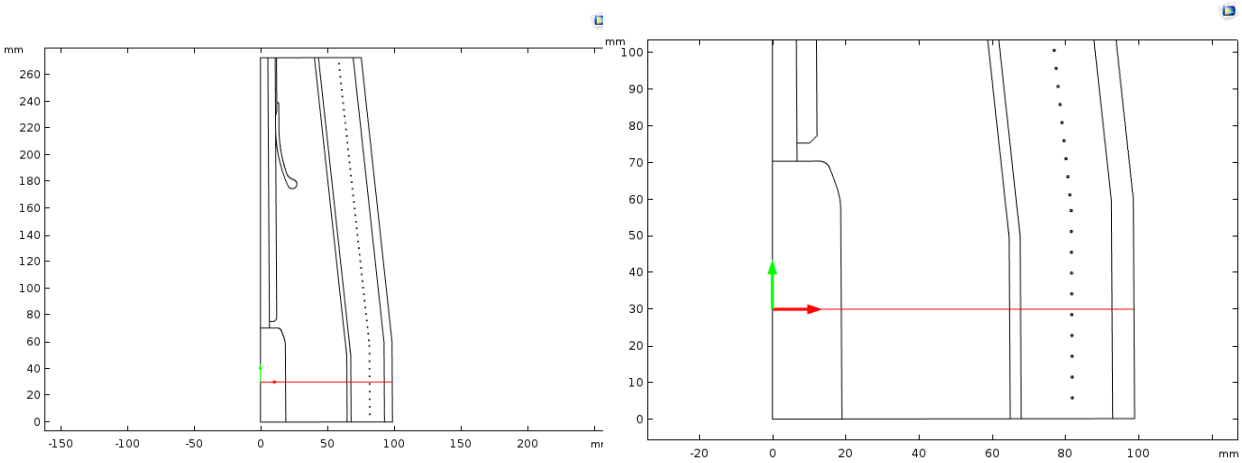

(a) Position of the cut-line in the joint

(b) Zoomed in cross-section

Figure 4.9: Cut-line made on Cable Connector + Joint Insulation

The electric field distribution at the cut line shown in figure 4.9 is given below:

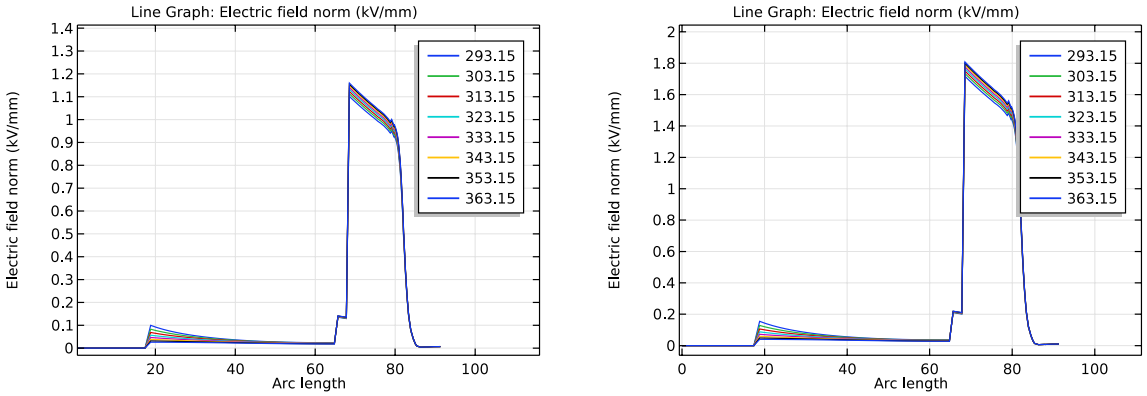

(a) Electric field distribution at 17 kV.

(b) Electric field distribution at 26.5 kV.

Figure 4.10: Electric Field distribution at 17 and 26.5 kV as per the cut line at the connector for different conductor temperatures.

In the above figure 4.10 we notice that for both cases of 17 kV and 26.5 kV given in figures 4.10a, 4.10b, the maximum field strength occurs in the Protolin resin accounting to about 1.1 and 1.8 kV/mm respectively. This is due to the same reason as explained earlier which is the lower conductivity of Protolin sees it experiencing higher field stress. It can be seen that the liquid dielectric insulation witnesses a very low electric field stress.

Electric Field Distribution

The knowledge of electric field distribution inside the joint model is important in understanding which location inside the joint are getting stressed under DC. The knowledge of such critical areas would help in making the necessary changes in design to mitigate the problem. The distribution of electric field inside the joint insulation is discussed below as three cases at conductor temperatures of 30°, 60° and 90° C for both voltage ranges ie 17 and 26.5 kV. The temperature at the joint body is realised from the measurement of joint thermal characteristics seen in section 6.4.3.

Case 1

The field distribution shown below shows the field strength witnessed in the joint model at a temperature of 30°C.

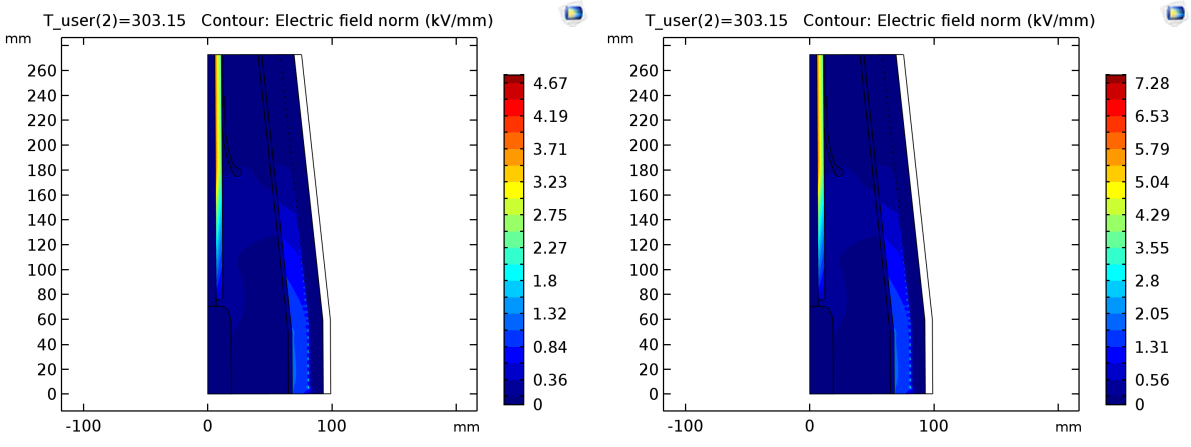

(a) Electric field distribution at 17 kV.

(b) Electric field distribution at 26.5 kV.

Figure 4.11: Electric Field distribution at 30°C for model with copper mesh.

In the above figure 4.11 we notice that at a temperature of 30°C for both cases (17 kV and 26.5 kV) the maximum field strength occurs at the copper mesh in the Protolin resin layer. The maximum field strength witnessed is about 4.67/7.28 kV/mm for the simulations at 17/26.5 kV respectively. The peak

field occurs in the periphery of the sharp edges of the copper mesh due to field enhancements. It can also be seen in figures 4.11a, 4.11b that the liquid Lovisil layer sees comparatively lower electric field strength compared to the XLPE and Protolin layer. The reason for this behavior is that in comparison to Protolin and XLPE, the liquid Lovisil is a more conductive material and electric field in DC moves to regions of lower conductivity. We also notice that in a case where we replace the copper mesh with a continuous copper strip, the field enhancement would be mitigated.

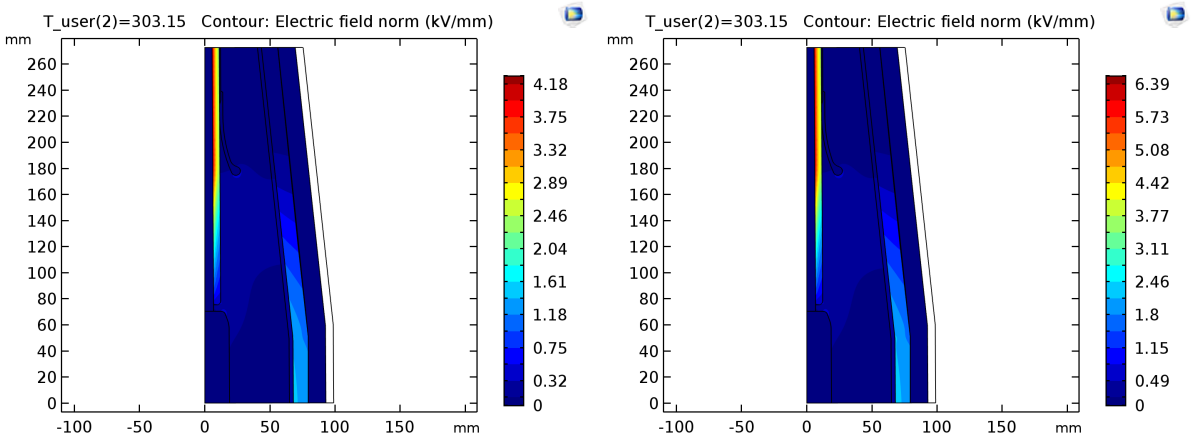

(a) Electric field distribution at 17 kV.

(b) Electric field distribution at 26.5 kV.

Figure 4.12: Electric Field distribution at 30°C for model with continuous copper strip.

In the above figure 4.12 we see the electric field strength for a joint model incorporating continuous copper strip instead of a copper mesh. It can be seen from that the maximum field strength for the model with a copper strip occurs in the XLPE layer. The maximum field strength witnessed for the cases with a potential of 17/26.5 kV is 4.18/6.39 kV/mm respectively. This is lower when compared to the simulations with a copper mesh shown in figure 4.11.

Case 2

The field distribution shown below shows the field strength witnessed in the joint model at a temperature of 60°C.

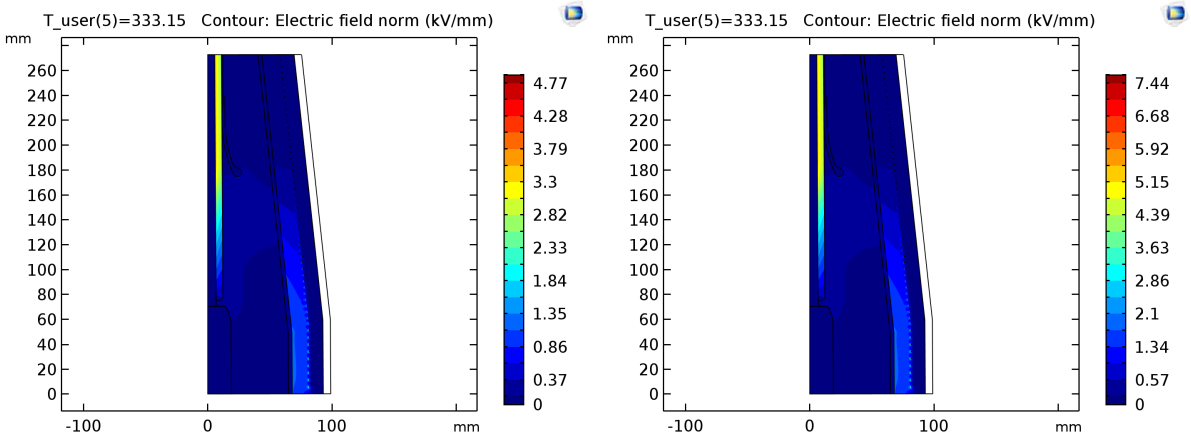

(a) Electric field distribution at 17 kV.

(b) Electric field distribution at 26.5 kV.

Figure 4.13: Electric Field distribution at 60°C for model with copper mesh.

In the above figure 4.13 we notice the same behavior as seen in figure 4.11. The field enhancement is witnessed at the periphery of the copper mesh in the Protolin layer at a temperature of 60°C. The

maximum field strength witnessed is about 4.77/7.44 kV/mm the simulations at 17/26.5 kV respectively. The difference when using a copper strip instead of copper mesh at 60°C can be given as follows:

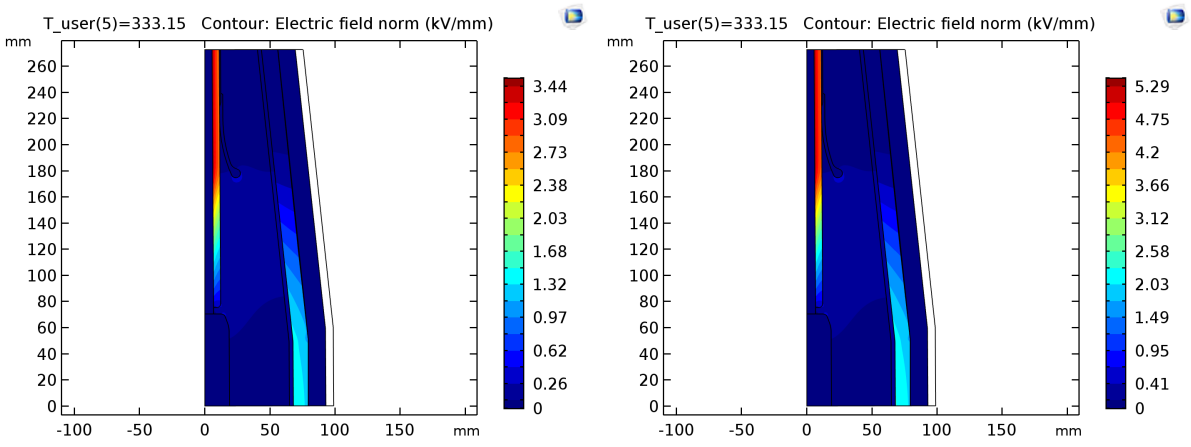

(a) Electric field distribution at 17 kV.

(b) Electric field distribution at 26.5 kV.

Figure 4.14: Electric Field distribution at 60°C for model with continuous copper strip.

The above figure 4.14 shows similar behavior to what is witnessed in 4.12. The maximum field strength is witnessed in the XLPE layer instead of the Protolin layer. This maximum strength is also lesser when compared to the case incorporating the copper mesh and it is 3.44/5.29 kV/mm for the potential of 17/26.5 kV respectively. The reduction in field strength at 60°C compared to the simulation for copper strip at 30°C is owing to the field inversion taking place inside the XLPE layer. The field inversion results in a drop in the peak field at the conductor side and shift of the the peak field towards the sheath.

Case 3

The field distribution shown below shows the field strength witnessed in the joint model at a temperature of 90°C.

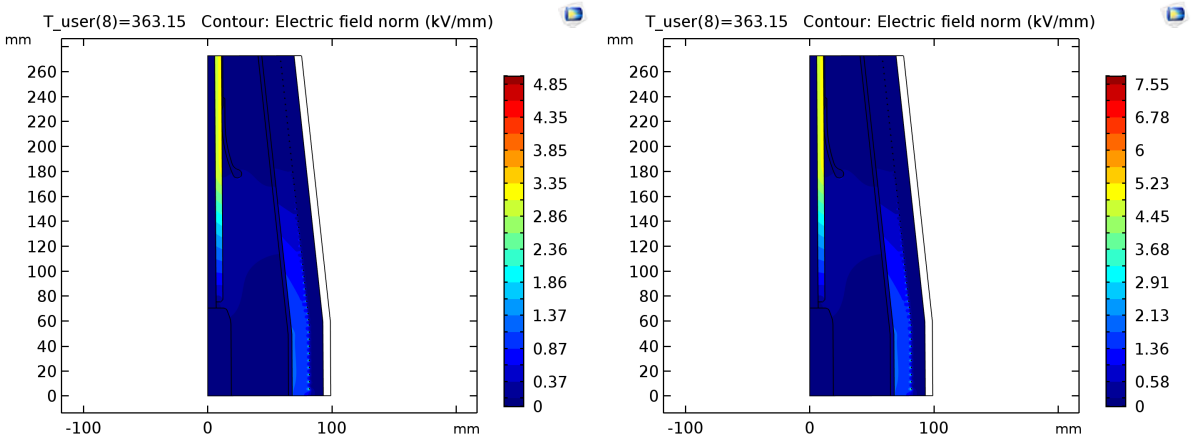

(a) Electric field distribution at 17 kV.

(b) Electric field distribution at 26.5 kV.

Figure 4.15: Electric Field distribution at 90°C for model with copper mesh.

In the above figure 4.15 we notice similar behavior to what is witnessed in previous cases in figures 4.11, 4.13. The maximum field strength witnessed is about 4.85/7.55 kV/mm for the simulations at 17/26.5 kV respectively. This value reduces when making use of a continuous copper strip instead of the copper mesh. The values of electric field strength when making use of a continuous copper strip, the value is about 3.28/5.09 kV/mm for the simulations at 17/26.5 kV respectively seen in figure 4.16. The drop in

peak field strength in figure 4.16 in comparison to figures 4.12 and 4.14 is owing to the field inversion phenomena taking place inside the XLPE layer.

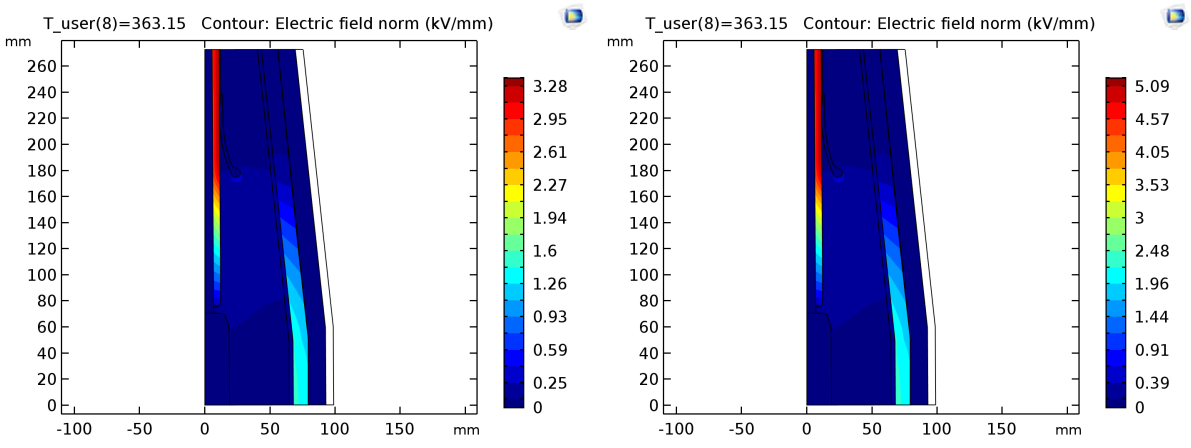

(a) Electric field distribution at 17 kV.

(b) Electric field distribution at 26.5 kV.

Figure 4.16: Electric Field distribution at 90°C for model with continuous copper strip.

4.3. Observations

- In the field distribution witnessed near the field grading as given in figures 4.6a and 4.6b we see that the maximum field strength is seen in the XLPE layer and this field strength is highest among all the three cut-lines.
- This maximum field strength witnessed in the XLPE layer is lower when compared to the DC breakdown strength of XLPE. The DC breakdown strength of AC XLPE is almost 60 kV/mm as per [41] which is way higher than the 3.8/5.6 kV/mm witnessed at both 17/26.5 kV respectively.
- It is stated in [55], [14] that the field inversion in DC would led to space charge build up which can then lead to critical field enhancement. As per our simulation we notice that the electric field doesn't rise to a critical value post field inversion, which thereby showcases that in medium voltage level the change in maximum field strength is not much when transitioning from no load to full load condition.

  This is similar to what is found in [17], the paper mentions how lower difference in max field stresses between no load and full load also results in lower concerns on the issues such as electric breakdown due to field inversion.
- As per field distribution seen in figures 4.6a, 4.6b, it can be seen that at a conductor temperature of 80°C there exists a uniform distribution of electric field across the cable insulation layer. This would thereby tends to stress the XLPE layer in a uniform manner rather than one end of the insulation getting excessively stressed in that particular location. This is of importance because as per the survey in [52], an operating temperature of 45°-60°C/75°-90°C is seen for URD (Underground Residential Distribution)/ feeder cable system respectively. These temperatures are in some cases lower or equal to the rated conductor temperature of the insulation.
- In the simulation as per the figure 4.8, in the presence of a sharp edge due to the copper mesh, the peak field occurs in the resin layer due to field enhancement at the copper mesh. This is in similarity to what is mentioned in [29], that in the presence of sharp defect in the insulation, a substantial field enhancement would be witnessed in the periphery of the defect. This field enhancement as per [29], may eventually lead to a breakdown.

  It is stated in [45], that metallic inclusions due to there lower thermal expansion coefficient when compared to surrounding material may lead to the formation of micro-voids in an already field enhanced location.

- In the simulations showcased for copper mesh at multiple conductor temperatures in figures 4.11, 4.13 and 4.15 we notice that the Protolin resin layer witnesses more field strength than the liquid Lovisil dielectric layer. The field tends to concentrate in the Protolin layer owing to its lower conductivity ($\approx 10^{-13}$ S/m).
- When making use of a continuous copper strip instead of a copper mesh, it was found that there was no more field enhancement in the Protolin layer. The max field in such a scenario as shown in figures 4.12, 4.14 and 4.16 took place in the cable insulation (XLPE).
- The AC breakdown strength of Protolin resin was found to be 9.9 kV/mm as per existing test report. It is stated in [31] that generally the breakdown strength of a insulating material is higher in DC in comparison to AC.

  The peak stresses witnessed in 4.11, 4.13 and 4.15 are lower than 9.9 kV/mm. Therefore the peak stresses are witnessed here are not critical to the Protolin layer.

4.4. Life Time Analysis

Insulation lifetime can be defined as the time duration under which owing to the application of multiple stresses a certain physical property important to the insulation behavior reaches its end of life [9]. Life models are used in order to understand the effect of these stresses on the insulation system, as per [33] these life models provide a correlation between the applied stresses and the insulation life. The major purpose of these life models are as follows [33]:

- Selection of proper cable insulation with respect to the applied stresses and tolerance.
- Selection of test voltage and test duration when performing tests such as the pre-qualification testing.
- The models can be used to estimate life time under operation.

The major stresses which are of importance when considering cable systems are as follows [33]:

- Mechanical Stress: Takes into account the mechanical activities (vibration, bending) which the cable system may endure during operation.
- Electrical Stress: This stress is present owing to the applied voltage.
- Environmental Stress: Takes into account the environmental conditions such as humidity and exposure to the ultra violet radiation.
- Thermal Stress: This stress is present owing to the heating and losses.

Electrical and Thermal stress are two of the most important stresses as they are elementary to cable design [33]. As per [39] these stresses (electrical and thermal) play major role in ageing and failure of the cable system. When considering life models to understand the effect of these stresses on the cable insulation, there are two general approaches [33]:

1. **Phenomenological models**: These model make use of ALT(Accelerated Life Testing) results and thereby understand the correlation of how the applied stress would impact the lifetime of the system.
2. **Physical life models**: These model state that prime reason of ageing is due the micro-defects present which undergo local degradation in a accelerated manner.

   The physical model are not discussed further as part of this study and [33] may be referred to understand more about these models. We would discuss the phenomenological models further as part of this thesis especially models concerning thermal stress, electrical stress and a combination of thermal and electrical stress.

Phenomenological models

The life models which are used for DC extruded cable system are derived from the models which are presently made into use for AC cable systems [33]. The models are derived such that we consider that the lifetime (L) of the insulation is affected by N different stress which do not change with respect to time.

$$L = L(S_1, ..., S_N)[33] \tag{4.4}$$

As part of this thesis based on the N stresses shown in equation 4.4, we would be mainly discussing electrical, thermal and a combination of both electrical and thermal the stresses.

Thermal Stress

As a part of early insulation design stated in [39], thermal stress were given high importance as the main objective was to send higher value of current and a comparatively smaller voltage value. This arrangement would in lower value of electrical stress [39]. In the equation 4.4 considering only thermal stress the value of parameters are therefore N=1 and S_1 = T' where T' is the thermal stress.

$$T' = \frac{1}{T_0} - \frac{1}{T}[33] \tag{4.5}$$

In the above equation 4.5, T represents the absolute temperature and T_0 represents the reference temperature [34].

The increase in temperature leads to the increase in chemical reaction such as oxidation in the insulation and also cross linking which leads to degradation [33], [39]. The model which is widely used to model thermal stress is the Arrhenius model and it can be expressed as follows [33]:

$$L(T) = L_0 exp[-B(\frac{1}{T_0} - \frac{1}{T})] = L_0 exp(-BT') \tag{4.6}$$

In the above equation 4.6:

- L_0: This is the life expected at the reference temperature T_0.
- T': Thermal stress as per equation 4.5.
- B = $\frac{\triangle W}{K_B}$
- $\triangle W$: Activation energy of thermal reaction. The sensitivity of the material in accordance to its rate of degradation in controlled by the activation energy [46].
- K_B: Boltzmann constant

Failure due to thermal ageing is characterised by the point after which any specific diagnostic property of the insulation reaches its limit value and post this point it tends to show dissatisfying behaviour [33].

Electrical Stress

If the only stress applied is voltage then in the equation 4.4, N=1 and S_1=E', here E' is the electrical stress which is the electric field strength present as a result of the applied voltage [33]. Inverse Power Model (IPM) as per [39] is widely used to model the lifetime insulation system when electrical stresses are concerned.

$$L(E) = L_0(\frac{E}{E_0})^{-n} \tag{4.7}$$

In the above equation 4.7

- L_0: This is the life expected at the reference electric field E_0.
- E_0: Reference electric field strength.
- E: Electric field strength at which the life of insulation is to be measured.
- n: Voltage endurance coefficient (VEC). Larger value of n indicates better endurance with respect to electrical stresses [39].

It is stated in [33] that Inverse Power Model is the most suitable model for the lifetime modelling owing to electrical stresses due to the following reasons:

- IPM finds wide application when considering high voltage DC cables of the extruded type. It is straightforward and thereby fits well when considering ALT for cables (AC and DC) of the extruded category.
- IPM is widely used as the international standard when undertaking life time modelling for high voltage DC cables of the extruded category.
- Theoretical and statistical reasoning as per the Weibull hypothesis forms the background of he model.

Electro-Thermal Stress

Electro-Thermal life modelling is considered when taking into account a multi stress condition where both thermal and electrical stress are acting on the insulation. Therefore in such a case when considering equation 4.4, N=2, and other parameters are $S_1 = E' = E$ and $S_2 = T'$ [33]. The life time is also represented as L(E,T) which can be seen as follows [33]:

$$L(E,T) = L_0(\frac{E}{E_0})^{-(n_0 - b_{ET}T')} exp(-BT') \tag{4.8}$$

In the above equation 4.8

- L_0: This is the life expected at the reference electric field E_0 and reference temperature T_0.
- E_0: Reference electric field strength.
- E: Electric field strength at which the life of insulation is to be measured.
- n_0: Voltage endurance coefficient (VEC).
- b_{ET}: Parameter of synergism between electrical and thermal stress.
- T': Thermal stress as per equation 4.5.
- B = $\frac{\Delta W}{K_B}$

The value of E and T in all life models discussed as per [33] is taken from the most stressed point inside the insulation. In the above equation 4.8, the term b_{ET} is of particular importance as the stress synergism factor sheds light on a point when multiple stresses act on the material and how it affects the ageing of the material in comparison to one stress alone [34]. In the absence of synergism and when stresses act independently, the ageing can be taken as the aggregate effect of stresses acting individually [34]. When the stresses are interacting with each a factor, a factor of synergism (K_S) can be defined as follows [34]:

$$K_S = \frac{L_{NS}}{L} = \frac{R(S_1, S_2, ..., S_N)}{\sum_{i=1}^{N} R_i} = \frac{1}{L[\sum_{i=1}^{N}(L_i)^{-1}]} \tag{4.9}$$

In the above equation 4.9:

- $R(S_1, S_2, ..., S_N)$: This is the ageing factor owing to multiple stresses.
- L_{NS}: Life without the effect of synergism.
- L: Life when under the interaction of multiple stresses.
- L_i: Life in the presence of on the i_{th} stress.

In the equation 4.9 when only considering two stresses, the equation can be rewritten as follows:

$$K_S = \frac{R(S_1, S_2)}{R(S_1) + R(S_2)} = \frac{R(S_1, S_2)}{R(S_2)[1 + \frac{R(S_1)}{R(S_2)}]} \tag{4.10}$$

The equation 4.10 shown above can be used to calculate the synergism factor given in the equation 4.8. In the above equation 4.10 when considering electro-thermal stress the two stress are electrical stress due to the applied voltage and thermal stress due to temperature. In the absence of synergism ($S_1 = 0$ or $S_2 = 0$), the above equation 4.10, the value of K_S = 1 [34]. When one stress dominates the other ($S_1 \gg S_2$ or $S_2 \gg S_1$), in such as case also as per [34] the value of synergism factor $K_S \approx 1$. When one of the stress in constant and other rises the value of K_S rises too and reaches a peak value beyond which it decreases as the condition of $S_2 \gg S_1$ or vice versa is achieved. In our case for DC application under a combination of electro-thermal stress we take the synergism factor as one.

In AC condition the field depends on the permittivity of the material which does not have a strong dependence on temperature [55]. As per [32], in HVAC cable insulation the highest stresses are owing to the temperature (joule losses and dielectric losses) and also the electric stress from voltage. These stresses occur at the interface of the conductor and insulation and the maximum electric stress would remain constant but the thermal stress would vary with the temperature change [32]. In contrast to this in DC the maximum field strength shifts due to the presence of a temperature gradient from the conductor to the sheath. In our simulations as observed in figures 4.11, 4.13 and 4.15, it is observed that the most stressed point lies in the resin layer at the periphery of the copper mesh. The maximum stress occurs due to the lower conductivity of resin layer in combination with the presence of sharp edges due to the copper mesh.

In the equation 4.8, the value of E_0 and T_0 are taken for condition such that L_0=$L(E$=E_0, T=$T_0)$ [33]. Here E_0 is the reference electric field while T_0 is the rated temperature of the insulation [33].

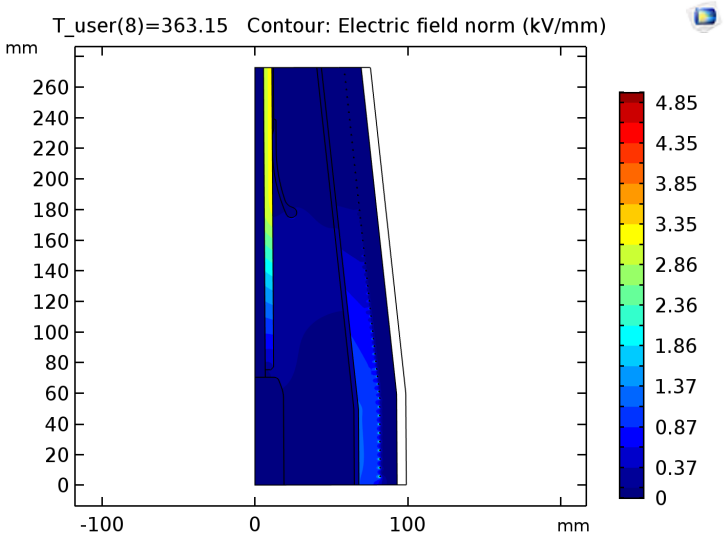

Figure 4.17: DC field distribution at rated voltage.

As per figure 4.17, the value of E_0 and T_0 is as follows:

- E_0 = 4.85 kV/mm
- T_0 = 363.15 K

The same model is simulated at higher stresses by applying a voltage of 26.5 kV. It is observed that the max field concentration occurs at the periphery of the copper mesh at a temperature of 363.15 K. As per equation 4.8, the value of E and T are taken at the most stressed point in the insulation. In figure 4.18, the value of E and T is as follows:

- E = 7.55 kV/mm
- T = 310.88 K

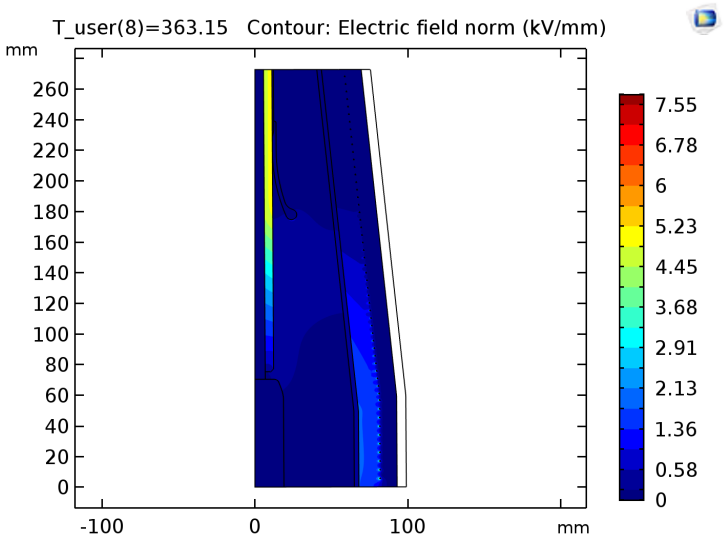

Figure 4.18: DC field distribution at elevated voltage.

In the equation 4.8, the value of B is given as follows:

$$B = \frac{\Delta W}{K_B} \tag{4.11}$$

Where,

- K_B : Boltzmann constant ($8.314 * 10^{-3}$ $[\frac{kJ}{mol.K}]$)
- ΔW: Activation energy $[\frac{kJ}{mol}]$

As per [33], a larger value of B would result in better performance of the material against thermal ageing. As seen in figure 4.18, the maximum stress occurs in the resin layer and therefore the activation energy of the resin layer needs to used in the calculation as per equation 4.8. The limitation in time restricted in calculating the activation energy of the Protolin resin and therefore the activation energy of a polyurethane resin used in electrical insulation is used for the lifetime calculation. In [44], activation energy for castor oil based polyurethanes used as insulators in electrical industry is discussed. Activation energy of castor oil based polyurethane adhesives with the ratio of NCO/OH as 1.5 is provided as 40.64 kJ/mol in [44] which is made use as part of the life time calculation.

```
n=13;
L0=40;
T0 = 363.15;          %Rated temperature of the insulation.
T = 310.88;           %Absolute temperature.
Tf = (1/T0-1/T);      %Thermal stress.
B_et = 1;             %Coefficient of synergism.
E0 = 4.85;            %Reference electric field strength.
E = 7.55;             %Electric field strength at elavated voltage.
Ef = log(E/E0);       %Electrical Stress
k = 8.314*10^-3;      %Boltzman constant [kJ/mol*K]
W = 40.64 ;           %Activation energy [kJ/mol]
B = (W/k);
L = L0*exp(-B*Tf)*(E/E0)^(-(n-B_et*Tf))
```

Substituting all the necessary values in equation 4.8 as show in the MATLAB script above, a life **(L) = 1.2 years** is obtained for the design life (L_0) = 40 years. It is assumed here that all the materials which are part of the joint assembly have a design life of 40 years. The end of the design life of the polyurethane resin may or may not cause the immediate breakdown of the joint as the liquid insulation dielectric is

separated by a polyester inner shell. In the longer run the end of life of the polyurethane resin may lead to the failure of the whole system.

5

Pre-Qualification Testing

A cable system would typically consist of a cable with accessories such as joints and terminations. There can be other accessories also which may form part of the cable system and which could be used for purposes such as measurement. A cable system is an essential part of the transmission and distribution network as it is responsible for the transfer of power from the generating point to the consumer.

Therefore, this makes it more and more critical to ensure that these cable systems work in the field for there desired lifetime and do not succumb to failure [58]. As per [58], the failure of cable system takes along time to repair which may go up to years for sub-sea connection. Reducing the investment cost and at the same time, providing a reliable power supply is very important in the present market scenario [48].

5.1. Pre-Qualification Testing

Pre-Qualification testing is a series of tests which performed on a cable system in order to ensure its long time performance in the field [3]. The pre-qualification tests also help in analysing the integrity of the insulation concerning conditions it may encounter during service [35].

The pre-qualification testing is undertaken once and repeated only for a drastic change in the construction such as design, stress (electrical) or the material of the system [3]. It needs to be analysed how these changes would affect the overall performance of cable system [3].

5.2. PQ for HVDC

The Pre-Qualification test for High Voltage DC cable systems up to 500 kV are done with respect to the document CIGRE TB 496 ”Recommendations for Testing DC Extruded Cable Systems for Power Transmission at a Rated Voltage up to 500 kV” [3].

As per [3], the test object is made to pass through a sequence of tests in the following order:

1. Long-Duration Voltage Tests
2. Superimposed impulse voltage test
3. Examination

5.2.1. Long Duration Voltage test

The long duration tests consist of a series of test taking place over 360 days. The temperature requirements as per standards are met for the temperature of the conductor and that across the sheath.

As per [3], different test sequences are recommended for the testing system based on LCC (Line Commuted Converter) or VSC (Voltage Source Converter) technology. A brief introduction of both the systems is given in the following paragraphs:

LCC: Line Commuted Converter or LCC is a type of converter system in which the bidirectional flow of power is attained by performing polarity reversal on the voltage [3]. LCC makes use of a thyristor based system for its operation, during power reversal the current flow remains in the same direction but the voltage polarity is reversed at both the stations [43]. These system in regards to there high reliability and low maintenance are widely popular [43].

The pre-qualification test sequence for a LCC bases system is given in [3] as follows:

Test	Number of Cycles	Test Voltage	Polarity
Load Cycle (LC)	30	V_{TP1}	+
Load Cycle (LC)	30	V_{TP1}	-
Load Cycle + Polarity Reversal (LC+PR)	20	V_{TP2}	
High Load (HL)	40	V_{TP1}	+
High Load (HL)	40	V_{TP1}	-
Zero Load (ZL)	120	V_{TP1}	-
Load Cycle (LC)	30	V_{TP1}	+
Load Cycle (LC)	30	V_{TP1}	-
Load Cycle + Polarity Reversal (LC+PR)	20	V_{TP2}	

Table 5.1: Test Sequence for LCC based systems [3].

VSC: Voltage Source Converter is a type of converter system which make use of IGBT (Insulated Gate Bipolar Transistor) Technology [43]. VSC system in order to attain bidirectional flow of power there is no requirement of change in polarity of the voltage [3]. In an urban power network as per [43], VSC based system adds flexibility owing to its ability to control both active and reactive power.

The pre-qualification test sequence for a VSC bases system is given in [3] as follows:

Test	Number of Cycles	Test Voltage	Polarity
Load Cycle (LC)	40	V_{TP1}	+
Load Cycle (LC)	40	V_{TP1}	-
High Load (HL)	40	V_{TP1}	+
High Load (HL)	40	V_{TP1}	-
Zero Load (ZL)	120	V_{TP1}	-
Load Cycle (LC)	40	V_{TP1}	+
Load Cycle (LC)	40	V_{TP1}	-

Table 5.2: Test Sequence for VSC based systems [3].

On observing the test sequences as per tables 5.1, 5.2 it is found that for the LCC based system, there is an additional polarity reversal test. As previously mentioned in the definition of line commuted converter system, the system undertakes polarity reversal to attain bidirectional flow of power. This polarity reversal is an additional stress on the system, and therefore, its effect needs to be tested as part of the testing sequence.

The tests mentioned in the tables 5.1, 5.2 are elaborated as follows based on [3]:

- **Load Cycle (LC):** Load cycle consist of the cable system being subjected to voltage application in combination with heating cycles. The heating cycles consist of a 8 hour period under the application of heating current post which the system is left for 16 hours to cool naturally. The choice of heating current can be either alternating or direct in nature. The voltage/current application mimics electrical/thermal stressing of the system, and these tests tend to replicate the stresses the cable system may experience during service [35].
- **Zero Load (ZL):** Zero load test consists of a constant voltage application, and it doesn't require the application of heating current.
- **High Load (HL):** High load test incorporates voltage application with a constant application of heating current throughout the test period.

The following temperature requirements should be satisfied as per [3] while performing tests which includes the use of heating cycles:

- $T_{cond,max}$: The maximum operational conductor temperature of the cable.

  As part of the load cycle test, $T_{cond,max}$ should be achieved for a minimum period of two hours in the eight hours under heating current application.
- ΔT_{max}: This is the maximum operational temperature gradient over the insulation layer in the absence of the semi-conductive screens.

The test voltages mentioned in both previous tables 5.1, 5.2 are elaborated as follows based on [3]:

- V_0: Rated DC voltage between conductor and earth screen for which the cable and accessories are defined.
- V_{TP1}: DC voltage to be used when performing load cycle, high load, zero load tests as part of the pre-qualification test procedure.

In tables 5.1 and 5.2 the number of cycles to be performed as part of each test is present. Every cycle is a period of 24 hours, and the cycle incorporates heating current application. These 24 hours would be divided into 8 hours of heating and 16 hours of cooling. While conducting these tests, it should be ensured that the test objects reaches the DC field distribution. This wait for reaching DC field distribution is because as mentioned in [3], the field distribution in DC is different from what it is in AC and depends on conductivity (σ) which has a high dependency on temperature and the electric field. The temperature is highest at the conductor and decreases towards the sheath, this causes a divergence [3]. A parameter t/τ is utilised to represent the aforementioned divergence. A value of 10 τ (10×time constant) needs to be attained to achieve the required DC distribution [3].

5.2.2. Superimposed Voltage Test:

A superimposed voltage test is performed post the series of test mentioned above in 5.2.1. The superimposed voltage test is conducted as a part of the pre-qualification test to ensure that the integrity of the insulation is maintained after performing the long duration test [3]. The test does not indicate the tolerance of test object to lightning impulses of a certain level [3]. The limitation in the test setup prevented us in including this test as part of the test program.

5.2.3. Examination

In the examination phase of the pre-qualification testing, the cable is dissected, and the accessories are dismantled. These examination steps would help to observe any anomalies such as degradation or deterioration, which would affect the performance of the system [3].

5.3. Test Program for MVAC

The testing for MVAC cable system is governed by [4] which is the standard known as NEN-HD 629-1 S3 for the ”Test requirements for accessories for use on power cables of rated voltage from 3.6/6(7.2) kV up to 20.8/36(42) kV - Part 1: Accessories for cables with extruded insulation”. These test qualify the following accessories for their use on the extruded power cables:

- Terminations (Indoor/Outdoor), Terminal Boxes
- Joints (Straight, Branch, Loop and Stop-ends) designed for indoor use or outdoor/underground use.
- Connectors (Screen/Unscreened-type, Bolted-type, Seperable-type)

The tests mentioned in [4] can be understood from the following table:

Test	Magnitude	Time	Expected Outcome
AC Voltage Withstand Dry	$4.5V_0$	5 minutes	No Breakdown or Flashover
Partial Discharge at Ambient Temperature	$2V_0$	-	A Maximum of 10 pC
Impulse Voltage at Elevated Temperature	10 impulses of each polarity	-	No Breakdown
Heating Cycle Voltage in Air	$2.5V_0$	63 cycles	No Breakdown
Heating Cycle Voltage in Water	$2.5V_0$	54 cycles	No Breakdown
Partial Discharge at Elevated and Ambient Temperature	$2V_0$	-	A Maximum of 10 pC
Impulse Voltage at ambient Temperature	10 impulses of each polarity	-	No Breakdown
AC Voltage Withstand Dry	$4.5V_0$	5 minutes	No Breakdown or Flashover
Partial Discharge at Ambient Temperature	$2V_0$	-	A Maximum of 10 pC

Table 5.3: Test Program as per NEN-HD 629-1 S3.

In the above table 5.3 the test procedure for the MVAC system as per the NEN-HD 629-1 S3 standard is found. The standard has separate test sequences for accessories, an amalgamation of the common tests are seen as per table 5.3. These tests are defined for both extruded and paper insulated cables. All the tests which are mentioned in table 5.3 are tested as per the test clauses stated in EN 61442: 2005 which is the standard known as ”Test methods for accessories for power cables with rated voltages from 6 kV (V_m=7.2 kV) up to 36 kV (V_m=42 kV) [1].

AC Voltage Withstand Dry

AC voltage withstand dry test is tested as per Clause 4 of EN 61442:2005. The test setup is prepared and it is ensured that that the accessories are free from moisture and dust prior to application of the test voltage. The standard states the method for the application of voltage should be as per the section 6 of IEC 60060-1 which is the standard for ”High Voltage Test Techniques - Part 1: General definitions and test requirements” [2]. The standard [2] suggests the following procedure for the application of voltage:

- The test voltage value used should be the root mean square voltage.
- The alternating test voltage is desired to be in the frequency range of 45-60 Hz. The desired voltage should have not more than 2% deviation between the peaks on either side.

- In test spanning less than 60 seconds, the voltage tolerance should be ±1%, and in the case for tests longer than 60 seconds, the voltage should be maintained within ±3% of the test voltage value.
- As per [2], the generation of the test voltage is via a transformer arrangement or by the utilisation of an series/parallel resonant circuit.
- Test Procedure:
    1. Initially the voltage application is started at a lower value in order to prevent disturbances (switching transients).
    2. The voltage should be raised with a per second rise of 2% of V. Once the voltage application crosses 75% of the applied value it is maintained for a pre-defined duration (one minute) after which it is decreased in a rapid fashion.
    3. The test object passes the test in the absence of any unruly discharge.

Partial Discharge at Elevated and Ambient Temperature

The tests for Partial Discharge at Ambient Temperature are performed as per Test clause 7 of EN 61442: 2005. The method for performing these tests are given as per the following IEC standards, which are IEC 60270 and IEC 60885-3.

When performing the tests at elevated temperature, it is ensured that the required connections are made for the supply of heating current. The conductor thermal requirements are almost similar to as previously mentioned in section 5.2. The difference lies in the duration of the heating cycle, a total period of 8 hours is seen in contrast to the 24 hours in [3]. The heating cycle as per [1] is shown below:

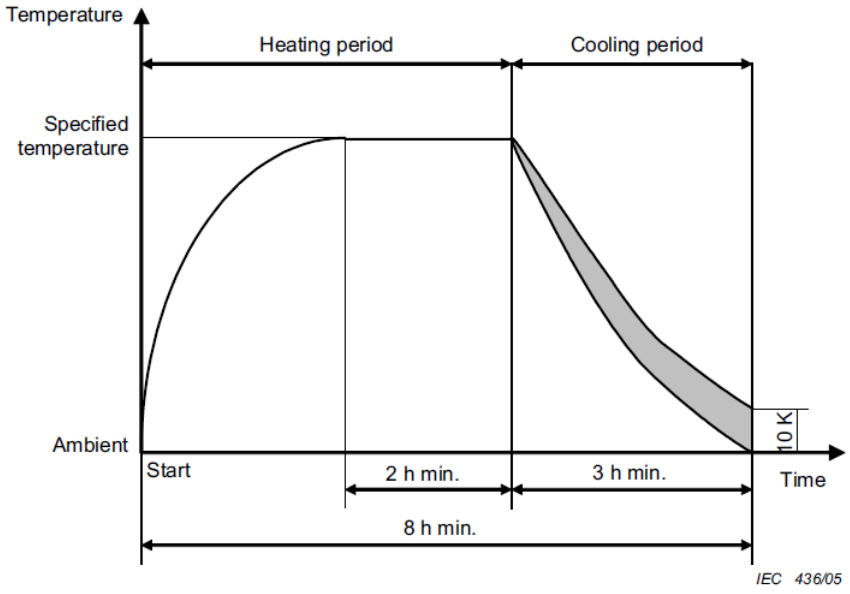

Figure 5.1: Heating cycle for tests at elevated temperature [1].

Impulse Test at Elevated and Ambient Temperature

Impulse Test at Elevated and Ambient Temperature is as per test clause 6 of the EN 61442: 2005. The clause also highlights that when testing three core accessories, it is ensured that at a certain point in time only one of the core is tested while other two cores should remain earthed. The method of performing these tests are as per the standard IEC 60230.

When testing at elevated temperature, we should ensure the following requirements:

- A cable core temperature of 5-10 K higher than the maximum core temperature should be attained and stabilized for 2 hours minimum during the heating phase for extruded cables.

- Similarly, a temperature of 0-5 K higher than the maximum core temperature should be attained and stabilized for 2 hours minimum during the heating phase for paper cables.

Heating Cycle Voltage Test in Air and Water

Heating Cycle Voltage test in air and water is as per clause 9 of the EN 61442:2005. When performing the Heating Cycle Voltage Test, the elevated temperature requirements mentioned previously for Impulse testing and as shown in figure 5.1 should be ensured. When testing in the air, the test object undergoes the aforementioned test cycles in combination with the application of the required voltage. When performing the test in water, the accessories under test should be immersed in water at room temperature to a height of 1.00+0.02m.

5.4. Modified Test Program

The test program mentioned in tables 5.1, 5.2 given by [3] is for the testing of DC cable systems up to 500 kV. This voltage range incorporates the medium voltage DC cable system also, and therefore naturally the question arises on the requirement of a separate test procedure for MVDC cable systems. It needs to be understood there are some significant differences between the cable systems used for both HVDC and MVDC application even when they share similarities at the design level, this can be seen as follows:

Paramater	**MVDC cable system**	**HVDC cable system**
Rated Voltage	10 - 50 kV	80 - 525 (640) kV
Conductor Cross-Section	95-630 mm^2	up to 3000 mm^2
Insulation Thickness	3.4, 5.5, 8.0 mm (based on MVAC cables)	5.5 - 26 mm
Mean Electric Stress	10 kV/mm	20 kV/mm
Insulation Material	XLPE	PE, XLPE, PP
Converter Technology	LCC, VSC	VSC

Table 5.4: Comparison of HVDC and MVDC cable systems [14]

It can be seen in the table 5.4 that the electric stress in medium voltage cable system is half of its high voltage counterparts, this reduction in the field stress is an important factor when considering space charge [14]. Given the difference between HVDC and MVDC cable system, the requirement for a modified test program is highlighted. As part of our research, we are looking at possibility of using MVAC cable system for DC application. The reason for finding the possibility of using MVAC cables for DC application is the availability of standard quality assurance methods and the presence of a stable supply chain [14]. The test voltages and test duration would be changed accordingly for the modified test program. The modified test program which is prepared for testing our test object show in section 6.1 can be understood as per the following table:

Test	Test Voltage (kV)	Duration (Days)	Polarity
Load Cycle (LC)	26.5	5	+
Load Cycle (LC)	26.5	5	-
High Load (HL)	26.5	5	+
High Load (HL)	26.5	5	-
Zero Load (ZL)	26.5	15	-
Load Cycle (LC)	26.5	5	+
Load Cycle (LC)	26.5	5	-

Table 5.5: Modified Test Program.

The modified test program is shown as in table 5.5, this test program is utilised for the testing of our medium voltage AC cable system under DC stress owing to the absence of a standard testing program. The voltages which are utilised here for testing as part of the modified testing program is 26.5 kV which is 1.56 times the DC safe voltage of 17 kV as per equation 4.3. The steps to the selection of the 1.56 test factor are explained below. The following points should be kept in consideration when performing the tests:

- The DC voltage is kept constant throughout all the tests only the polarity is reversed as per the test requirements.
- The test object is subjected to heating current for 8 hours and then allowed to naturally cool down for 16 hours during LC (Load Cycle) tests.
- In tests involving heating current, a temperature more than max conductor temperature and max sheath temperature is obtained for a minimum of 2 hours during the heating cycle.
- In between tests, the test object is rested for 24 hours with the presence of only heating current.

This test program in table 5.5 is motivated by referring to ”Recommendations for testing DC extruded cable systems for power transmission at rated voltage up to 500 kV” by the CIGRE Working Group 1.32 given in the CIGRE Test Brochure 496. In combination to that the testing procedures for MVAC cable accessories given as ”NEN-HD 629-1 S3, ”Test requirements for accessories for use on power cables of rated voltage from 3.6/6(7.2)kV up to 20.8/36(42)kV-Part 1: Accessories for cables with extruded insulation” is also referred.

The modified test program given in table 5.5 is similar to the test program as per table 5.2 given as per CIGRE TB 496. The decision to exclude polarity reversal test as seen in table 5.1 is on the assumption that the future distribution network would make use of modern voltage source converters that do not require polarity reversal for bidirectional flow of power. As these VSC based systems do not face voltage reversal and therefore, the test object needs not to be tested for its performance under the same. It is mentioned in [55], how an increase in usage of XLPE cables has been seen as the modern VSC based systems do not undergo polarity reversal for the bidirectional flow of power. This increasing trend is taken into account when selecting a test program which does not include polarity reversal tests.

When comparing the test program in table 5.5 to the test program for MVAC accessories given in table 5.3 under section 5.3 we see that the partial discharge tests are not undertaken for DC. Partial Discharges in AC or DC is a representation of the performance of the insulation [50]. The decision was made not to consider the partial discharge tests when testing an MVAC system under DC stress because as per [40], partial discharge has very less magnitude and does not have the same recurrence in DC to what seen in for the AC conditions. In [50] it is mentioned that the partial discharge rate in DC depends on the τ on the insulation, which depends on material characteristics while in AC the partial discharge has a dependence on the $\frac{dv}{dt}$. The dependence of τ is important as the value of τ is magnitudes higher than the value which would provide similar partial discharge recurrence rate as what is seen for AC [50], [19]. We also consider the fact that the partial discharge inception voltage is higher for DC when compared to AC [40], [17].

AC voltage withstand dry as per table 5.3 for the testing of MVAC accessory is similar to the zero load test in the test for HVDC cable system and the testing of MVAC cable system under DC stress as per

out test program in table 5.5. The variation lies in the duration of the tests and the method of voltage application. Heating cycle voltage in air test as per the table 5.3 is similar to the Load Cycle test in the test for HVDC cable with the difference lying in the duration of the heating cycle and the number of test cycles. The test factor is different in the test cases as it depends on the selection of test duration and life constant value. The selection of these constants in deducing the parameters for the modified test program is explained below.

Test voltages here can be understood as given in section 6.2, the value of n was selected as 13 and the testing duration was taken to be 45 days. These change in values would have a effect on value of multiplying factor K_1. The value of K_1 when calculated now is as follows:

$$K_1 = \sqrt[13]{\frac{40 \times 365}{45}} = 1.56 \tag{5.1}$$

Therefore the test voltage for our modified test program would be obtained as follows:

$$\text{AC Peak Voltage} \times 1.56 = 17 \times 1.56 = 26.5\text{kV} \tag{5.2}$$

The selection of the test duration, which is 45 days here is different from the 360 days mentioned by CIGRE work group in [3]. The selection of n is also different from what is suggested as n = 10 by CIGRE in [3] which they mention is selected in conservative manner. In [28], it is stated that defects such as treeing may cause a breakdown in the long term at the operating voltage. At elevated voltages these defects may lead to a breakdown in a matter of hours to minutes, the author mentions how as per inverse power law the life of a test object varies inversely to the electric field (E) applied raised to a power n. This behaviour is given as the following equation as in [28] :

$$L = \frac{c}{E^n} \tag{5.3}$$

It should be noted here that the equation 5.3 is similar to the equation used by the committee in [3] to calculate the voltage factor for their tests. As per [28], the value of n ranges between 9 to 12 and the voltage life (L) depends on the size of the defect. Thereby, it is understood that for a larger defect the voltage life would be shorter at a definite value of field strength (E). The value of c, which is a constant lays its dependency on the defect size [28].

As per [14], the value of ranges from 12 up to 15 for cables under AC and the value under DC would be generally larger what is stated for AC. The authors mention in [14] how a life exponent of 15 would help in reducing the test duration but here attention needs to be given to the the time constant (τ) and test requirements. The test factor for various test duration for different values of n, this can be shown in the figure below:

Design life, test duration	Life exponent	Test factor
40 years, 360 / 90 / 60 days	10.0	1.45 / 1.66 / 1.73
	12.5	1.34 / 1.50 / 1.55
	15.0	1.28 / 1.40 / 1.44

Figure 5.2: Test factor or different test duration and life exponent values [14]

The life constant of 13.7 as per [14] provides a test factor of 1.45 for a test duration of 90 days. The test factor used in [14] and [3] are similar, but the value of life-constant changes and there is a considerable reduction in the duration of tests from 360 days to 90 days. In [30], a life constant of 13.4 is used for XLPE samples under DC.

The value of n based on these recommendations for our tests as part of the modified test program is **n=13**. The same value is used to calculate the test factor for a test duration of **45 days**. The value of life constant as 13 for AC XLPE cable is also seen in [41] on performing the V-t characteristics for both AC and DC XLPE materials. It needs to mentioned here that the value of 13 selected here is higher than what is stated by [3] of n=10.

In the modified test program given as per table 5.5 the load cycles have heating cycles of 8 hours of heating and 16 hours of cooling, which is similar to [3], shown as per table 5.1, 5.2. According to [14], the duration mentioned above can be adjusted as per the thermal characteristics of the cable. When considering a medium-voltage DC cable of insulation thickness 5.5 mm, a heating cycle duration of 4/8 hours or 6/6 hours can be utilised [14]. As mentioned earlier, it is important to ensure that the test object reaches DC field distribution in the selected test duration. The knowledge of volume resistivity of various insulation material and how it changes with respect to change in temperature is important for the same.

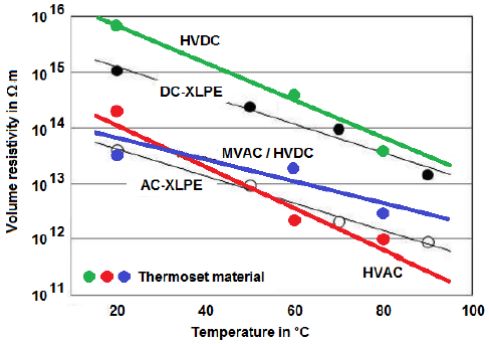

Figure 5.3: Change in Volume resistivity with temperature [14]

It is understood from above figure 5.3 that the volume resistivity for AC XLPE cable like the one used in our tests is almost ten times lower than the DC XLPE cable at a temperature of 20°C. At the higher temperature of 90°C, the volume resistivity of AC XLPE is lower to the DC XLPE in a similar fashion. The value of DC XLPE at different temperatures can be seen in the following table:

Temperature (C)	ϵ (F/m)	ρ (Ω.m)	Time for stability, 10τ (hours)
20	$2 \times 10^{-11} < \epsilon < 3 \times 10^{-11}$	$10^{15} < \rho < 5 \times 10^{16}$	55<10τ<4300
60	$2 \times 10^{-11} < \epsilon < 3 \times 10^{-11}$	$2 \times 10^{13} < \rho < 5 \times 10^{14}$	1<10τ<43
90	$2 \times 10^{-11} < \epsilon < 3 \times 10^{-11}$	$10^{12} < \rho < 5 \times 10^{13}$	0.06<10τ<4.3

Table 5.6: Resistivity, Permitivity and Time for stability of DC XLPE cables [3]

In the above table 5.6, it is seen that at 20°C, the time constant (τ) is anywhere between 55 hours to 4300 hours. As per 5.3, at 20° C, the volume resistivity of AC XLPE is lower by ten times when compared to the DC XLPE. Therefore the time constant would end up to be in the range 5.5 to 430 hours instead of staying in the range of 55 to 4300 hours when utilising AC XLPE instead of DC XLPE.

Work Group part of [3] takes the time for stability values measured at 10τ condition, which ensured 100% DC field distribution. The author in [14] mentions how 99% DC field distribution can be attained at 5τ. Utilising the time for stability as per 5τ, the time constant for the test object would reduce from 5.5 hours as follows:

$$0.5 \times 10\tau = 0.5 \times 5.5 = 2.75 hours \tag{5.4}$$

This time constant of 2.75 hours shown above in equation 5.4 for AC XLPE cable is lower to the 55 hours of DC XLPE cable at 20°C. Similarly, at higher temperatures like 90°C, the volumetric resistivity of AC XLPE is material is almost 100 times lower than what is witnessed for DC XLPE material [41].

Therefore from this, we understand that the dielectric time constant for AC XLPE cable would be much lower than the value for DC XLPE cable.

Every cycle as part of the test program comprises of 8 hours of heating and 16 hours of cooling as mentioned previously. With respect to our calculations, we understand that our AC XLPE cable under the application of DC stress would reach a resistive distribution in a period of about 2.75 hours at 20°C. This thereby shows that the selected test cycle allows ample time in the heating cycle for the test object to reach the required resistive distribution.

6

Experiments

The modified test program proposed and motivated as part of section 5.4 needs to be examined. The test object (MVAC cable system) would be subjected to this modified test program, and the effect of the applied stresses would be understood in a detailed examination phase. Thermal characteristics of the cable and the joint are measured in order to verify if the temperature requirements are being met.

6.1. Test Object

Test object in our research can be defined as a certain length of cable or the cable accessories which is to be put under testing. As part of this research, the test object utilises a 150 mm^2 12/20 kV AC Cross-Linked Polyethylene (XLPE) cable. The cable is combined with accessories such as a geometrically graded 12 kV AC cable joint and termination at both ends with similar field grading as of the joint. The total length of the test object comes to an approximate of 3 m. The test object can be seen in the following figure:

Figure 6.1: Test Object.

6.1.1. Cable

The cable used is a 150 mm^2 XLPE cable with aluminum conductor and the construction characteristics of the cable can be given as per the following table:

Standardization	NEN-HD 620 S2 - Part 10J / IEC 60502-2
Conductor Cross-section	150 mm^2
Conductor Material	Aluminum
Conductor Screen	Weakly Conducting Compound
Core insulation	Vulcanized polyethylene (XLPE)
Earth screen construction	Round wire copper + copper tape in counter spiral
Jacket Material	MDPE

Table 6.1: Cable Construction Characteristics [57]

The temperature and electrical characteristics of the cable are given in the following table:

Max. operating Temperature	70° C
Max. permissible conductor temperature	90° C
Nom. voltage V_0	12 kV
Nom. voltage V	20 kV
Nom. voltage V_{max}	24 kV
Conductor short circuit temperature	250° C
Nom. conductor diameter	13.3 mm
Insulation thickness	5.5 mm

Table 6.2: Cable Temperature and Electrical Characteristics [57]

The preparation of the cable as part of the construction of the test setup can be understood from the following representative figure.

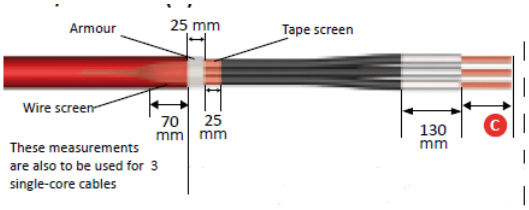

Figure 6.2: Cable Preparation.

As seen in figure 6.2, the cable is stripped layer by layer to expose the conductor. This exposed conductor is attached to the cable lug as shown in figure 6.3. Cable lugs allows the secure connection/termination of cable conductors to electrical equipment or electrical sources. The cable lug connected to either end of the cable in the test object prepared can be shown in the following figure.

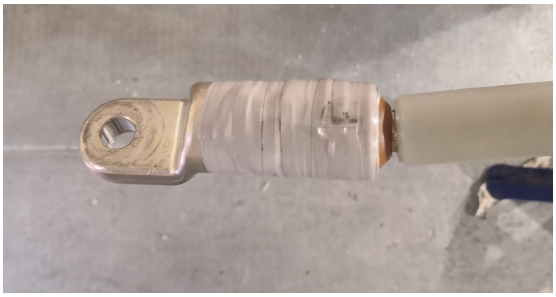

Figure 6.3: Cable lug attached to the cable end.

6.1.2. Joint

Lovink Enertech B.V. manufactures the Lovisil medium voltage cable joints which are available in a range from 12-36 kV. The joints due to there construction mechanism which consist of an outer shell, Lovisil insulation and polyurethane resin is highly resistant against moisture and any type of pollutants present in the soil. The speciality of Lovisil cables is that it makes use of the Lovisil fluid silicon insulation, which works well with both polymeric and paper insulated cables [5]. The liquid silicon has a property by which it fills all voids and thereby prevents any damage caused by unfilled voids [5]. Silicone insulation can be called polysiloxanes or polymerised siloxanes, and these are prepared from the polymerisation process of siloxanes to an inorganic chain of atoms of silicon and oxygen [23]. In general, such liquid silicon insulation can be represented by a formula:

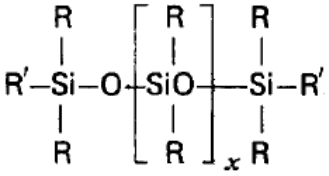

Figure 6.4: General Formula for liquid silicon [23].

The general formula is given in figure 6.4 can be modified by changing the R with Metyl, Alkyl or Aryl and the R ' can be replaced using Alkyl, Alkoxy, Hydroxide or H [23]. The chemical formula for liquid Lovisil is not added here as is protected by the Patent rights of Lovink Enertech B.V.

The Lovisil liquid used as insulation in the joints has some major advantages [5]:

- It is a perfect insulant for all the components inside the joint.
- It cures and forms a sealant rubber when in contact with moisture/water.
- It tends to reduce the number of partial discharge in the joint.

The joint which is used as a part of the test object is an MVAC 12 kV straight joint of the M85 type which is manufactured by Lovink Enertech B.V. The joint showcased here for representative purpose in fig 6.5 is a three core joint of the M85 type. As part of our test process the test object is made of a polymeric single core joint.

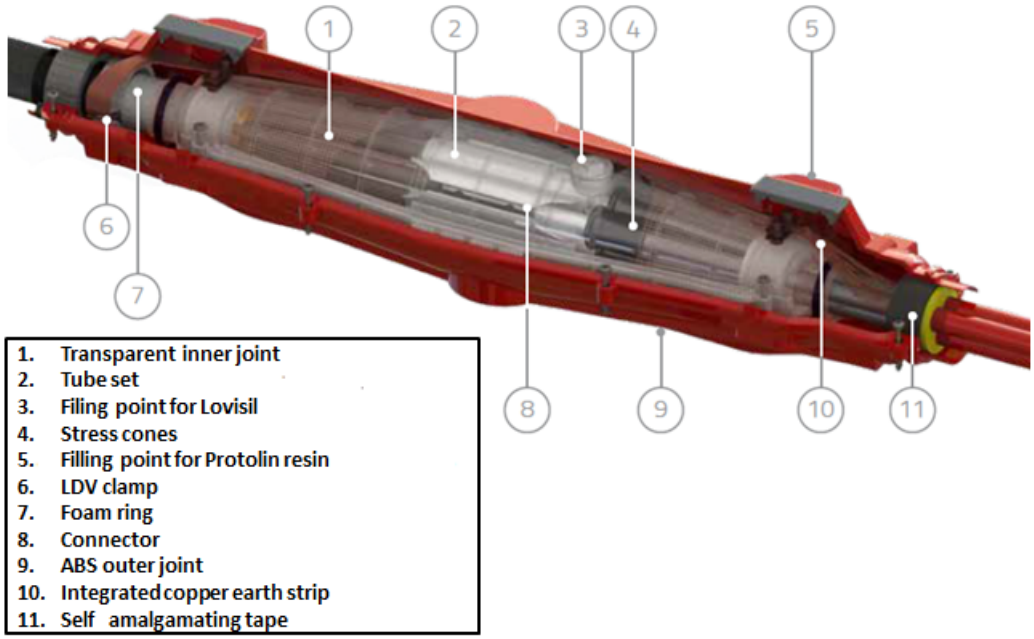

Figure 6.5: M85 Joint.

The joint is made of of a two shell structure, the inner shell which is made of polyester compound holds the liquid dielectric. This liquid silicon insulation stays predominantly in liquid form, and this helps in minimising the discharges from the dried paper when using the joint for paper insulation type cables. The outer shell, red in colour is made using ABS (Acrylonitrile Butadiene Styrene), this provides mechanical protection to the joint. The space between the outer and inner shell is filled with a special polyurethane resin called Protolin, which is manufactured at Lovink Enertech. The resin provides safety against moisture ingress and also guarantees an excellent seal owing to its exceptional bonding to the ABS outer shell.

There is present inside the joint a copper mesh which acts as the electrical screen. It should also be noted the ϵ_r value of Lovisil insulation is virtually identical to the insulation of XLPE/EPR cables and this value doesn't change when the insulation is cured in the presence of water [5]. This property ensures a homogeneous electric field distribution during AC operation as AC field distribution depends on permittivity ϵ_r of the material.

The construction of the M85 joint utilised as a part of the test object involves first stripping down both cable to their conductors, as shown in figure 6.2. The conductors are then connected using a connector of appropriate size. A pair of deflectors are put over on either side of the connector over the semi-conductive layer. The interruption of the semi-conductive layer which occurs in cable preparation may lead to field concentration as shown in figure 1.3, this field concentration would need to be mitigated. The deflector when mounted at this point over the semi-conductive screen interruption helps in shaping the field and thereby avoiding any field concentrations. The various components present in the joint prior to filling it with the liquid dielectric and enclosing with the ABS shell can be seen as per figure 6.6.

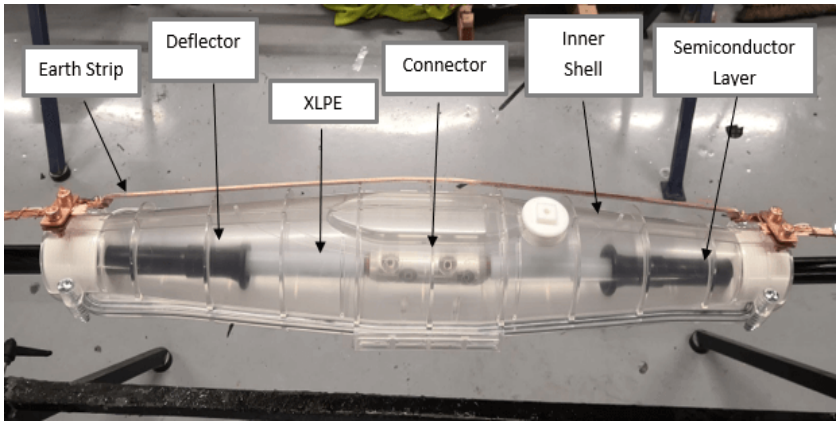

Figure 6.6: Cable Joint Built till Inner Shell.

In figure 6.7, the earth screen of the cable is connected to the earth strip of the joint on either side. This provides thereby a continuous path for cable neutral and fault current.

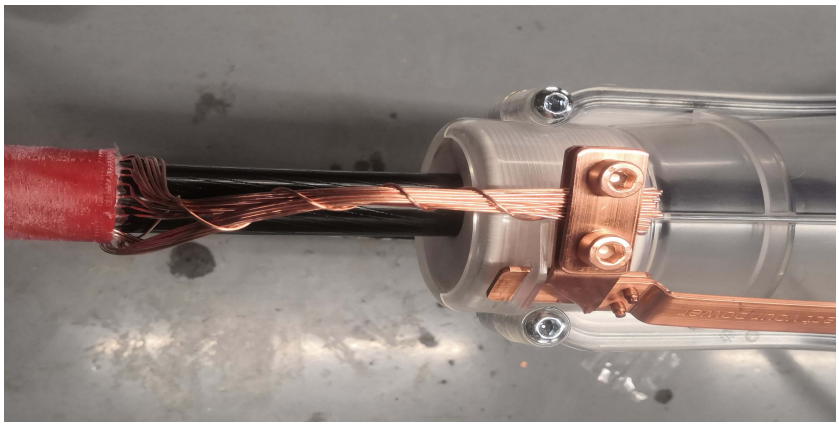

Figure 6.7: Earth Strip Connection of Cable and Joint.

The transparent inner shell shown in figure 6.6 is filled with Lovisil insulation. The inner shell is then wrapped with a copper mesh, this copper mesh thereby acting as a Faraday cage which prevents the field from straying outside as shown in figure 6.8.

Figure 6.8: Inner shell covered with Copper mesh.

The inner shell which is wrapped with copper mesh is then placed inside the outer shell made of ABS,

this provides mechanical protection to the joint. In the space between the outer and inner shell, a special resin manufactured at Lovink is added, and it helps in protecting against moisture. The joint built for the test is shown in the figure below:

Figure 6.9: M85 Joint Built for Test.

6.1.3. Termination

Termination is an important accessory when considering the cable system and are used for terminating the cable system. Terminations are also used when there arises a need to interface the cable with other electrical systems [45]. The termination used as part of the test setup was a 12/20 kV termination with geometric type field control. Geometric field control as shown in figure 1.5 makes use of a funnel/deflector at the semi-conductor screen interruptions to prevent field concentration [45].

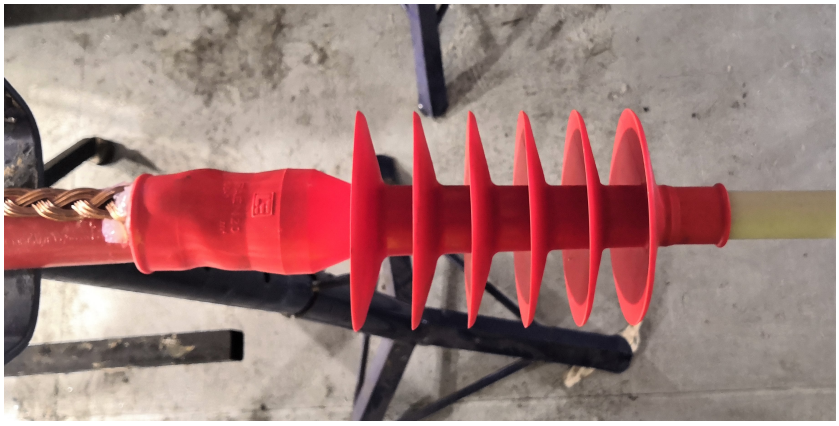

Figure 6.10: Termination with geometric field control.

6.2. Test Voltages

The selection of test voltages is very critical in performing testing, the voltage used in testing is higher than the voltage in normal operation, and this higher voltage is used to understand more about the voltage life of the component. Voltage life of a component can be understood as the lifetime of the component at that certain voltage level [29]. The accessories used in the cable system have rated voltages as the following as per [4]:

- V_0: Rated voltage between the conductor and earth screen for which it is designed.
- V: Rated voltage between a pair of conductors for which it is designed.
- V_m: Highest voltage for which the accessory is designed.

The test voltages mentioned in tables 5.1, 5.2 mentions a set of test voltages which are explained under the section 5.2. The selection of these test voltage has a dependency on the life constant 'n' and also the testing duration 't_1'. In [3] it mentioned that the test factors for the tests in tables 5.1, 5.2 are based on the knowledge of the voltage-time (V-t) characteristics. The exact behaviour of V-t characteristics of is unknown when considering DC, but as per the workgroup in [3] the use of Inverse Power Law model is a good approach.

The approach in [3] can be understood as follows:

$$V^n \times t = Constant \tag{6.1}$$

In the equation 6.1 :

V: Voltage

t: Time

n: Life constant

The DC voltage V_{dc} can be given as follows:

$$V_{dc} = V_0 \times K_1 \tag{6.2}$$

In the equation 6.2:

V_0 : System Voltage

K_1 : Voltage Multiplication Factor

K_1 can be calculated with the following equation:

$$K_1 = \sqrt[n]{\frac{t_0}{t_1}} \tag{6.3}$$

In the equation 6.3:

t_0 : Design life of the test object

t_1 : Duration of the test

As per [3] the design life of the cable systems t_0 is taken to be 40 years, and the duration of the test was taken as 360 days for pre-qualification tests. As the knowledge of life constant n is limited, the workgroup made use of a conservative approach and kept the value to a lower limit of n=10. These values would now be used to find the voltage test factor k_1.

Therefore the known values in equation 6.3 is as follows:

t_0 = 40 years

t_1 = 360 days [Pre-qualification tests]

n = 10

Substituting the above values in equation 6.3:

$$K_1 = \sqrt[10]{\frac{40 \times 365}{360}} = 1.45 \tag{6.4}$$

The value of test factor k_1 is found as **1.45**. The nominal electric stress in DC polymeric cable, which is around 20 kV/mm in HV cable would be enhanced by 1.45 times when performing pre-qualification tests [55].

6.3. Test Setup

Test Setup consists of the test object and the required accessories for performing the required tests as per section 5.4. The test setup built in the high voltage lab of Lovink Enertech B.V.

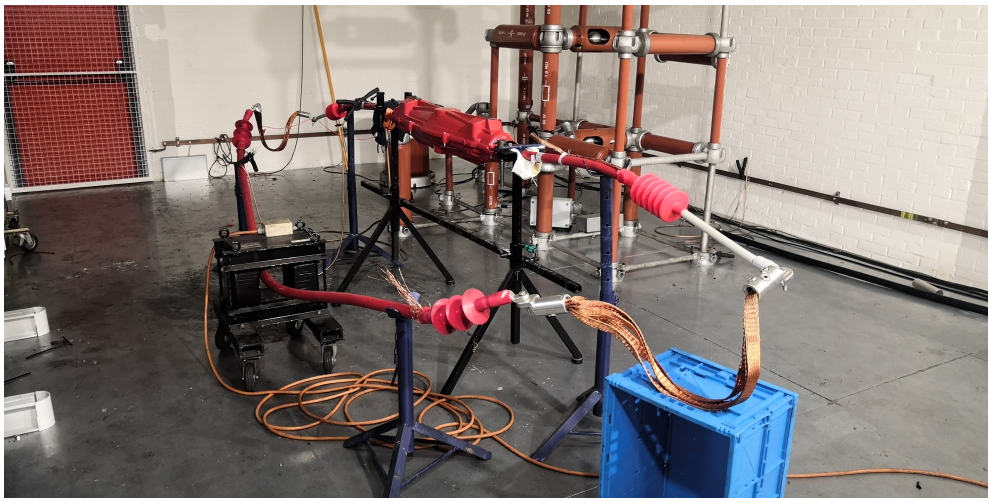

Figure 6.11: Test Setup for Load Cycle on AC cable system.

The test setup consists of a current transformer which is required to pass the required current of 498 A into the circuit for achieving the desired heating pattern for the tests. The selection of 498 A as the heating current is explained under section 6.4. A service cable of the same type as that of the test cable is used for making the test object passes through the current transformer. The XLPE cable has a conductor cross-section of 150 mm^2. The test object, as explained in section 6.1, consists of a Lovisil joint and also a pair of geometric field graded terminations on either end. The test setup also consists of an AC source which supplies the DC voltage to the test arrangement after rectifying the AC to DC using a set of diodes. The built-in diodes in the test setup arrangement can be reversed in direction to obtain a voltage of opposite polarity. The DC voltage from the diode passes a capacitor arrangement which smoothens it for application as the test voltage. The AC source and diode setup can be shown in the following figure:

Figure 6.12: Diode Arrangement to Obtain Desired Polarity.

The smoothening capacitor arrangement can be seen as per the following figure:

Figure 6.13: Capacitor for smoothenening the DC output voltage.

6.3.1. Conditions for tests

Insulation Thickness Verification

The insulation thickness is to be verified on the test cable prior to performing the pre-qualification test. The insulation thickness of the sample should not deviate too much from the nominal thickness mentioned by the manufacturer [3]. This can be understood in the following scenarios [3]:

- If the deviation between the insulation thickness and nominal thickness is less than 5%, then the test voltages remain unaltered.
- If the deviation between the insulation thickness and nominal thickness is more than 5% and less than 15%, then the test voltages are multiplied by a factor α.

$$\alpha = \frac{t}{t_n} \tag{6.5}$$

  - t: measured thickness of the test cable.
  - t_n: nominal thickness mentioned by the manufacturer

- If the deviation between the insulation thickness and nominal thickness is more than 15%, then the testing needs to be halted.

6.4. Thermal Characteristics of Cable and Accessories

Reference cable is a definite length of cable which belongs to same roll of cable being put under test. Reference cable is used to understand the electrical and thermal behavior of the object under test. The cable provides an understanding about the correlation between the heating current, temperature of the core and the temperature of the sheath. In our case the cable under test is a 150 mm^2 12/20 kV XLPE AC cable with a maximum conductor temperature of 90°C as shown in table 6.2. The maximum conductor temperature for a variety of cable insulation types can be given as the following table [45]:

Dielectric	Impregnated Paper	LDPE (Low Density Polyethylene)	HDPE (High Density Polyethylene)	XLPE (Cross Linked Polyethylene)	EPR (Ethylene Propylene Rubber)
Operating Temperature [C]	85/90	70	80	90	90
Short Circuit Temperature [C]	160/180	150	180	250	250

Table 6.3: Permissible conductor temperature for cables with different insulation types [45]

6.4.1. Preparation of Reference Cable

The preparation of reference cable involves taking a desired length of the cable and then adding thermocouples to it for monitoring its electrical and thermal characteristics. The calibration of the cable needs to be done in order to realise the thermal behaviour of the conductor during actual testing [4]. Calibration is done by passing a certain current and observing the conductor temperature behaviour for that current with the help of thermocouples [31]. The placement of thermocouples on the cable is as per what is given in [1].

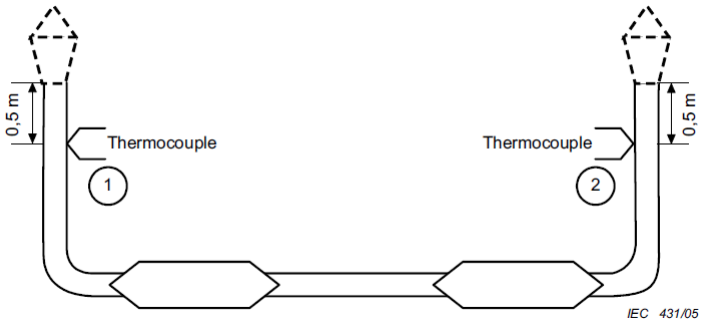

Figure 6.14: Joints tested in air [1].

As shown in figure 6.14, two thermocouples are placed 0.5 m from either end of the cable which has a minimum length of 2 m. These two thermocouples as per [1], are attached on the conductor and also on the external surface. Another thermocouple is used additionally while testing, which would provide the reading of the ambient temperature of the surrounding. As part of the test preparation, when using thermocouples on the reference cable of the same type as that of the test cable helps in understanding if the desired temperature characteristics are met for the cable. The desired temperature characteristics are as follows [2]:

- Achieving a temperature of 5-10 K above the maximum conductor temperature for a minimum period of 2 hours in the heating cycle when considering extruded insulation cables.
- Achieving a temperature of 0-5 K above the maximum conductor temperature for a minimum period of 2 hours in the heating cycle when considering paper insulated cables.

In order to place the thermocouple on the conductor, the cable needs to be dismantled layer by layer in the position where we need to place the sensor. Once the thermocouple is placed, the cable is built back in the same fashion. The whole process can be understood by the following figures:

(a) Water Blocking Sheath.

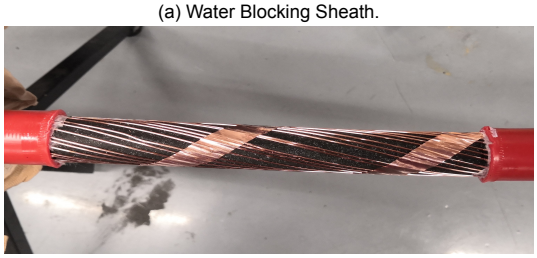

(b) Copper Sheath.

(c) Water Blocking Sheath.

Figure 6.15: Dismantling the initial three layers of the cable.

(a) Semi-conductive layer over the XLPE.

(b) Aluminium Conductor.

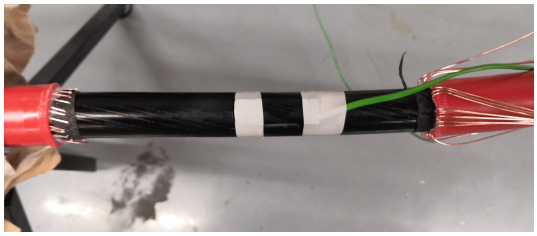

(c) Thermocouple placed on conductor.

Figure 6.16: Dismantling the final layer and placing thermocouple.

In the above figure 6.15 the dismantling of the first three layers of the cable. After removing the jacket of the cable, the water blocking sheath 6.15a is seen, and on removing that layer the copper sheath shown in 6.15b is found. Under the copper sheath, there is another layer of water blocking sheath which is shown in figure 6.15c. The figure 6.16 showcases the dismantling of the cable and placing the thermocouple on the conductor. The figure 6.16a showcases the semi-conductive layer, which is below the water blocking sheath. This semi-conductive layer is extruded on top of the cable insulation made of XLPE. After removing the XLPE layer, the aluminium conductor of the cable is visible as shown in 6.16b. The thermocouple is placed on the conductor, and the layer is built as they were initially prior to dismantling. The layers need to be built back in the same manner in order to understand the thermal characteristics of the cable with respect to the applied current in the most appropriate manner.

In figure 6.17, the cable can be shown after the thermocouple being placed at the conductor. The dismantled layers are held down using tapes to ensure that the thermocouple does not get dismantled during the testing phase. These thermocouple arrangement on either side record the conductor temperature and this would be checked to ensure if the necessary requirements are being met.

Figure 6.17: Rebuilt Cable after Placing the Thermocouple.

6.4.2. Thermal Characteristics of the Cable

As per [4], the cable needs to be calibrated for a temperature of 95°C at the core to ensure that the conditions mentioned previously for both load cycle (LC) and high load (HL) are satisfied. A suitable current needs to be selected, which ensures a temperature of 95°C on the conductor for at least two hours of the total heating period of 8 hours.

From initial testing, it was understood that a current of 408 A would result in a conductor temperature of 65°C. Therefore a comparatively higher current in the order of 588 A was passed through the reference cable. It was observed that for 588 A, the conductor temperature was 135°C. Therefore it was understood that the temperature almost doubled for an increase in 180 A (408 A + 180 A) and thereby if this increase in current was halved to a value of 90 A (408 A + 90 A), we would get a conductor temperature in the range of 97°C.

In order to verify this, a current of 498 A is passed through the circuit. The heating current heats the cable for 8 hours and then its left to cool for 16 hours, this completes one cycle. As previously mentioned in 6.4.1 there are four thermocouples on the cable, these thermocouples are connected to a data logger with multiple channels by assigning each thermocouple to a specific channel. The computer stores the temperature data for the whole cycle. On observing the temperature at the conductor after a few hours it was at 95°C, this was the desired temperature, and thus the thermal behaviour of the cable was understood. Post completion of the total cycle, the data plotted to observe the temperature variation.

Figure 6.18: Reference cable testing setup.

In figure 6.18, the current transformer inputs the set current into the service cable, which has a conductor size of 400 mm^2. This current is passed onto our reference cable of 150 mm^2, which is red in colour. Due to the smaller conductor cross-section of the reference cable, it heats up faster in comparison to the service cable. The reference cable is fixed with thermocouples as mentioned previously, and they measure the temperature at the definite points.

The graph for the temperature data during one cycle can be shown in the following graph:

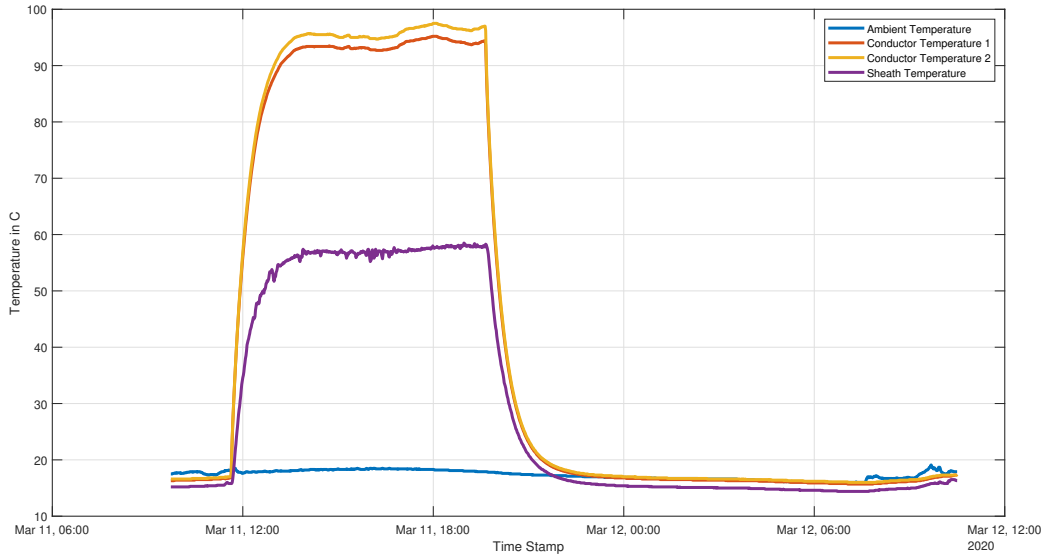

Figure 6.19: Temperature Distribution in the Cable.

It is seen from figure 6.19 that initially there is a sharp increase in temperature, and after reaching the set temperature, it remains constant. This is because initially the core heats up owing to the losses and this creates a gradient inside the cable geometry. The temperature of the sheath and core rises owing to the losses due to the current and eventually reaches a saturated as the maximum heat produced due to the input current is reached. If we further increase the current, after a certain point, the sheath would not be able to dissipate heat at the same rate the core produces and would result in thermal degradation.

From the above figure 6.19 we understand the following:

- The current flow starts at 11:38 AM, this is understood by the rise of temperature across the thermocouple 2,3,4 owing to the heat produced.
- A saturation temperature of 95° C is reached in the following 2 hours.
- The ability to reach this temperature within 2 hours satisfy the condition laid by [4] to have a temperature higher than the maximum conductor temperature for at least 2 hours in the heating cycle.
- A total of 6 hours is spent at 95° C, which is higher than the maximum conductor temperature.
- The temperature at the sheath during this time is 57° C, which leads to a gradient of 38° C across the insulation.
- At 19:38 PM the cable finishes 8 hours of the heating cycle and thereby the cooling phase starts.

6.4.3. Thermal Characteristics of the Joint

The joint model has comparatively larger cross-section compared to the cable and thereby would dissipate heat better. The knowledge of the temperature at the outer surface of the joint would help in understanding the temperature gradient formed inside the joint. In order to understand the gradient, four thermocouples are placed at multiple points on the joint body. Additionally, a thermocouple has also been placed on the cable sheath to understand the difference between both the joint body and the cable sheath.

(a) Thermocouple at the centre and the beginning of the joint body.

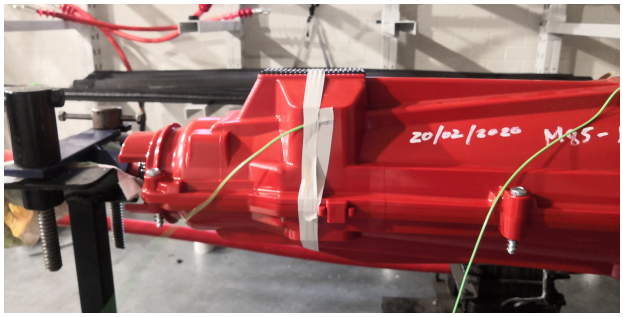

(b) Thermocouple zoomed in.

Figure 6.20: Thermocouples placed at multiple locations on the joint body.

A total of five thermocouples are added to the arrangement, the position of the thermocouple are as follows:

- Top of the joint
- Bottom of the joint
- Either end of the joint
- Sheath of the Cable

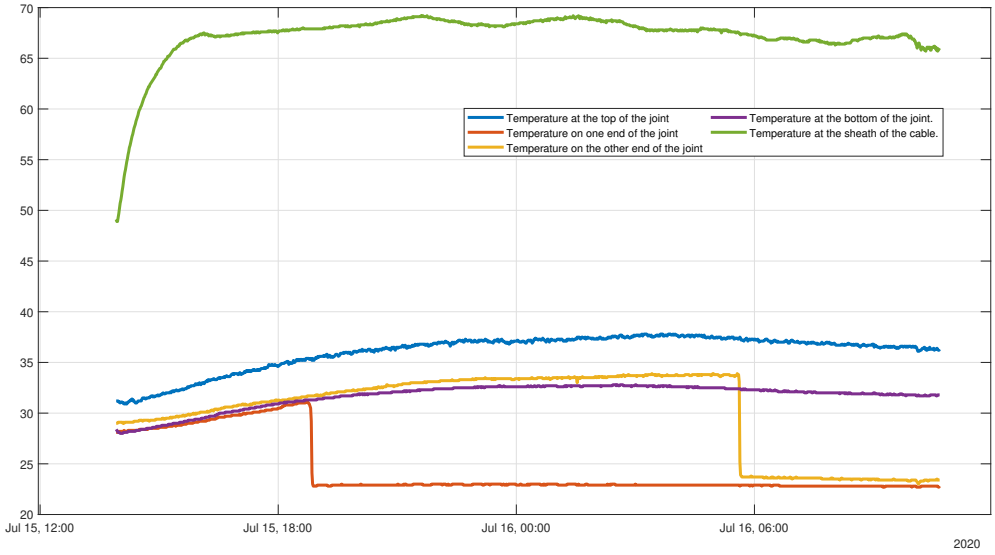

Figure 6.21: Temperature Distribution on the Joint.

As per the figure 6.21, the temperature at various locations on the joint body and on the cable sheath is seen. The difference in the temperature at the cable sheath in figures 6.19, 6.21 is owing to the difference in ambient temperature and also because when performing this test some additional current was added to account for the current drop. The ambient temperature is higher by almost 6°C when observing the thermal characteristics of the joint. The higher ambient temperature facilitates the sheath reaching a higher temperature as seen as part of this test.

The temperature at the sheath is the highest and stays relatively stable between 65°C to 68°C. The temperature at the top of the joint is the highest among all thermocouples and reaches the maximum of 37.7°C at 4:30 AM. The sensors at the bottom and either end of the joint follow a very similar trend until around 7:30 PM. The sensors on both the end of the joint slipped and fell on the ground at 7:30 PM and 5:00 AM next day respectively, this is the reason for the sudden drop in temperature at either end of the joints. In accordance with the initial behaviour, we can extrapolate that the same behaviour would be continued by the sensors if they had not slipped from the test arrangement.

6.5. Testing Sequence

The test object shown in section 6.1 was put under testing as per the modified test program found in table 5.5. The choice of test voltages and the duration of tests is seen in section 5.4. The sequence of the test program and the parameters of the test can be further explained as follows:

Load Cycle

As per table 5.5, the load cycle tests were the first type test to be conducted on our test object. A voltage of 26.5 kV was applied on the test object in combination of heating cycles with 8 hours of heating and 16 hours of cooling. The diodes seen in figure 6.12 were arranged in a manner such that a positive voltage is attained at the output. The heating current given to the circuit was a total of 498 A calculated as seen in sub-section 6.4.2. The current ensures the temperature requirements of the pre-qualification testing $T_{cond,max}$,ΔT_{max} seen in section 5.2 are fulfilled.

After completing the test for a total of 5 cycles (1 cycle is 8 hour of heating and 16 hours of cooling) with a constant voltage of 26.5 kV, the load cycle under positive polarity is completed. The test object is rested for a total of 24 hours as advised in [3]. In this 24 hour rest period, the heating current of 498 A is applied throughout, but the test object is disconnected from the voltage source. The load cycle is

repeated in the same manner for five more cycles post the rest period. In these next 5 cycles, the diodes are re-arranged to obtain a voltage of 26.5 kV of negative polarity, and the rest of the parameters are kept similar to the previous load cycle under positive polarity.

High Load

High load test is the second type of test which are conducted on the test object as per the modified test program in table 5.5. As part of the high load test, the DC voltage of 26.5 kV is kept constant throughout for the five cycles, where every cycle is 24 hours of voltage and heating current application. The diodes are arranged to achieve positive voltage polarity, and the heating current of 498 A is achieved from the current transformers part of the test setup.

After completing the test for five cycles the test setup is rested for 24 hours under the application of heating current, but it is kept disconnected from the voltage source. The high load is repeated for five more cycles after the rest period with the application of voltage and heating current. In these next 5 cycles, the diode is re-arranged to obtain 26.5 kV under negative polarity.

Zero Load

Zero load test is the third type of test performed on the test object as part of the modified test program. The zero load test, as the name suggests, doesn't require the heating current application. The test consists of 15 cycles, where every cycle is 24 hour of voltage application. The voltage of 26.5 kV at negative polarity is kept constant throughout the 15 cycles.

Load Cycle

The load cycle, which was the first type of tests conducted on the test object as part of the modified test program, is repeated after the zero load test. The load cycle test is performed for a total of 10 cycles, where five cycles are under positive and rest under negative polarity. As part of the load cycle, the heating current is applied to the test object where each cycle consists of 8 hours of heating and 16 hours of cooling.

6.6. Examination

The examination is a very important part of the pre-qualification test procedure, as previously mentioned in section 5.2. It helps in observing and understanding the effect of the test program if any on the test object, and the effects may range from cracks, corrosion, tracking, leakage of dielectric insulation or the evidence of overheating [4], [13]. The following points of visual inspection have taken inspiration from [4] for the inspection of MVAC accessories post-testing and serve as the phase 1 of examination.

Point of Examination	Yes	No
Corrosion on the metallic parts		No
Electrical degradation on the cable insulation.		No
Electrical degradation on the joint insulation		No
Indication of mechanical/thermal degradation.		No
Leakage of the insulating media.		No
Visible shrinkage of the cable components.		No
Displacement in the accessories.		No

Table 6.4: Visual inspection post testing as per modified test program.

Post completion of the tests, the visual examination of the test object shown in figure 6.1 is conducted as per the visual indicators from [4] stated above. In order to further examine the cable system, it is dissected at multiple locations and subjected to visual inspection [13]. In phase 2 of the examination,

using a drill, a hole is made on either side of the joint. This hole is to remove the liquid Lovisil from the inner shell of the joint as per figure 6.6.

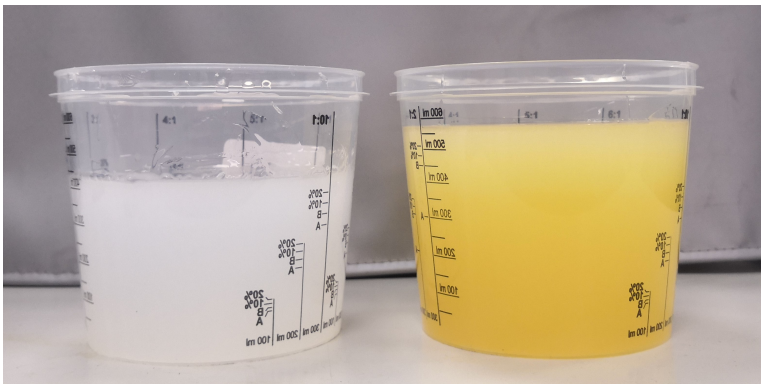

Figure 6.22: Discoloration of liquid Lovisil post testing.

It is seen from figure 6.22, that post completion of the tests the liquid silicon dielectric, undergoes discolouration. The reason for the discolouration is the ageing which the liquid Lovisil underwent as part of the modified test program given in table 5.5.

As mentioned earlier in section 6.1, the cable is stripped layer by layer to attach the joint and termination. In the absence of a suitable field grading there would be field enhancement at the semi-conductive layer interruption as see in figure 1.3. In order to avoid this field enhancement, the test object makes use of geometric field grading, as seen in figure 1.5. In phase 3 of the examination, the geometric field grading present as part of the termination and the joint is removed to check for any possible electrical degradation such as tracking.

1. Termination

   The termination as in figure 6.10 is used as part of the test object. A scalpel is used to cut open the cold shrink termination. In figure 6.23a, the encircled part showcases the geometric field grading as part of the termination. As per [61], the deflector arrangement with its geometrical shaping decreases the field enhancement at the semi-conductive screen interruption.

   Figure 6.23b showcases the semi-conductive screen interruption at the termination end. The encircled part in figure 6.23b shows no burnt marks or tracking due to electrical degradation. This showcases that the geometric field grading would effectively control the field enhancement at the semi-conductive screen interruption.

2. Joint

   Similar to as seen in the termination, the cable is stripped layer by layer before it enters in joint housing. The semi-conductive screen interruption present would cause field enhancement and therefore, geometric field grading is utilised using a deflector arrangement as seen in figure 6.6.

   Post testing the deflector is removed from the joint housing as seen in figure 6.24a. The deflector is removed using scalpels, and the semi-conductive interruption can be seen in figure 6.24b. It is seen from figure 6.24b that there are no burnt marks or tracking on the XLPE insulation. This indicated that as part of the modified test program, the cable insulation did not undergo electrical degradation at the semi-conductive screen interruption. The difference in the colour between the cable insulation as seen in figure 6.23b and figure 6.24b is because the latter is submerged in liquid Lovisil inside the joint inner shell.

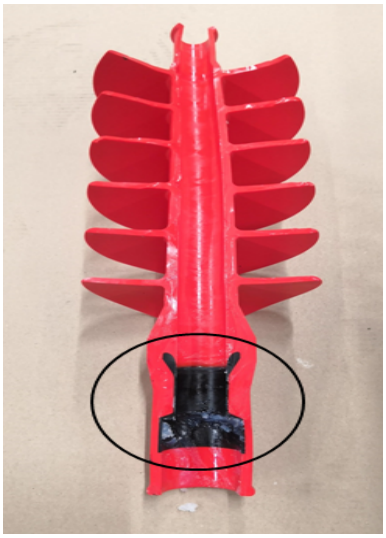

(a) Geometric field grading as part of the termination.

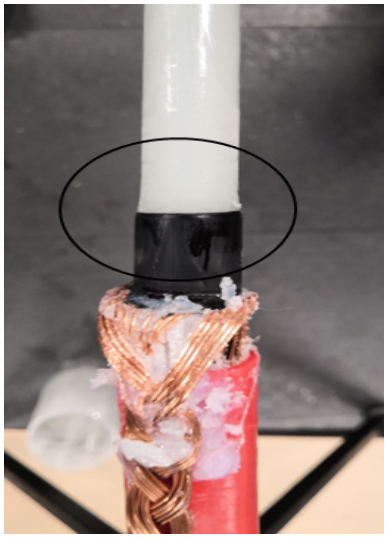

(b) semi-conductive screen interruption at the termination end.

Figure 6.23: Examination of the termination post testing.

(a) Geometric field grading as part of the joint.

(b) semi-conductive screen interruption inside the joint.

Figure 6.24: Post testing examination of the deflector inside the joint.

Figure 6.25: Examining the bolted connector present inside the joint housing.

In figure 6.25, the cable entering the connector from either end is showcased. The encircled part showcases the XLPE insulation of the cable entering the connector from either end. It is noticed that the cable shows no sign of electrical/thermal degradation at the proximity of the connector.

In phase 4 of the examination, the cable is dissected at multiple locations to check for any possible electrical degradation such as tracking/treeing.

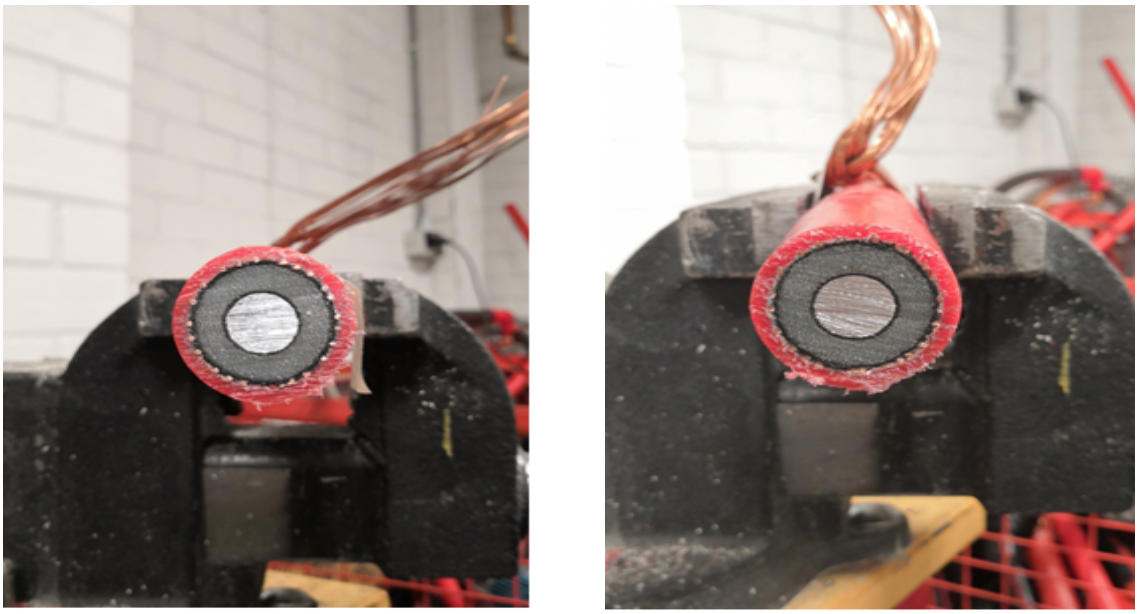

(a) Cable dissected at location 1.

(b) Cable dissected at location 2

Figure 6.26: Cable dissected at multiple locations.

(a) Cable dissected at location 3 inside the joint.

(b) Cable dissected at location 4 inside the joint.

Figure 6.27: Cable dissected at multiple locations inside the joint.

In the figure 6.26 and 6.27, the cross-section of cable dissection at multiple locations is seen. The figure 6.26 showcase the cable located outside the joint while 6.27 showcase the stripped part of the cable found inside the joint housing. It can also be noticed that the XLPE insulation which forms the cable insulation shows no signs of visible electrical degradation. In the multiple locations checked as part of the examination, there were absent any signs of electrical/thermal degradation.

In phase 5 of the examination, the joint assembly is dissected at multiple locations to check for any form

of electrical/thermal degradation. It can be seen from simulations as per figures 4.11, 4.13, 4.15 that the presence of a copper mesh in the resin layer results in field enhancements. As part of the dissection, special attention is given to the copper mesh in the resin layer to check for any visible degradation.

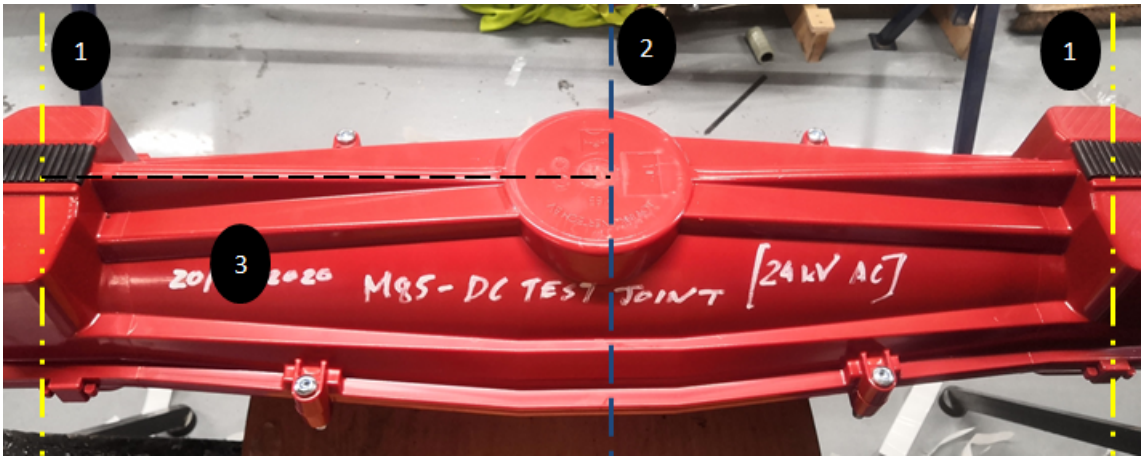

Figure 6.28: Axis for joint dissection.

As shown and indicated in figure 6.28, the joint is at first dissected along the yellow lines indicated with axis 1. Post which the joint is dissected from the centre along the blue line indicated with axis 2. The joint in the last stage is dissected along the black line, this allows to examine the cross-section inside the joint for any form of degradation.

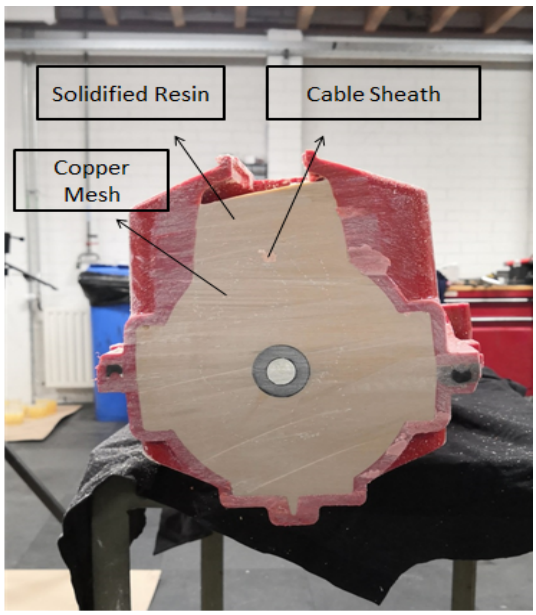

(a) Joint dissection.

(b) Zoomed in cross-section of dissection.

Figure 6.29: Joint dissected along axis 1 as per figure 6.28

(a) Joint dissection.

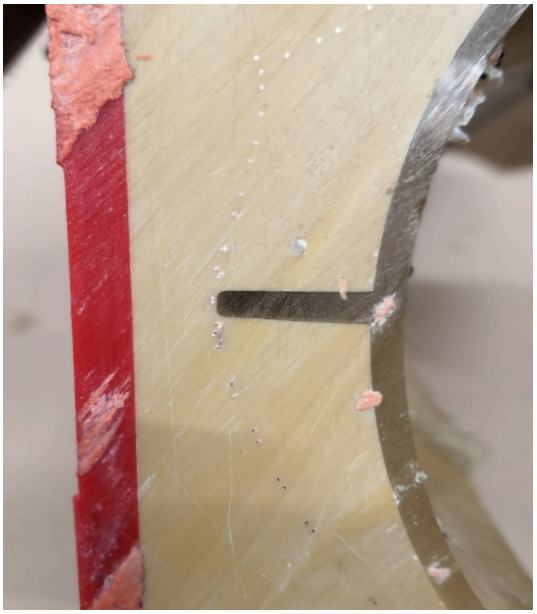

(b) Zoomed in cross-section of dissection.

Figure 6.30: Joint dissected along axis 2 and 3 as per figure 6.28

It is seen from figures 6.29 and 6.30 that the peak field witnessed at the mesh does not cause any visible electrical degradation to the polyurethane resin layer. It can also be seen from figure 6.30b that the solidified resinous layer has a very smooth texture and there is an absence of any visible voids. This is a positive sign when utilising the MVAC accessory for DC, but the possibility of micro-voids and the difference in coefficient of thermal expansion for both copper and resin layer cannot be ignored.

The successful completion of the modified test program as per table 5.5 showcase the ability of MVAC cable system to provide satisfactory long term performance when re-purposed for DC application. The absence of any visible electrical/thermal degradation checked as part of visual examination post the testing phase adds to the ability of the system to transition effectively for DC application.

7

Discussion and Conclusion

The research presented as part of this thesis focused on the applicability of an MVAC cable system for the future distribution network. The absence of standard test procedures for pre-qualification and also to understand the field distribution in the accessory when stressed under DC, the following research questions were formulated:

1. How do the existing MVAC accessories behave under DC stress, will DC due to its complex field distribution be critical to the accessory?
2. Will the MVAC cable system when put under a modified Pre-Qualification test program ensure a long term performance of the system for operation under DC stress?

The discussion as per section 7.1 takes into account the observations from the FEM simulations found in chapter 4. The lifetime analysis, which is also a part of chapter 4 aims at finding the lifetime of the most stressed layer in the insulation. The test object prepared as part of the research is subjected to the modified test program in order to understand its long term performance under DC stress. The discussion also takes into account the observations made as part of the examination phase performed post-testing found in section 6.6.

7.1. Discussion

The FEM simulations in chapter 4 showcase the field distribution inside the MVAC joint when simulated for DC stressing. The simulation shows that the difference in conductivity between materials inside the MVAC joint would lead to field concentration in the material with lower values of conductivity. It can be seen from the simulation in section 4.2 that the liquid Lovisil due to its higher conductivity in comparison to both XLPE and Protolin resin witnessed a comparatively lower electric stress. It should also be highlighted here that the maximum electric strength seen in the XLPE and liquid Lovisil layer are lower when compared to there respective breakdown strengths. The maximum field strength witnessed in the Protolin layer as part of the simulations is also lower than the known AC breakdown strength of the material. It is stated in [31] that generally, the breakdown strength of insulating material is higher in DC in comparison to AC. This further ensures that the maximum field strength witnessed as part of the simulations in the Protolin layer would not be critical to the material.

The presence of copper mesh leads to field enhancement in the Protolin layer at the periphery of the mesh. At higher voltages, the presence of such field enhancement would lead to electrical degradation of the material. At a conductor temperature of 80°C as seen in figures 4.6a, 4.6b an equalisation of electric field is observed in the cable insulation. This equalisation of the electric field would lead prevent uneven electrical stressing of the XLPE insulation layer in that cutline region. The electro-thermal lifetime calculation due to accelerated ageing performed on most stressed layer indicated a lifetime of 1.2 years for the Protolin resin.

The test object in figure 6.1 prepared as part of our test program is made to undergo the modified test program as per table 5.5. The selection of test duration and the life constant (n) influences the

test voltage. The test voltage selected is a voltage higher than the DC safe voltage to make the test object undergo accelerated ageing. The load cycles and high load tests investigate the performance of the cable under thermal and electric stressing. The behaviour of the test object under constant DC stressing was investigated as part of the zero load tests. The effect of the stresses during the test on the test object is investigated during the examination phase. The test object is at first visibly examined for any form of degradation post which it is dissected, and accessories are dismantled to check for possible degradation.

7.2. Conclusion

The first research question focuses on the field distribution inside the MVAC accessory when simulated under DC condition. This is of importance because the MVAC accessory is manufactured to facilitate AC electric field distribution which depends on the permittivity of the material.

In order to answer the first research question, simulations are performed on the AC accessory under DC stress using COMSOL multiphysics. The simulations give an overview of the electric field distribution in the accessory as in DC the electric field is dependent on both temperature and electric field. Electro-thermal life laws are used to understand the lifetime of the most stressed layer from the simulation under accelerated stressing.

The simulation done as part of chapter 4 motivate us in stating that when simulating the MVAC accessory under DC stress, no critical field stresses are observed in any part of the accessory. The Protolin resin, which witnessed the maximum electrical stress due to the presence of copper mesh, would showcase a lifetime of 1.2 years under accelerated electro-thermal ageing.

The second research questions aims to find the possibility of using an MVAC cable system in the future distribution network. It needs to be ensured that these MVAC cable systems provide the desired long term performance when used under DC stress.

In order to answer the second research question, long term performance of the MVAC cable system under DC stress needs to be evaluated. The knowledge of the pre-qualification rules for both HVDC and standard testing procedures for MVAC are referred for the same. A modified test program is proposed and motivated to carry out the pre-qualification test for the MVAC cable system. The test object post completion of the test program needs to be examined to understand the effect of the applied stresses. The test object post visual inspection would be dissected and dismantled for further inspection.

The successful completion of the modified test program as per table 5.5, thereby showcases the ability of the MVAC cable system to provide the desired long term performance when re-purposed for DC application. The absence of any form of visible thermal/electrical degradation in the examination phase showcased in section 6.6 thereby supports the agreement of re-purposing an MVAC cable system for DC application.

8

Future Recommendations

In this research we make use of a combination of COMSOL simulation and testing to understand the possibility of using an MVAC cable system under DC conditions. The simulations showcased no critical field enhancement in any part of the joint, although there is a considerable amount of field in the resin layer compared to the joint insulation. In order to mitigate this field concentration in the resin layer, the conductivity of the resin layer can be altered for it to see lower field concentrations. The increased conductivity of the resin layer would thereby not accumulate electric field and the field enhancement around the mesh would also be mitigated. The possibility of using a continuous copper strip as shown in section 4.2 instead of the copper mesh would also mitigate the issue of field enhancement witnessed in the resin layer at the periphery of the copper mesh.

The life time calculations showcase the resin material to have a lifetime of 1.2 years under accelerated stress. In order to have a more accurate lifetime value it is important to calculate the activation energy of the Protolin resin. Pre-qualification testing showcase the ability of the MVAC cable system to providing satisfactory long term performance when re-purposed for peak AC voltage (safe DC voltage), this thereby paves the way to test and re-purpose the cable system for higher DC voltages. In such a condition when testing at higher voltages, it is recommended to measure the DC breakdown strength of the Protolin resin. The limitation of the test setup deterred the possibility of performing a superimposed voltage test post the long term testing. When testing at higher voltages, it would be recommended to perform the superimposed voltage test to ensure the integrity of the insulation.

Bibliography

[1] Test methods for accessories for power cables with rated voltages from 6 kV (Um = 7,2 kV) up to 30 kV (Um = 36 kV). Standard IEC: 61442:2005, International Electrotechnical Commission, Geneva, Switzerland, 2005.

[2] High-voltage test techniques - part 1: General definitions and test requirements. Standard IEC: 60060-1:2010, International Electrotechnical Commission, Geneva, Switzerland, 2010.

[3] *Recommendations for testing DC extruded cable systems for power transmission at a rated voltage up to 500 kV*. CIGRÉ, 2012.

[4] Test requirements for accessories for use on power cables of rated voltage from 3.6/6(7.2)kv up to 20.8/36(42)kv - part 1: Accessories for cables with extruded insulation. Standard NEN-HD 629-1 S3, Nederlands Normalisatie-instituutn, Netherlands, 2019.

[5] LoviSil® technology, Apr 2020. URL `https://www.lovink-enertech.com/en/over-ons/lovisil-technologie/`.

[6] War of the currents, Mar 2020. URL `https://en.wikipedia.org/wiki/War_of_the_currents`.

[7] H. Al-Khalidi and A. Kalam. The Impact of Underground Cables on Power Transmission and Distribution Networks. In *2006 IEEE International Power and Energy Conference*, pages 576–580, 2006.

[8] D. Antoniou, A. Tzimas, and S. M. Rowland. DC utilization of existing LVAC distribution cables. In *2013 IEEE Electrical Insulation Conference (EIC)*, pages 518–522, 2013.

[9] L. V. Badicu, L. M. Dumitran, P. V. Notingher, R. Setnescu, and T. Setnescu. Mineral Oil Lifetime Estimation Using Activation Energy. In *2011 IEEE International Conference on Dielectric Liquids*, pages 1–4, 2011.

[10] G. Bathurst, G. Hwang, and L. Tejwani. MVDC - The New Technology for Distribution Networks. In *11th IET International Conference on AC and DC Power Transmission*, pages 1–5, 2015.

[11] B.Gholizad. Lecture notes in Special Cables., March 2019.

[12] R. Bodega, G. Perego, P. H. F. Morshuis, U. H. Nilsson, and J. J. Smit. Space charge and electric field characteristics of polymeric-type MV-size DC cable joint models. In *CEIDP '05. 2005 Annual Report Conference on Electrical Insulation and Dielectric Phenomena, 2005.*, pages 507–510, 2005.

[13] A. Braun, J. Brueggmann, M. Krause, T. Schrank, F. Martin, S. Poehler, O. Sener, F. Exl, and T. Klein. PQ Test of Extruded HVDC 525-kV-Underground Cables: Results and Conclusion. 06 2019. Jicable 2019 : 10th International Conference On Insulated Cables ; Conference date: 23-06-2019 Through 27-06-2019.

[14] A. Buchner and U. Schichler. Review of CIGRE TB 496 regarding Prequalification Test on Extruded MVDC Cables. *Proceedings of the Nordic Insulation Symposium*, 08 2019. doi: 10.5324/nordis.v0i26.3286.

[15] A. Andreas Buchner and U. Schichler. Application of extruded MVAC Cables for DC Power Transmission. 6 2019. Jicable 2019 : 10th International Conference On Insulated Cables ; Conference date: 23-06-2019 Through 27-06-2019.

[16] S. Buddhawar, A. Lewarkar, R. A. Mor, and D. Bergsma. DC Characterization Of Liquid Silicon Insulation Material. In *2019 IEEE 20th International Conference on Dielectric Liquids (ICDL)*, pages 1–7, 2019.

[17] A. Burstein, V. Ćuk, and E. d. Jong. Determining potential capacity gains when repurposing MVAC cables for DC power transportation. *CIRED - Open Access Proceedings Journal*, 2017(1):1691–1694, 2017.

[18] W. Choo and G. Chen. Electric field determination in DC polymeric power cable in the presence of space charge and temperature gradient under dc conditions. In *2008 International Conference on Condition Monitoring and Diagnosis*, pages 321–324, April 2008. doi: 10.1109/CMD.2008.4580292.

[19] H. Ghorbani, M. Jeroense, C. Olsson, and M. Saltzer. HVDC Cable Systems—Highlighting Extruded Technology. *IEEE Transactions on Power Delivery*, 29(1):414–421, Feb 2014. ISSN 1937-4208. doi: 10.1109/TPWRD.2013.2278717.

[20] H. Gramespacher and Y. Hanyu. Reliability of HVDC Cable Joints: Today Future Challenges, INMR World Congress. 10 2019.

[21] H. He, C. Beverwijk, P. Kuijpers, and W. Sloot. Cost-effective and practical solutions for testing HVDC cable systems. 06 2019. Jicable 2019 : 10th International Conference On Insulated Cables ; Conference date: 23-06-2019 Through 27-06-2019.

[22] M. Hu, S. Xie, J. Zhang, and J. Xue. Design and test of China first ±160kV DC cable for flexible DC transmission project. In *2014 China International Conference on Electricity Distribution (CICED)*, pages 1680–1684, 2014.

[23] P. Huber and W. Kaiser. Silicone fluids: Synthesis, properties and applications. *Journal of Synthetic Lubrication*, 3(2):105–120, 1986. doi: 10.1002/jsl.3000030204. URL https://onlinelibrary.wiley.com/doi/abs/10.1002/jsl.3000030204.

[24] D. HÄRING, G. SCHRÖDER, and J. KAUMANNS. Investigation and Qualification of 320 kV HVDC cable systems for VSC and LCC applications. 06 2019. Jicable 2019 : 10th International Conference On Insulated Cables ; Conference date: 23-06-2019 Through 27-06-2019.

[25] J. Karlstrand, G. Bergman, and H. . Jonsson. Cost-efficient XLPE cable system solutions. In *Seventh International Conference on AC-DC Power Transmission*, pages 33–38, 2001.

[26] H. Kasuga, H. Miyake, and Y. Tanaka. Space charge formation in XLPE at polarity reversal under high temperature. In *2017 International Symposium on Electrical Insulating Materials (ISEIM)*, volume 2, pages 535–538, Sep. 2017. doi: 10.23919/ISEIM.2017.8166544.

[27] Frederik H. Kreuger. *Industrial high voltage: 1. Electric Fields, 2. Dielectrics, 3. Constructions*. Delft Univ. Press, 1991.

[28] Frederik H. Kreuger. *Industrial high voltage: 4. Co-ordinating, 5. Measuring, 6. Testing*. Delft Univ. Press, 1992.

[29] Frederik H. Kreuger. *Industrial high DC voltage: 1. fields, 2. breakdowns, 3. tests*. Delft Univ. Press, 1995.

[30] T. Liu, Z. Lv, Y. Wang, K. Wu, L. A. Dissado, Z. Peng, and R. Li. A new method of estimating the inverse power law ageing parameter of XLPE based on step-stress tests. In *2013 Annual Report Conference on Electrical Insulation and Dielectric Phenomena*, pages 69–72, 2013.

[31] Y. Liu, X. Cao, and M. Fu. The Upgrading Renovation of an Existing XLPE Cable Circuit by Conversion of AC Line to DC Operation. *IEEE Transactions on Power Delivery*, 32(3):1321–1328, 2017. doi: 10.1109/tpwrd.2015.2496178.

[32] G. Mazzanti. The combination of electro-thermal stress, load cycling and thermal transients and its effects on the life of high voltage ac cables. *IEEE Transactions on Dielectrics and Electrical Insulation*, 16(4):1168–1179, 2009.

[33] G. Mazzanti. Life and Reliability Models for High Voltage DC Extruded Cables. *IEEE Electrical Insulation Magazine*, 33(4):42–52, 2017.

[34] G. Mazzanti, G. C. Montanari, and L. Simoni. Study of the synergistic effect of electrical and thermal stresses on insulation life. In *Proceedings of Conference on Electrical Insulation and Dielectric Phenomena - CEIDP '96*, volume 2, pages 684–687 vol.2, 1996.

[35] K. P. Meena, B. N. Rao, Thirumurthy, and G. K. Raja. Failure analysis of Medium Voltage Cable accessories during qualification tests. In *2012 IEEE 10th International Conference on the Properties and Applications of Dielectric Materials*, pages 1–4, 2012.

[36] I. A. Metwally, A. H. Al-Badi, A. S. Al-Hinai, F. A. Kamali, and H. Al-Ghaithi. Influence of design parameters and defects on electric field distributions inside MV cable joints. In *2016 18th Mediterranean Electrotechnical Conference (MELECON)*, pages 1–6, 2016.

[37] M.Ghaffarian Niasar. Lecture notes in Cable Accessories, Cable Ampacity and Cable Installation., February 2019.

[38] M.Ghaffarian Niasar. Lecture notes on Space Charge, May 2019.

[39] G. C. Montanari, G. Mazzanti, and L. Simoni. Progress in Electrothermal Life Modeling of Electrical Insulation During the Last Decades. *IEEE Transactions on Dielectrics and Electrical Insulation*, 9 (5):730–745, 2002.

[40] E. A. Morris and W. H. Siew. A comparison of AC and DC partial discharge activity in polymeric cable insulation. In *2017 IEEE 21st International Conference on Pulsed Power (PPC)*, pages 1–4, 2017.

[41] Y. Murata, M. Sakamaki, K. Abe, Y. Inoue, S. Mashio, S. Kashiyama, O. Matsunaga, T. Igi, M. Watanabe, S. Asai, and S. Katakai. Development of High Voltage DC-XLPE cable System. pages 55–62, 04 2013.

[42] T. Nguyen, H. Yoo, and H. Kim. A comparison study of MVDC and MVAC for deployment of distributed wind generations. In *2016 IEEE International Conference on Sustainable Energy Technologies (ICSET)*, pages 138–141, 2016.

[43] O. E. Oni, I. E. Davidson, and K. N. I. Mbangula. A review of LCC-HVDC and VSC-HVDC Technologies and Applications. In *2016 IEEE 16th International Conference on Environment and Electrical Engineering (EEEIC)*, pages 1–7, 2016.

[44] Mitesh Ramanlal Patel, Jignesh Markandray Shukla, Natvarbhai Khodidas Patel, and Ketan Haribhai Patel. Biomaterial based novel polyurethane adhesives for wood to wood and metal to metal bonding. *Materials Research*, 12:385 – 393, 00 2009. ISSN 1516-1439. URL http://www.scielo.br/scielo.php?script=sci_arttext&pid=S1516-14392009000400003&nrm=iso.

[45] E. Peschke and R. von Olshausen. *Cable Systems for High and Extra-High Voltage: Development, Manufacture, Testing, Installation and Operation of Cables and their Accessories*. Publicis MCD Vlg., 1999. ISBN 9783895781186. URL https://books.google.nl/books?id=JORSAAAAMAAJ.

[46] P. K. Ramteke, A. K. Ahirwar, N. B. Shrestha, V. V. S. Sanyasi Rao, K. K. Vaze, and A. K. Ghosh. Thermal ageing predictions of polymeric insulation cables from Arrhenius plot using short-term test values. In *2010 2nd International Conference on Reliability, Safety and Hazard - Risk-Based Technologies and Physics-of-Failure Methods (ICRESH)*, pages 325–328, 2010.

[47] Ravi. Comparison between overhead lines and underground cables, Oct 2019. URL http://electricalarticle.com/comparison-between-overhead-lines-underground-cables/.

[48] N. Schaik, E.F. Steennis, J. Eerde, B.J. Grotenhuis, A. Kerstens, M.J. Riet, and C.J. Verhoeven. Standardisation, prequalification, diagnostics, as part of cable system management. pages 15–15, 02 2001. ISBN 0-85296-735-7. doi: 10.1049/cp:20010676.

[49] A. Shekhar, E. Kontos, A. R. Mor, L. Ramírez-Elizondo, and P. Bauer. Refurbishing existing mvac distribution cables to operate under dc conditions. In *2016 IEEE International Power Electronics and Motion Control Conference (PEMC)*, pages 450–455, 2016.

[50] A. Shekhar, X. Feng, A. Gattozzi, R. Hebner, D. Wardell, S. Strank, A. Rodrigo-Mor, L. Ramirez-Elizondo, and P. Bauer. Impact of DC Voltage Enhancement on Partial Discharges in Medium Voltage Cables—An Empirical Study with Defects at Semicon-Dielectric Interface. *Energies*, 10: 1968, 11 2017. doi: 10.3390/en10121968.

[51] O. Siirto, J. Vepsäläinen, A. Hämäläinen, and M. Loukkalahti. Improving reliability by focusing on the quality and condition of medium-voltage cables and cable accessories. *CIRED - Open Access Proceedings Journal*, 2017(1):229–232, 2017.

[52] M. Smalley, E. Wen Shu, B. Richardson, Y. Hawig, R. Hartlein, and N. Hampton. Operating Extruded Distribution Cable Systems at Elevating Temperatures. 06 2019. Jicable 2019 : 10th International Conference On Insulated Cables ; Conference date: 23-06-2019 Through 27-06-2019.

[53] C. Stancu, P. V. Notingher, L. Dumitran, L. Taranu, A. Cernat, and A. Constantin. Thermal ageing effect on the DC cable joints insulations. In *2016 International Conference on Applied and Theoretical Electricity (ICATE)*, pages 1–6, Oct 2016. doi: 10.1109/ICATE.2016.7754670.

[54] R. Tarimo. Going underground: European transmission practices, Sep 2019. URL https://www.power-grid.com/articles/powergrid_international/print/volume-16/issue-10/features/going-underground-european-transmission-practices.html.

[55] M. Tefferi, Z. Li, Y. Cao, H. Uehara, and Q. Chen. Novel EPR-insulated DC cables for future multi-terminal MVDC integration. *IEEE Electrical Insulation Magazine*, 35(5):20–27, Sep. 2019. ISSN 1558-4402. doi: 10.1109/MEI.2019.8804331.

[56] K. Terashima, H. Sukuki, M. Hara, and K. Watanabe. Research and development of /spl plusmn/250 kV DC XLPE cables. *IEEE Transactions on Power Delivery*, 13(1):7–16, Jan 1998. ISSN 1937-4208. doi: 10.1109/61.660837.

[57] *Voedingskabel >= 1 kV, voor vaste aanleg*. TKF CONNECTIVITY SOLUTIONS, 3 2020.

[58] Y. Del Valle, N. Hampton, J. Perkel, and C. Riley. *Underground Cable Systems*, pages 11158–11187. Springer New York, New York, NY, 2012. ISBN 978-1-4419-0851-3. doi: 10.1007/978-1-4419-0851-3_758. URL https://doi.org/10.1007/978-1-4419-0851-3_758.

[59] B. Van Maanen, C. Plet, P. Van Der Wielen, S. Meijer, F. De Wild, and F. Steenis. Failure in Underground Power Cables - Return of Experience. 06 2015. Jicable 2015 : 9th International Conference On Insulated Cables ; Conference date: 21-06-2015 Through 25-06-2015.

[60] K. Wu, Y. Wang, X. Wang, M. Fu, and S. Hou. Effect of space charge in the aging law of cross-linked polyethylene materials for high voltage DC cables. *IEEE Electrical Insulation Magazine*, 33 (4):53–59, 2017.

[61] H. Ye, T. Fechner, X. Lei, Y. Luo, M. Zhou, Z. Han, H. Wang, Q. Zhuang, R. Xu, and D. Li. Review on HVDC cable terminations. *High Voltage*, 3(2):79–89, 2018.

[62] J. Yu, K. Smith, M. Urizarbarrena, N. MacLeod, R. Bryans, and A. Moon. Initial designs for the ANGLE DC project; converting existing AC cable and overhead line into DC operation. In *13th IET International Conference on AC and DC Power Transmission (ACDC 2017)*, pages 1–6, 2017.